ON THE QUESTION OF PILOT DETERIORATION DURING LOW ALTITUDE FLIGHT

P. Schulz

Translation of "Zu Fragen der Pilotenschädigung beim Tiefflug". In: Turbulenzmodell in Bodennaehe und Flug in Turbulenter Atmosphaehre (Turbulence Model at Low Altitudes and Flight in a Turbulent Atmosphere), Deutsche Gesellschaft fuer Luft- und Raumfahrt, Cologne, West Germany, Report DLR-Mitt-70-12, Presented at the Meeting of the DGLR Science Commission on Flight Performance and Flight Characteristics, Darmstadt, West Germany, 12-13 November, 1970. pp. 99-117.

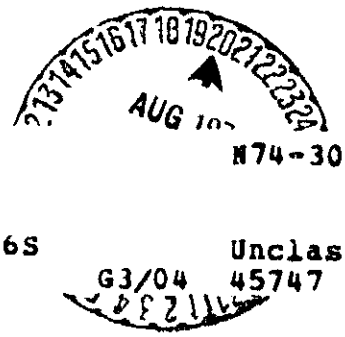

NATIONAL AERONAUTICS AND SPACE ADMINISTRATION
WASHINGTON, D. C. JULY 1974

STANDARD TITLE PAGE

1. Report No. NASA TT F-15,799	2. Government Accession No.	3. Recipient's Catalog No.
4. Title and Subtitle ON THE QUESTION OF PILOT DETERIORATION DURING LOW ALTITUDE FLIGHT		5. Report Date July 1974 6. Performing Organization Code
7. Author(s) P. Schulz		8. Performing Organization Report No. 10. Work Unit No.
9. Performing Organization Name and Address SCITRAN box 5456 Santa Barbara, CA 93108		11. Contract or Grant No. NASw-2483 13. Type of Report and Period Covered Translation
12. Sponsoring Agency Name and Address National Aeronautics and Space Administration Washington, D.C. 20546		14. Sponsoring Agency Code

15. Supplementary Notes Translation of "Zu Fragen der Pilotenschädigung beim Tiefflug". In: Turbulenzmodell in Bodennaehe und Flug in Turbulenter Atmosphaehre (Turbulence Model at Low Altitudes and Flight in a Turbulent Atmosphere), Deutsche Gesellschaft fuer Luft- und Raumfahrt, Cologne, West Germany, Report DLR-Mitt-70-12, Presented at the Meeting of the DGLR Science Commission on Flight Performance and Flight Characteristics, Darmstadt, West Germany, 12-13 November, 1970. pp. 99-117.

16. Abstract

The problem of pilot performance estimates during the aircraft design phase is discussed. The following are found to influence such estimates: low-altitude turbulence model, aircraft model, mission model and pilot response model. Pilot response to stochastic gust disturbances are evaluated and the aircraft transfer functions are calculated. Flight controllers are needed for low-altitude flight. Elastic degrees of aircraft motion should be included in the calculation.

17. Key Words (Selected by Author(s))	18. Distribution Statement
	Unclassified - Unlimited

19. Security Classif. (of this report)	20. Security Classif. (of this page)	21. No. of Pages	22. Price
Unclassified	Unclassified	20	

A SIMULATOR INVESTIGATION OF ENGINE FAILURE COMPENSATION FOR POWERED-LIFT STOL AIRCRAFT

Albert W. Nieuwenhuijse

and

James A. Franklin

Ames Research Center
Moffett Field, California 94035

ABSTRACT

A piloted simulator investigation of various engine failure compensation concepts for powered-lift STOL aircraft was carried out at the Ames Research Center. The purpose of this investigation was to determine the influence of engine failure compensation on recovery from an engine failure during the landing approach and on the precision of the STOL landing. The various concepts included (1) cockpit warning lights to cue the pilot of an engine failure, (2) programmed thrust and roll trim compensation, (3) thrust command and (4) flight-path stabilization. The aircraft simulated was a 150 passenger four-engine, externally blown flap civil STOL transport having a 90 psf wing loading and a .56 thrust to weight ratio. Results of the simulation indicate that the combination of thrust command and flight-path stabilization offered the best engine-out landing performance in turbulence and did so over the entire range of altitudes for which engine failures occurred.

ON THE QUESTION OF PILOT DETERIORATION DURING LOW ALTITUDE FLIGHT

P. Schulz*

1. Introduction

/99*

The ride qualities of an aircraft represent one of several multi-discipline problems which are related to the development of a controller for the high velocity low altitude flight regime. The usual criteria for evaluating the ride qualities of an aircraft are the variances of accelerations at the location of the pilot seat. Since the factors which influence the minimization of the aircraft response to gusts also influence the flight properties of the system, we should also consider the following:

1. Stability and control, and
2. Instabilities induced by the pilot,

i.e., a gust aid system cannot be designed in a manner which is too stable, otherwise, the pilot will have difficulties in flying the aircraft.

However, these problems will not be discussed in this paper, which is only concerned with the calculation of the ride qualities during the project and definition phases. In order to be able to /100 calculate the ride qualities in a satisfactory manner, the accuracy of the following models is important:

*VFW-Fokker GmbH., Bremen.

**Numbers in the margin indicate the pagination of the original foreign text.

1. the turbulence model for low altitudes,
2. the aircraft model,
3. the aircraft mission model,
4. the pilot model which is loaded by the accelerations.

The first calculations can be made using a rigid aircraft. Later on, when the elastic and aerodynamic properties are better known, it is possible to include the elastic degrees of freedom. There are two possibilities for calculating the transfer function of the aircraft:

1. the equations for longitudinal motion of the point mass aircraft,
2. buildup of a relatively simple discrete aircraft model and use of the rigid degrees of freedom for calculating the transfer function.

Both methods will be discussed because they give different results for aircraft with large sweepback angles.

The tolerance limits of human beings to accelerations have not yet been determined even today, because not enough data have been collected.

The pilot deterioration should be the general criterion for the ride qualities, and not the variance of the accelerations at the pilot seat. This requirement is a consequence of the fact that two different power spectra can have the same variance (because of the integration) but could result in different degrees of pilot deterioration. Therefore, this lecture will primarily deal with this topic.

The sensitivity of an aircraft to atmospheric turbulence /101
primarily depends on the ratio of the force produced by the gust and the mass of the aircraft, as well as the tendency of the aircraft to turn into the relative wind. In order to calculate the gust sensitivity at the center of gravity and at the pilot seat, we can use the equations for the longitudinal motion as a first approximation [3]. The results of these calculations will be very useful for the following investigations:

1. the influence of the angle of attack oscillation on the gust sensitivity at the center of gravity. The result is that there is a decrease in $\sigma_{n_{z_s}}$ when ζ and ω_0 are increased (Figure 1).

2. the influence of the angle of attack oscillation and of the dynamic amplification factor on the gust sensitivity at the pilot seat (Figure 2).

Since these various parameters for optimum ride qualities also influence the flight property criteria, for example, ω_0^2/n_{z_α}, Z_α/ω_0 and n_{z_α}/ω_0, the proper selection of these quantities depends on both the ride qualities and the flying qualities.

2. The Behavior of Humans under the Influence of Stochastic Disturbances

Not much data is available which describes the fatigue of /102
humans caused by stochastic accelerations. When these data are applied to high velocity, low altitude flight, one encounters the problem of whether and how the pilot can solve tactical and flight handling tasks if he is subjected to a stochastic acceleration spectrum. All of the data on this subject apply for sinusoidal accelerations with a certain variance and frequency,

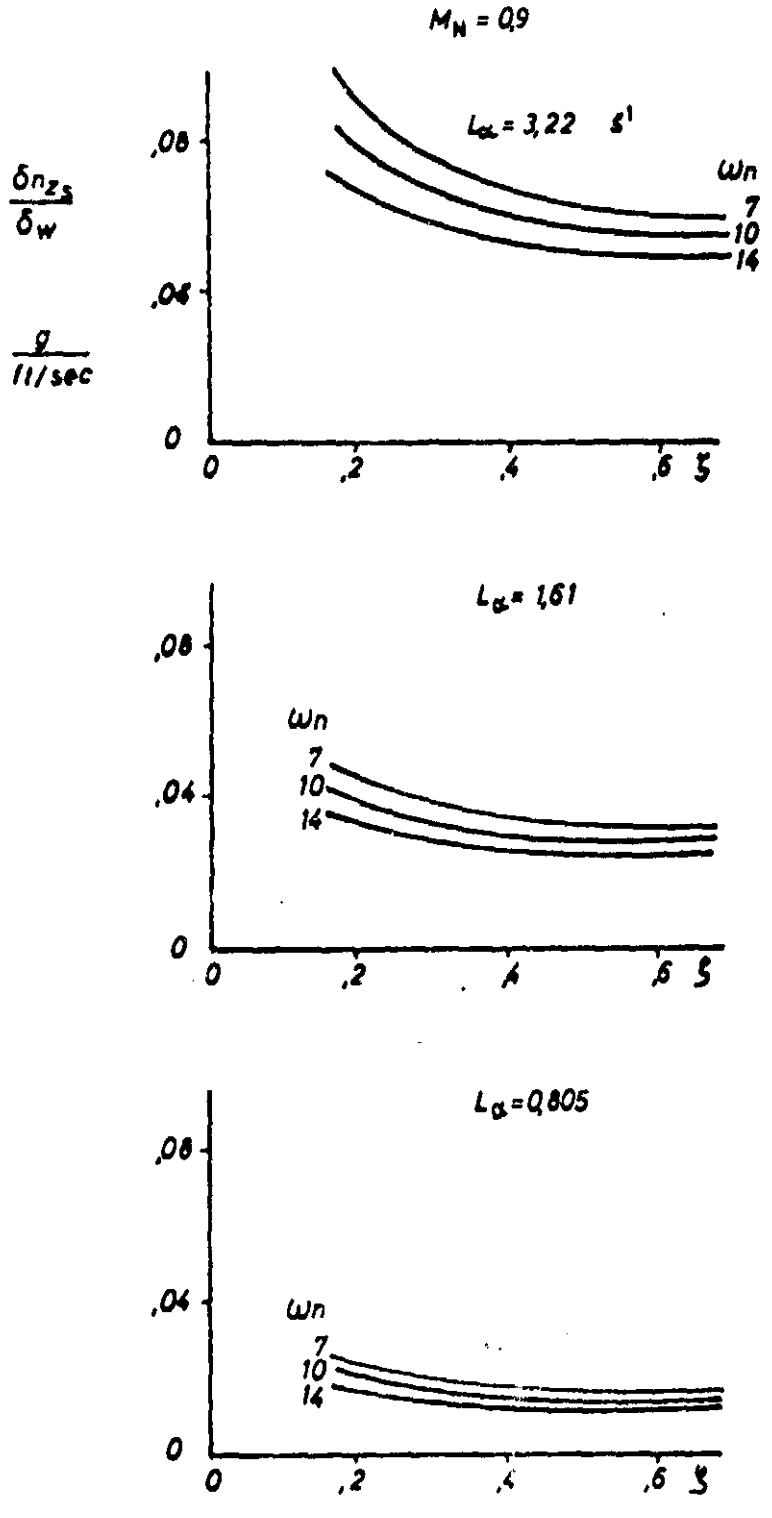

Figure 1. Influence of angle of attack oscillation on the gust sensitivity at the center of gravity.

From Ralph C. A. Harrah. Maneuverability and Gust Response Problems Associated with Low Altitude, High Speed Flight.

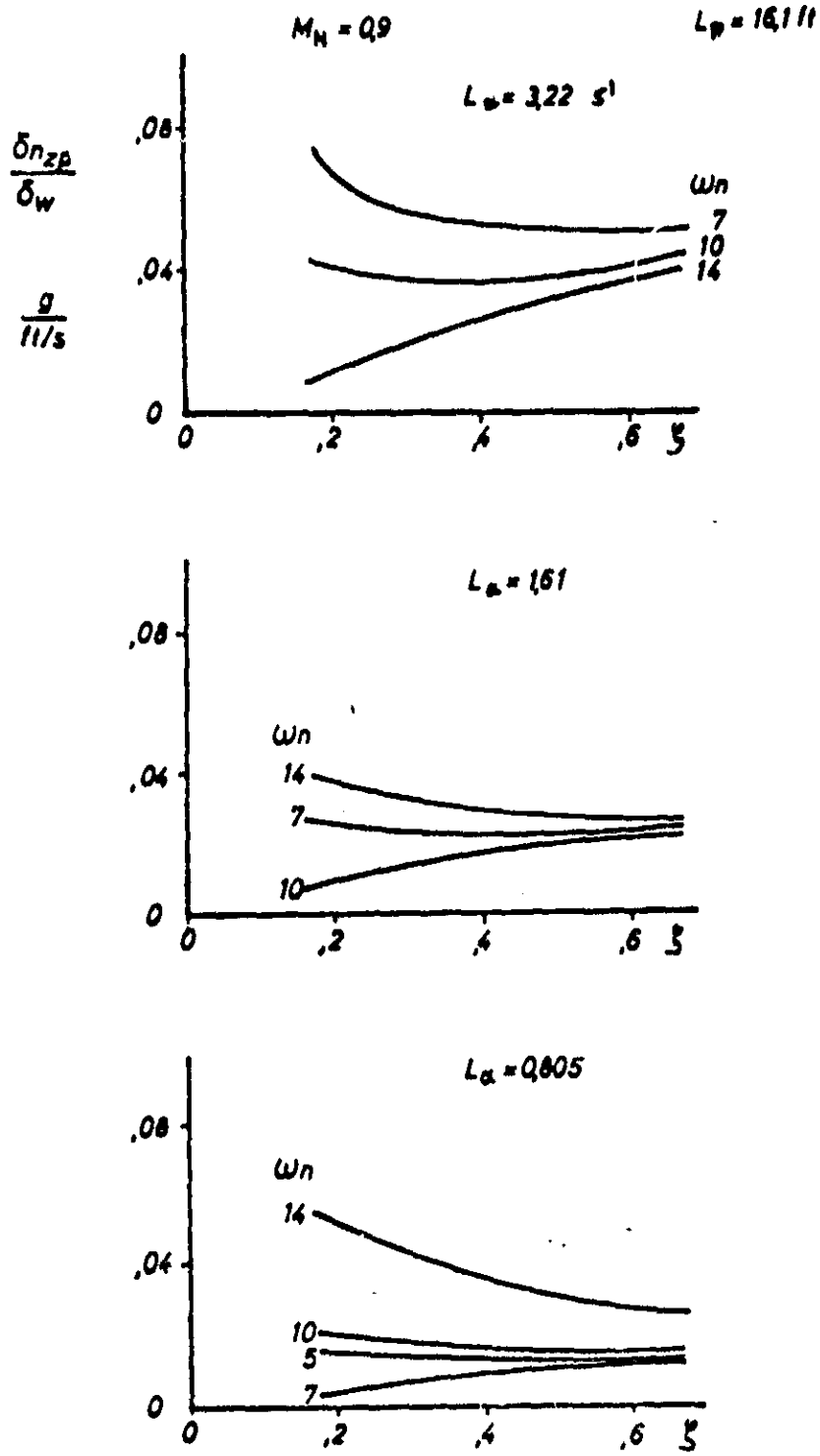

Figure 2. Influence of angle of attack oscillation on the gust sensitivity at the pilot seat location.

From Ralph C. A. Harrah. Manueverability and Gust Response Problems Associated with Low Altitude, High Speed Flight.

for example, see [1]. This will be used here as a basis for calculating the pilot deterioration due to gusts. This reference indicates that the acceleration within six octaves must be integrated to obtain partial values of the variance, i.e.,

$$\sigma^2_{part_i} = \int_{\omega_i}^{2\omega_i} \Phi_B(\omega)\, d\omega$$

where $\Phi_B(\omega)$ = power spectrum of accelerations. Using these partial values of the variance of the accelerations, the permissible loading times t_{z_i} are calculated from the load capacity curves (Figure 3). The reciprocal $S_i = 1/t_{z_i}$ is then the pilot deterioration. The deterioration from all octaves is then summed and one finds the total deterioration due to the existing power spectrum of accelerations at the pilot seat location.

The method given in this reference uses a type of average value of accelerations in this octave for calculating the deterioration. Since the permissible loading times depend very greatly on the variance and frequency of the accelerations, the pilot deterioration will change drastically when the octaves are displaced (Figure 4). Therefore, it would be desirable to have a method which does not use the average value of the accelerations but a method which averages the permissible loading times for the /103 deterioration. This can be done by means of the following substitution

$$\omega = \omega_0 \cdot 2^x$$

$$\Rightarrow \quad d\omega = \ln 2 \cdot \omega_0 2^x\, dx$$

$$\sigma^2_{part_i} = \int_{x_i}^{x_i+1} \omega_0 2^x \ln 2\, \Phi_B(\omega)\, dx$$

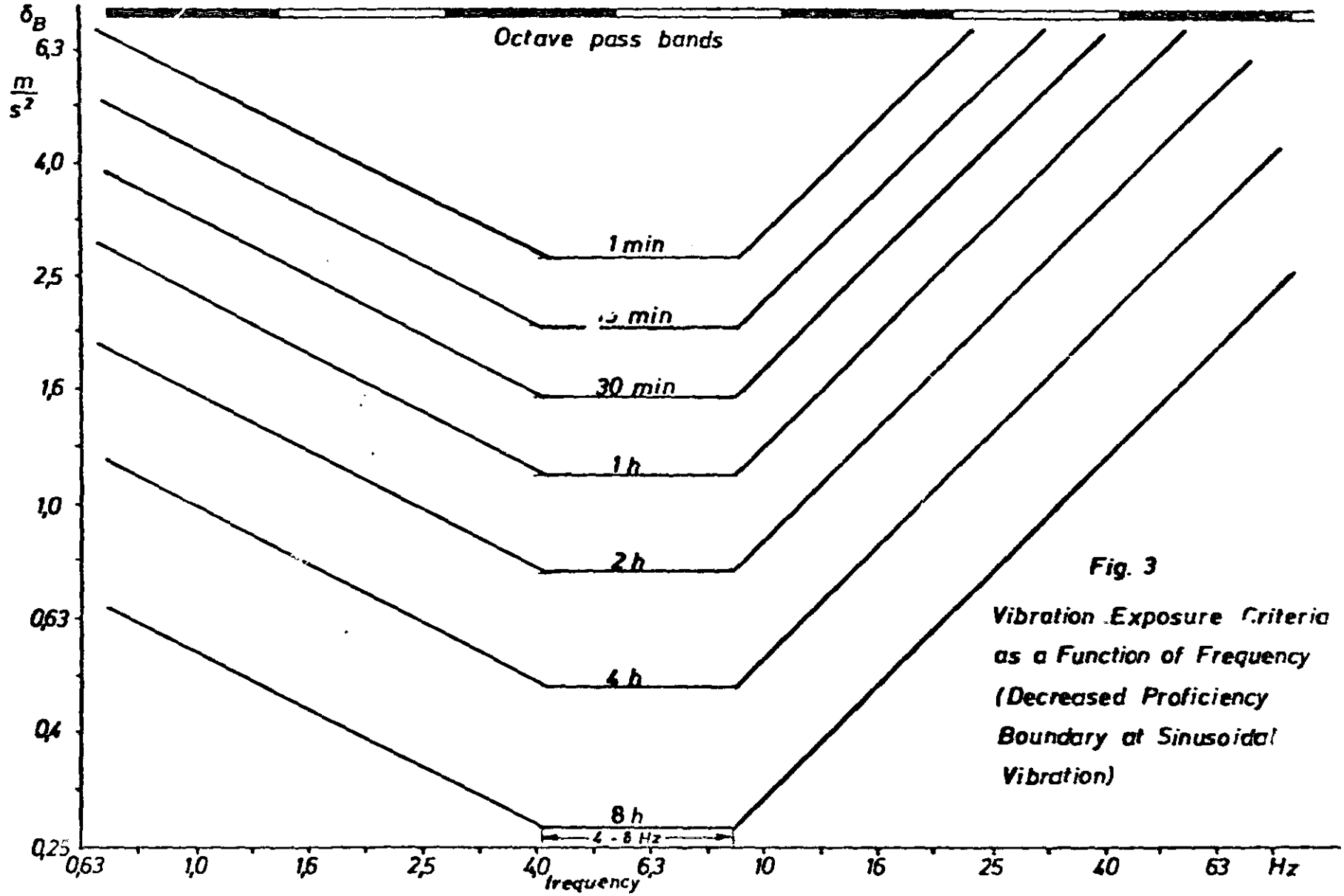

Fig. 3

Vibration Exposure Criteria as a Function of Frequency (Decreased Proficiency Boundary at Sinusoidal Vibration)

Figure 3. Vibration exposure criteria as a function of frequency (decreased proficiency boundary at sinusoidal vibration).

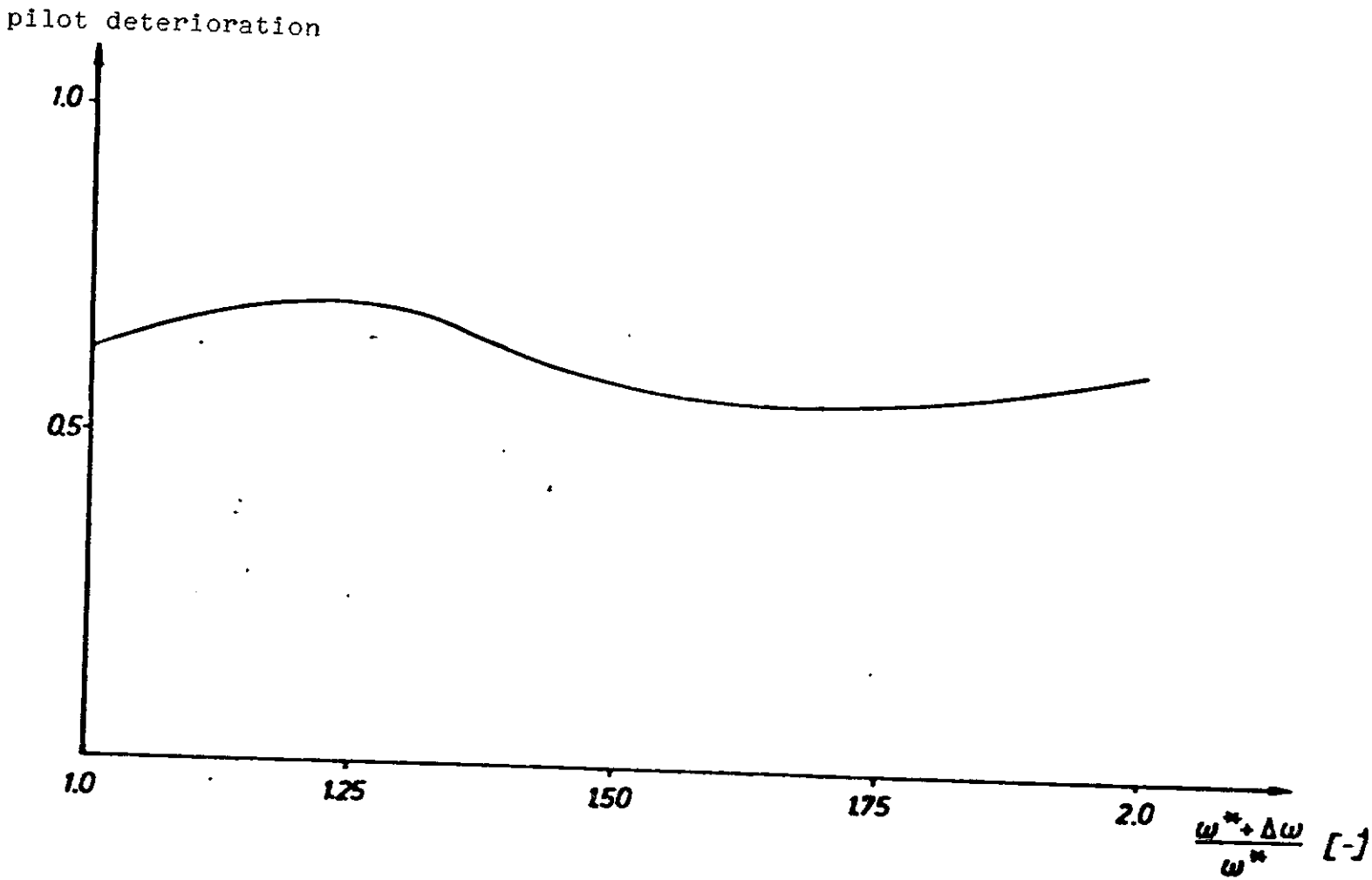

Figure 4. Reduced performance capacity as a function of octave changes.

In this formula, x is a dimensionless quantity, i.e., the integrand has the same dimensions as σ^2.

Therefore, we make the following substitution

$$\sigma^{*2}_{(x)} = \omega_0 2^x \ln 2 \, \Phi_B(x)$$

and we obtain the following for the variance of octave i

$$\sigma^2_{part_i} = \int_{x_i}^{x_{i+1}} \sigma^{*2}_{(x)} \, dx$$

This expression has the advantage that $\sigma^{*2}_{(x)}$ is a continuous function and has the same dimensions as $\sigma^2_{part\ i}$. Therefore, σ^2_{part} is the average of the function $\sigma^{*2}_{(x)}$ of the octave i, because the length of the integral is 1. Therefore, the deterioration curve $S^*(\sigma^*, x)$ is calculated from the continuous function $\sigma^*_{(x)}$ and the permissible load curves (Figure 3). The earlier summation of partial deterioration values is then replaced by an integration of the deterioration curve.

$$S = \int S^*_{(x)} \, dx$$

The disadvantage of the old method is that it averages $\sigma^{*2}_{(x)}$.

This fact and the variation of the permissible load curves /104 are the reasons for the change in the results when the octaves are displaced.

The question of the applicability of the permissible load curves to stochastic accelerations becomes rather unimportant by making a transfer to the continuous function $\sigma^*_{(x)}$ from the partial values of variance. These permissible load curves are then established for sinusoidal accelerations with a certain frequency and amplitude. Discrete points of the curve σ^*, i.e., the corresponding power spectrum of accelerations, can be looked upon as representatiors of sinusoidal functions with frequencies and variances corresponding to the selected points. Therefore, the reference mentioned above can also be applied for stochastic accelerations

3. Pilot Deterioration Due to Stochastic Accelerations

A pilot can withstand an acceleration spectrum with a certain variance for only a limited time t_z, which is a function of the average value of accelerations and the frequency of the gusts. This function was taken from [1] mentioned above. The variance of the load multiple σ_w at the pilot seat is given by

$$\sigma_n^2 = \int_0^\infty \Phi_n(\omega)\, d\omega$$

$$= \frac{1}{V} \int_0^\infty |F(\omega)|^2 \cdot \Phi_w(\omega)\, d\omega$$

$\Phi_n(\omega)$ is the power spectrum of the load multiple; $\Phi_w(\omega)$ is the power spectrum of the gusts; F(w) is the transfer function /105 of the aircraft $\Delta n_z/w$.

During the mission, the transfer function of the aircraft changes because of the decrease in aircraft weight. Other reasons for this are the changes in weather, velocity, and flight altitude during the flight. In order to include these changes in the

load multiple in the calculation, the influence of any effective time is explained by means of a damage accumulation [2].

The "damage rate", which varies in time, has been given by

$$\frac{dS}{dt} = \frac{1}{t_z(t)}$$

where $t_z(t)$ = instantaneous permissible load time due to $\sigma_z(t)$. The instantaneous damage is then the ratio of the loading time --dt — and the permissible loading time $t_z(t)$.

In this way, the total damage over the mission becomes

$$S = S(T_M) = \int_0^{T_M} dS = \int_0^{T_M} \frac{dt}{t_z(t)}$$

where T_M = mission time.

Since any mission differs from any other mission because of the change in the weather and because only the statistical distribution of the gusts is known, it is impossible to calculate the actual damage during a certain mission. Therefore, it is only possible to calculate the expectation value of pilot deterioration:

$$E[S(T_M)] = \int_{-\infty}^{\infty} S(\sigma_w)\, dW(\sigma_w) = \int_{-\infty}^{\infty} S(\sigma_w)\, w(\sigma_w)\, d\sigma_w$$

/106

where $W(\sigma_w)$ = probability function and $w(\sigma_w)$ = probability density function.

It is defined in [4] as follows:

$$w(\sigma_w) = \frac{P_1}{b_1}\sqrt{\frac{2}{\pi}}\, e^{-\frac{\sigma_w^2}{2b_1^2}} + \frac{P_2}{b_2}\sqrt{\frac{2}{\pi}}\, e^{-\frac{\sigma_w^2}{2b_2^2}}$$

where the parameters P_1 and P_2 are the ratio of flight time or flight path for nonstormy and stormy turbulence. b_1 and b_2 are the scale parameters for the individual probability distributions of σ_w for the two types of turbulence.

The power spectrum for the vertical turbulences is given by the Dryden or the Karmann spectrum.

4. The Calculation of the Aircraft Transfer Function

As already mentioned above, there are two possibilities for calculating the transfer function of a rigid aircraft.

1. The equations of motion for the point mass aircraft

2. If a relative simple discrete model is used, it is possible to employ the rigid body motions for calculating the transfer function.

The main differences between the method are in the treatment of the unsteady aerodynamic effects and the sweepback angle. /107

In order to calculate the transfer function of the rigid aircraft due to vertical gusts for the longitudinal motion, the equations of motion are taken from [5]

$$\ddot{\vartheta} - M_q \dot{\vartheta} - M_\alpha \alpha - M_{\dot{\alpha}} \dot{\alpha} = M_\alpha \frac{w}{V}$$

$$\dot{\alpha} - \dot{\vartheta} + L_\alpha \alpha = -L_\alpha \frac{w}{V}$$

The unsteady aerodynamic effects are not contained in these equations. Since the deflections of individual wing points cannot be determined in this model, it is only possible to consider the Kuessner function. Therefore, for the right side,

we obtain

$$\frac{w}{V} = \int_0^t \frac{\dot{u}(\tau)}{V} \psi(t-\tau)\, d\tau + \frac{u(0)}{V} \psi(t)$$

where ψ = Kuessner function.

The transfer function is obtained from the two equations given above by using the Laplace transformation. The pitch moment term in the moment equation can be split up into components for the wing-fuselage and for the elevator, in order to include the dead time between these two components. The Kuessner function of the elevator can be ignored because the chord length of the elevator is small compared with that of the wing and the aerodynamic response can therefore be approximated by a jump function.

The transfer functions for the two degrees of freedom of the system α and ϑ are calculated from the two equations of motion. With this it is possible to then calculate the load multiple at the center of gravity and the additional load multiple caused by rotation around the center of gravity.

/108

$$\frac{\Delta n_{z_s}}{u} = \frac{V\dot{\gamma}}{u_g}$$

$$\frac{\Delta n_{z_2}}{u} = \frac{l_p \ddot{\vartheta}}{u_g}$$

The transfer function for the total load multiple is then the sum of both

$$\frac{\Delta n_{z_p}}{u} = \frac{\Delta n_{z_s}}{u} + \frac{\Delta n_{z_2}}{u}$$

The calculation of the transfer function of the elastic aircraft will be outlined here. Starting with the general matrix equation of an elastic equation, it is possible to determine the displacements and rotations of the discrete points of the aircraft. These are then built up from the contributions of the individual eigen modes and of a time function, according to the Bernoulli separation theorem. When a transfer is made from the time region to the frequency region, this then becomes the transfer function of the system. Because of the fact that the deflections are known, it is possible to apply the Kuessner and the Wagner force under these unsteady aerodynamic conditions. In our calculations, we only considered the circulatory components caused by vertical motion of the profile and of the rotation around the C/4 point in the Wagner force.

The advantage of an aircraft built up of discrete points is that it also becomes possible to consider the influence of the wing sweepback. In the case of a wing with a strong sweepback, a straight gust front will reach the individual points of the wing at different times and, therefore, the response of the aircraft will be softer. Another advantage is the possibility of being able to consider the Kuessner and the Wagner forces under unsteady aerodynamic conditions.

These two facts are the reasons for the differences in the two curves given in Figure 5. This is also the reason for their general appearance. Even though one wishes to only calculate the rigid aircraft, the discrete model can be used because the rigid degrees of freedom and the eigen modes can be used for describing the aircraft and its motion. In addition, later on, the elastic eigen modes can be incorporated relatively easily into the computer program. /109

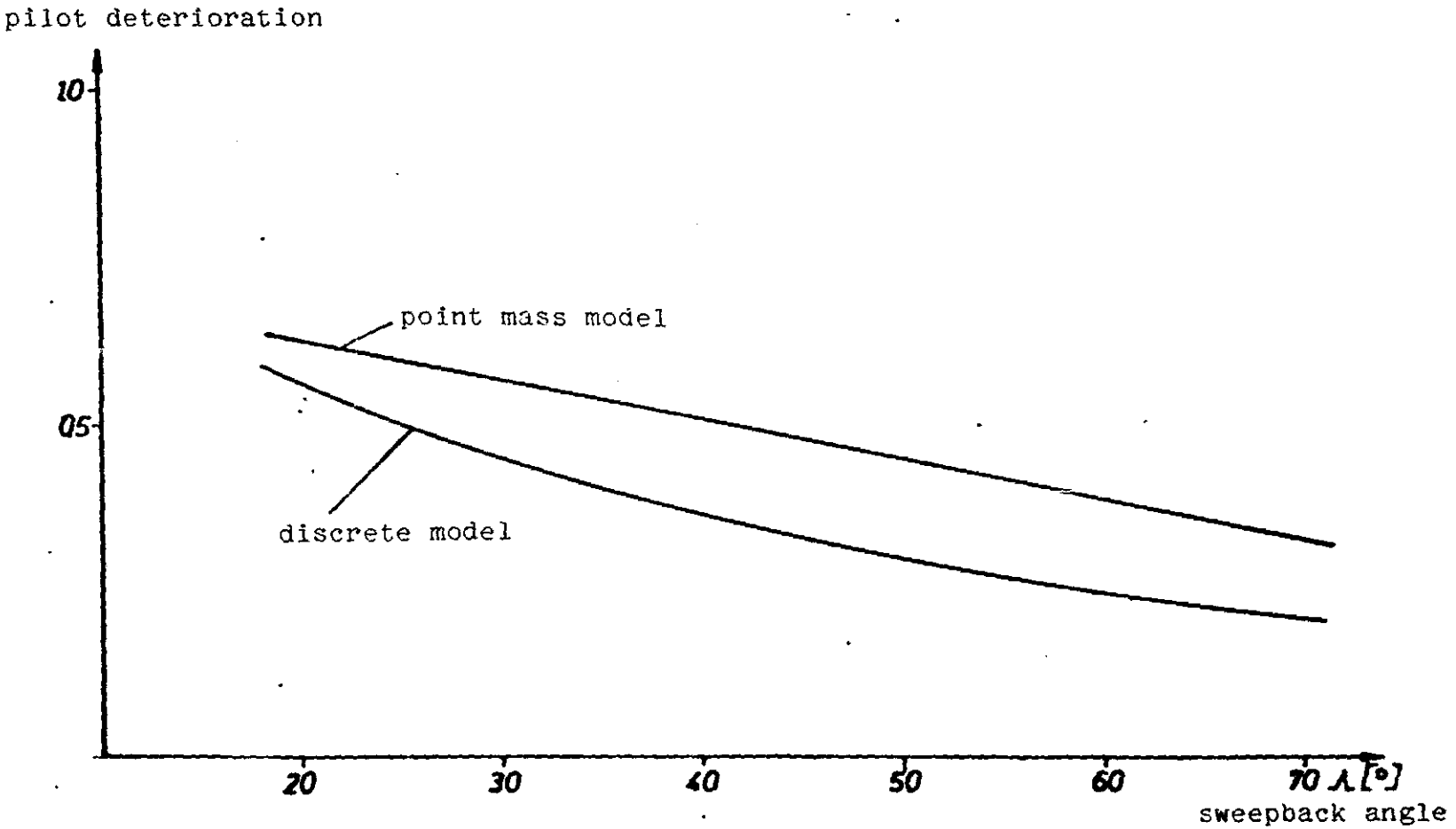

Figure 5. Reduced performance capacity for the two different models.

5. Summary

The calculation of pilot deterioration for high velocity, low altitude missions is a multi-layered problem. The improved method of considering the physiological data of humans represents only a small step towards the exact calculation of ride qualities. Because of the difficult situation of a pilot during a terrain-following mission, it is necessary to have a flight controller for controlling the aircraft. Therefore, a complete aircraft model for calculating the pilot deterioration should contain this controller.

The load on the pilot caused by maneuver stresses during terrain following flights is very high. Therefore, it is necessary to consider these accelerations in the calculation. However, we encounter the following difficulty: if one superimposes the acceleration caused by vertical gusts with those of the terrain following flight, one then indirectly is saying that there is no relationship between the gusts and the terrain shape. Even if we have a noise generator and a filter during a real time simulation, which produces the statistical gust distribution along the flight path, one has still not yet made any statement about the relationship between these two quantities. Another difficulty is the low frequency at which the maneuver loads of terrain following flight occur. The permissible load curves given in [1] extend to a frequency of down to f = 0.7 Hz. After about /110
1 Hz, one encounters the region of seasickness, which was intentionally excluded in this report, because not enough is known and, in addition, the available data is contradictory.

For the first calculations of pilot deterioration during the project phase, it is not necessary to consider the elastic degrees of freedom. Since the influence of the elastic oscillations on the pilot is considerable even for small aircraft, one should

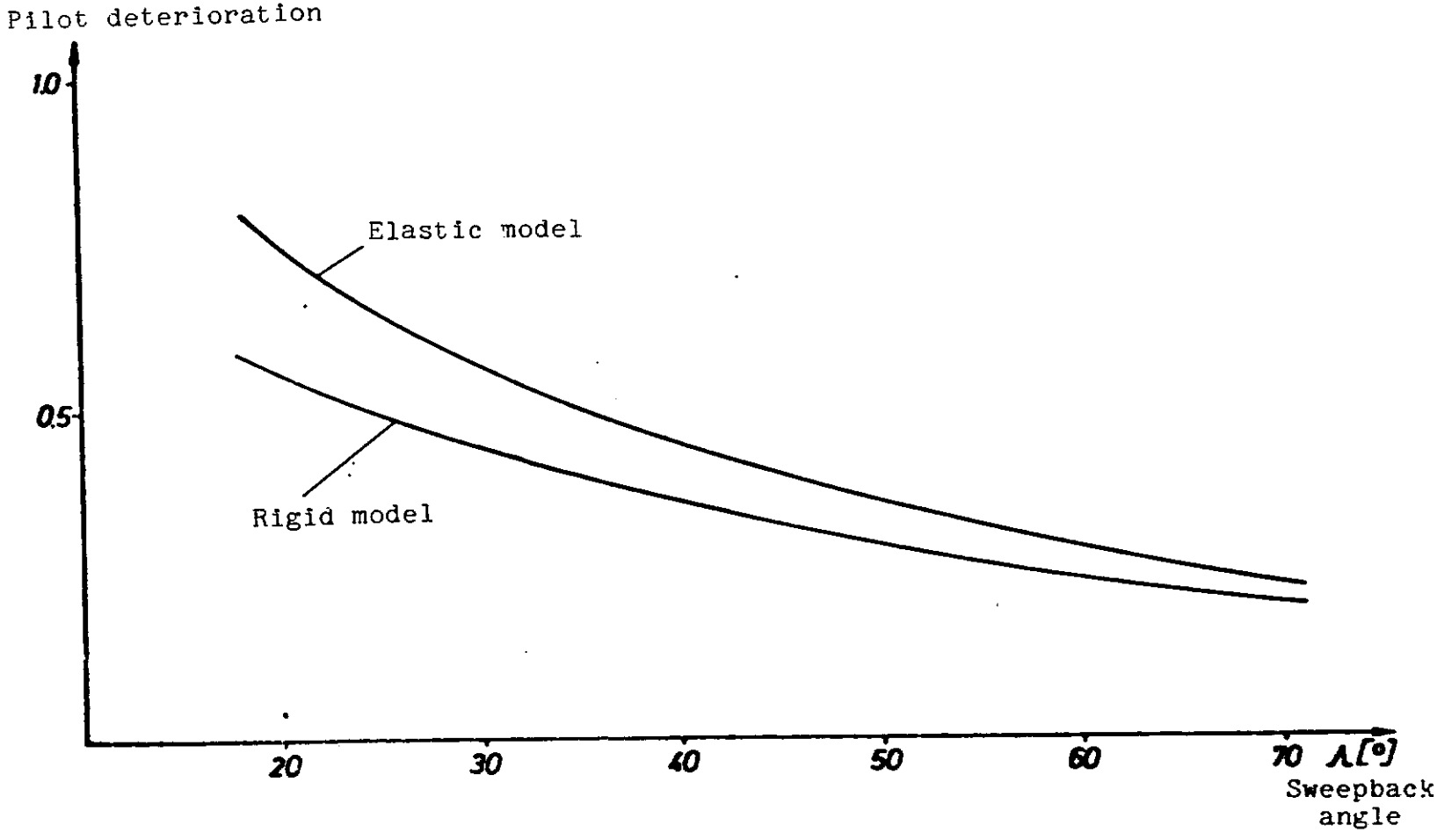

Figure 6. Reduced performance capacity for rigid and elastic discrete model.

include the elastic degrees of freedom as soon as possible in the calculations. The curves given in Figure 6 show the influence of the elastic degrees of freedom. The slight difference between the two curves at large sweepback angles was produced by the fact that the moments of inertia of the wing segments were too small.

The method for calculating the pilot deterioration is the same for sideways motion. Only the permissible load curves are somewhat different in this case.

REFERENCES

1. ISO-Bericht: Evaluation Exposure of Humans to Whole Body Vibration, May, 1968.

2. Staufenbiel, Dr. Influence of Gusts on the Design of Low Altitude, High Velocity Aircraft. VFW-Report EM-351-65.

3. Harrah, R. C. A. Maneuverability and Gust Response Problems Associated with Low Altitude, High Speed Flight. AGARD Flight Mechanics Panel, Report 556, October 1967.

4. Press, H. and R. Steiner. An Approach to the Problem of Estimating Serve and Repeated Gust Loads for Missile Operations. NACA TN-4332.

5. Chalk, R. Fixed Base Simulator Investigations of L_α and True Speed on Pilot Opionion of Longitudinal Flying Qualities. ASD-TDR-63-399.

Translated for National Aeronautics and Space Administration under Contract No. NASw-2483 by SCITRAN, P. O. Box 5456, Santa Barbara, California, 93108.

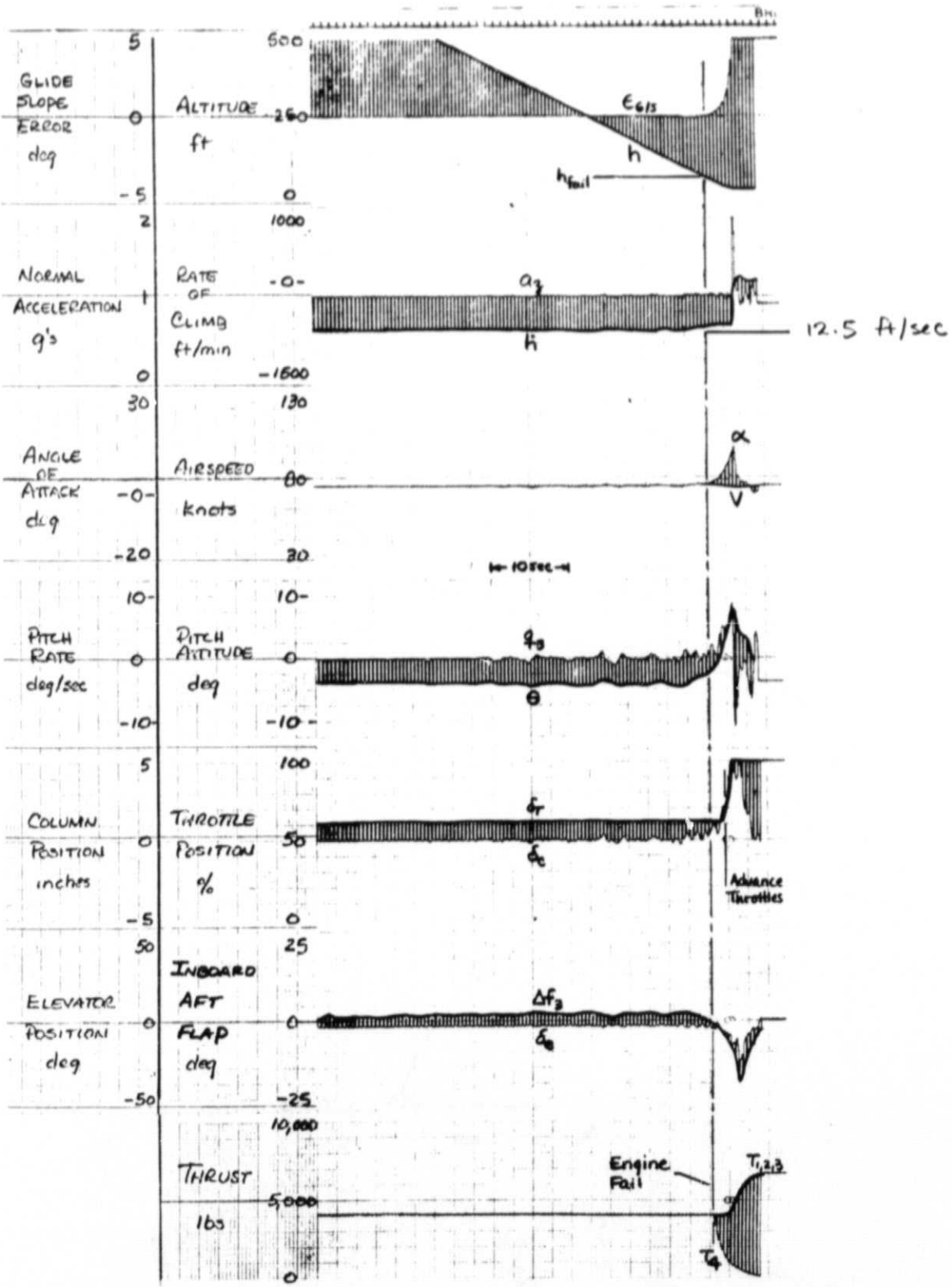

Figure 1. Time History of STOL Landing
Following an Engine Failure at 50 Feet

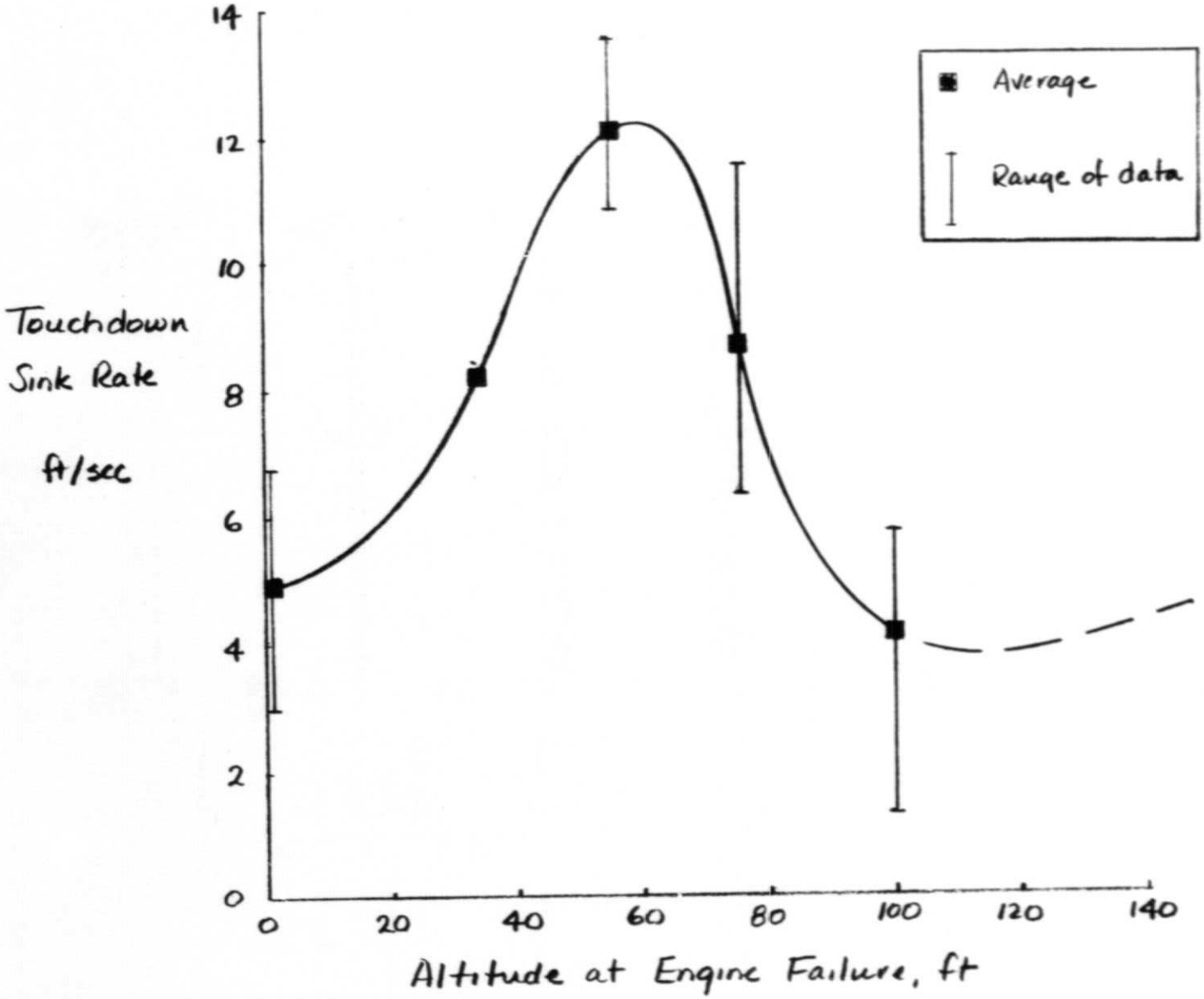

Figure 2. Trends of Engine-Out Touchdown Sink Rate with Altitude at Engine Failure

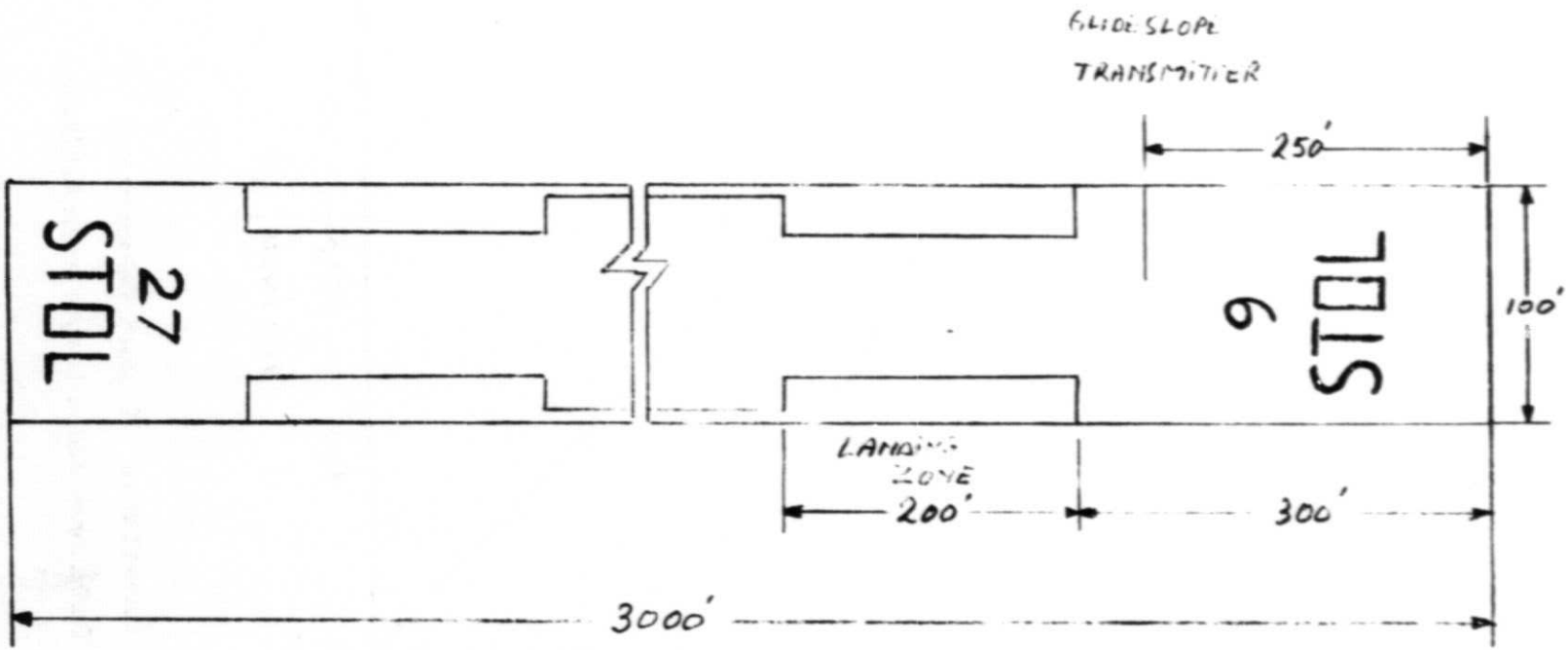

Figure 3. STOLPORT Layout

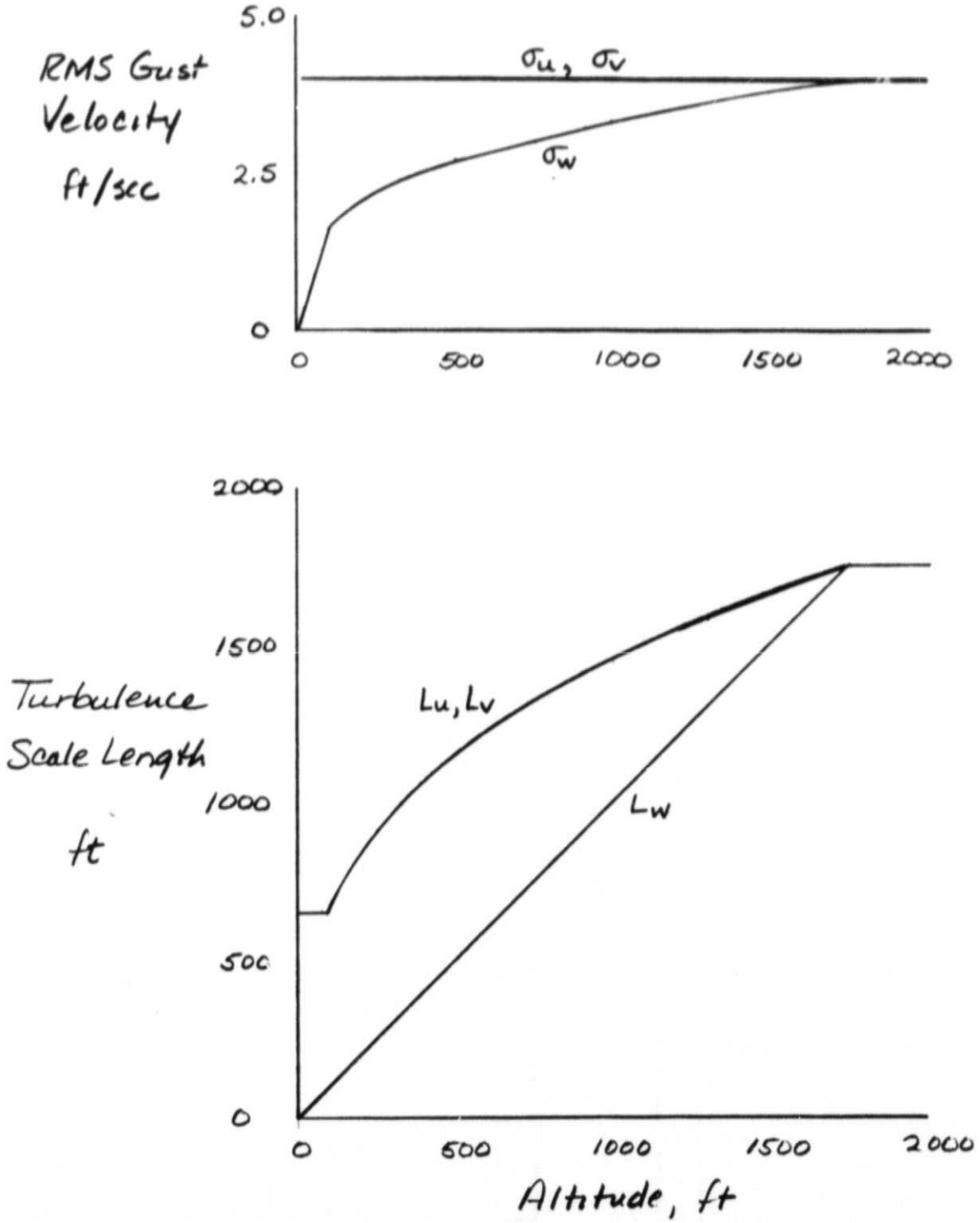

Figure 4. Variation of RMS Gust Velocity and Turbulence Scale Length with Altitude

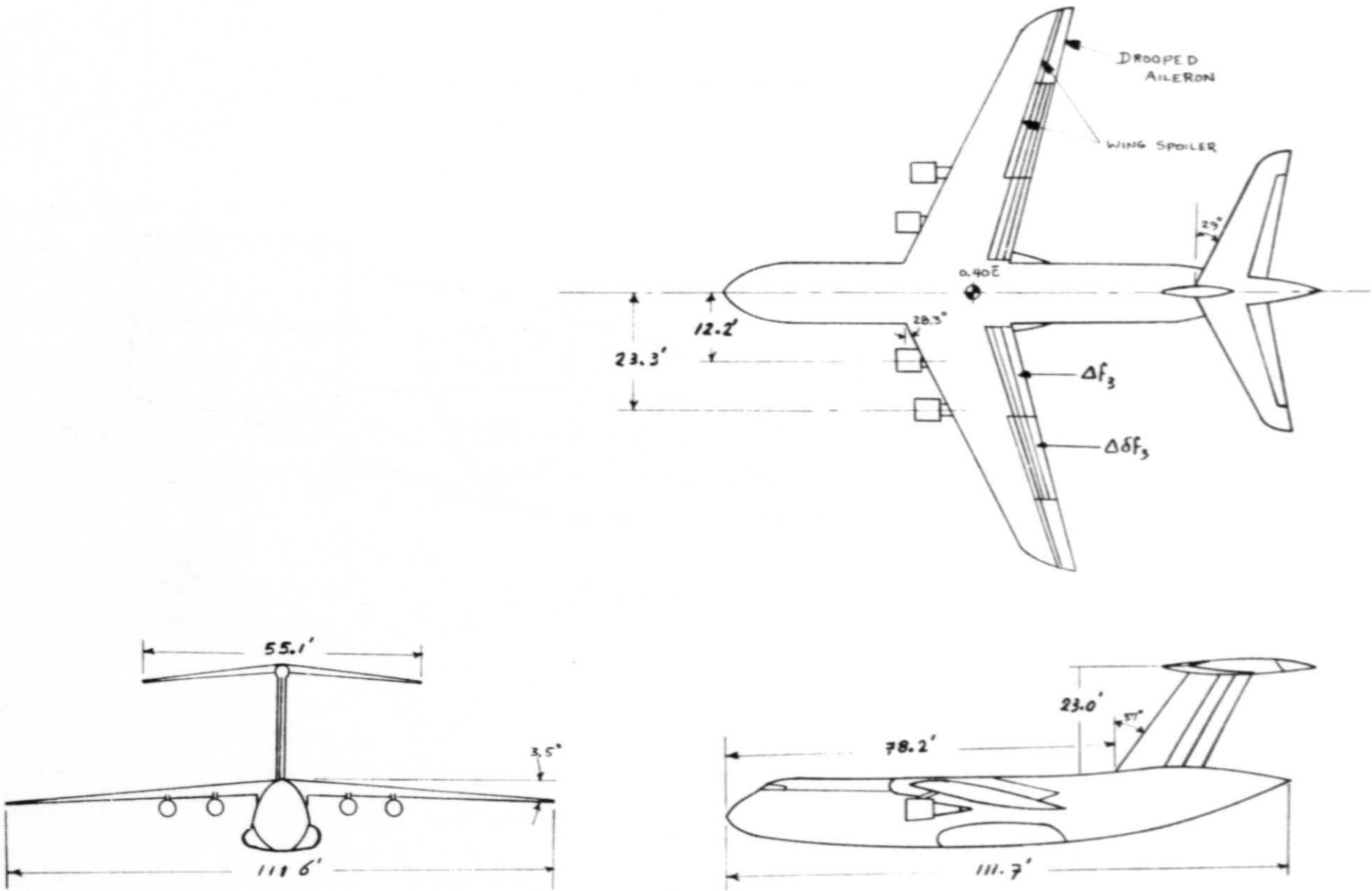

Figure 5. Three View Schematic of Simulated Aircraft

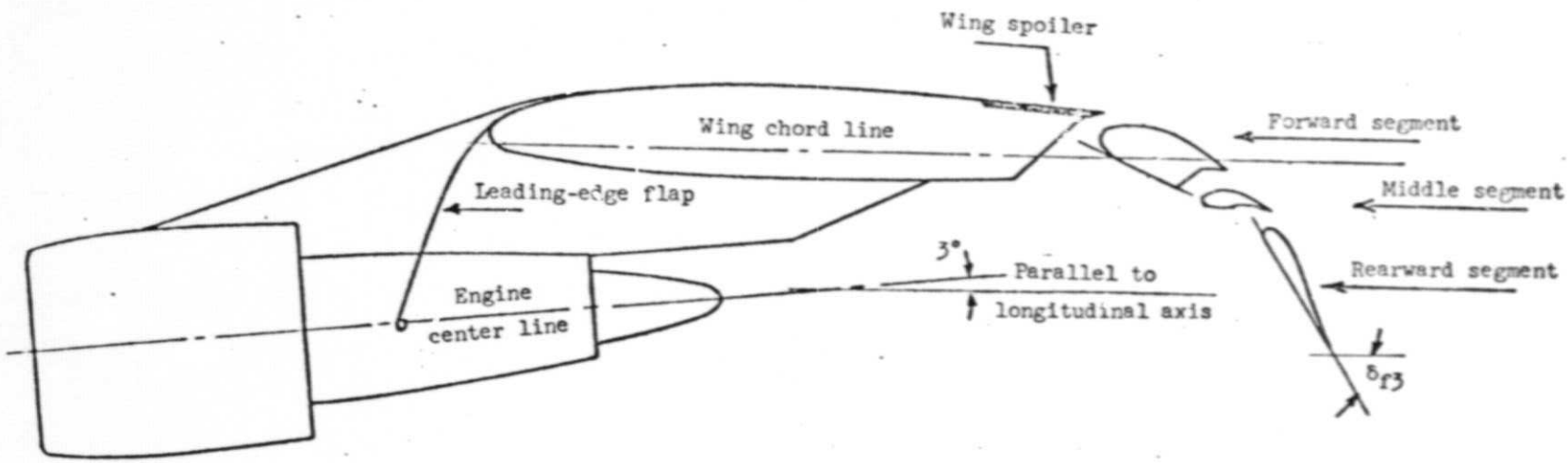

Figure 6. Flap Assembly and Engine Pylon Detail

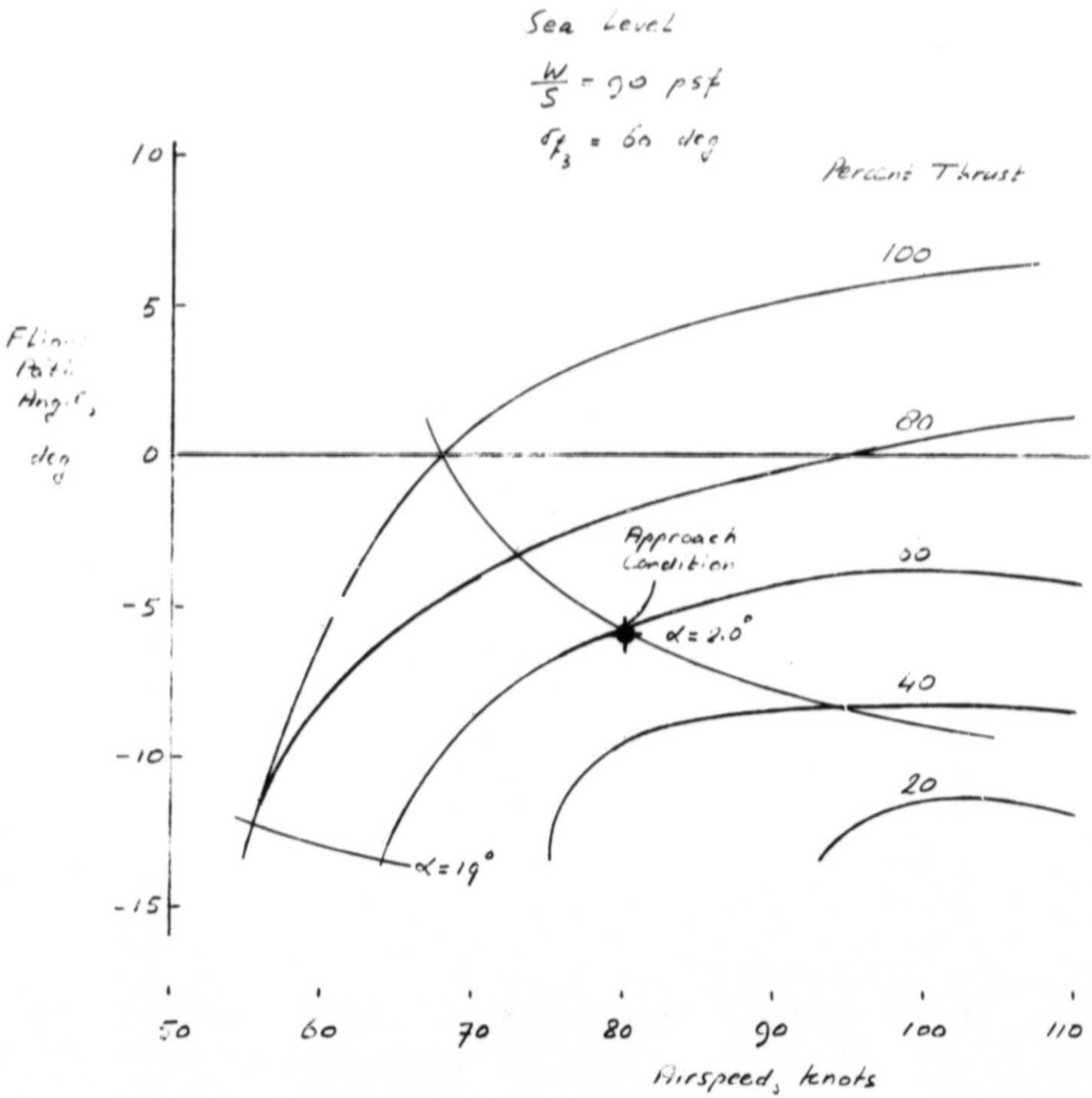

Figure 7. Performance Characteristics of Approach Configuration - ALL Engines Operating

OUTBOARD ENGINE FAILED

Trimmed in roll with ailerons, spoilers and outboard flaps ($\Delta\delta_{f_a}$) as noted

Sea Level $\quad W/S = 90$ psf $\quad \delta_{f_3} = 60$ deg

	Thrust (%)	Δi_{t_3} (deg)	$\Delta\delta_{f_a}$ (deg)
1.	60	0	20
2.	100	0	20
3.	100	-25	20
4.	60	0	0
5.	100	0	0

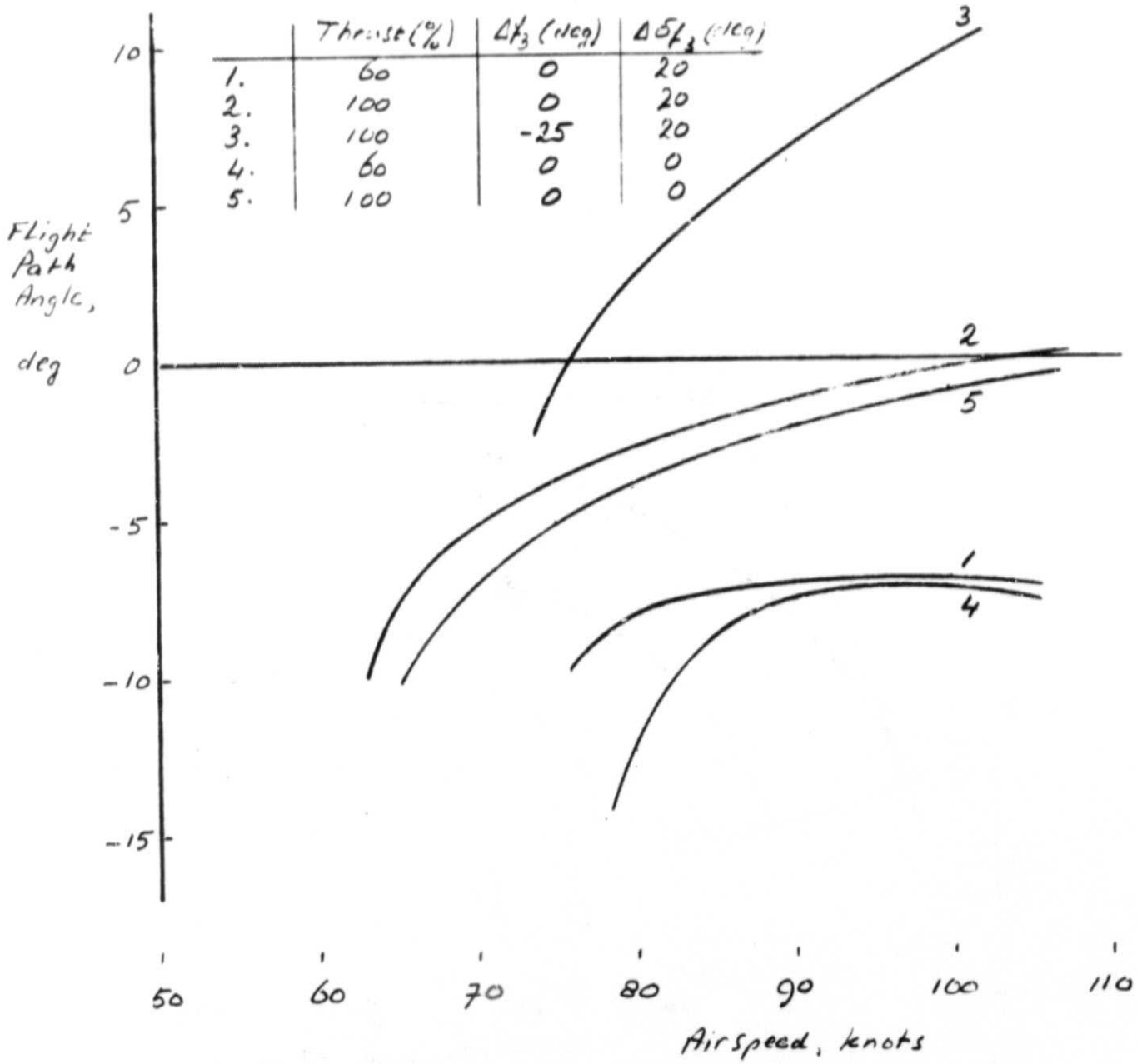

Figure 8. Performance Characteristics of Approach Configuration - Outboard Engine Failed

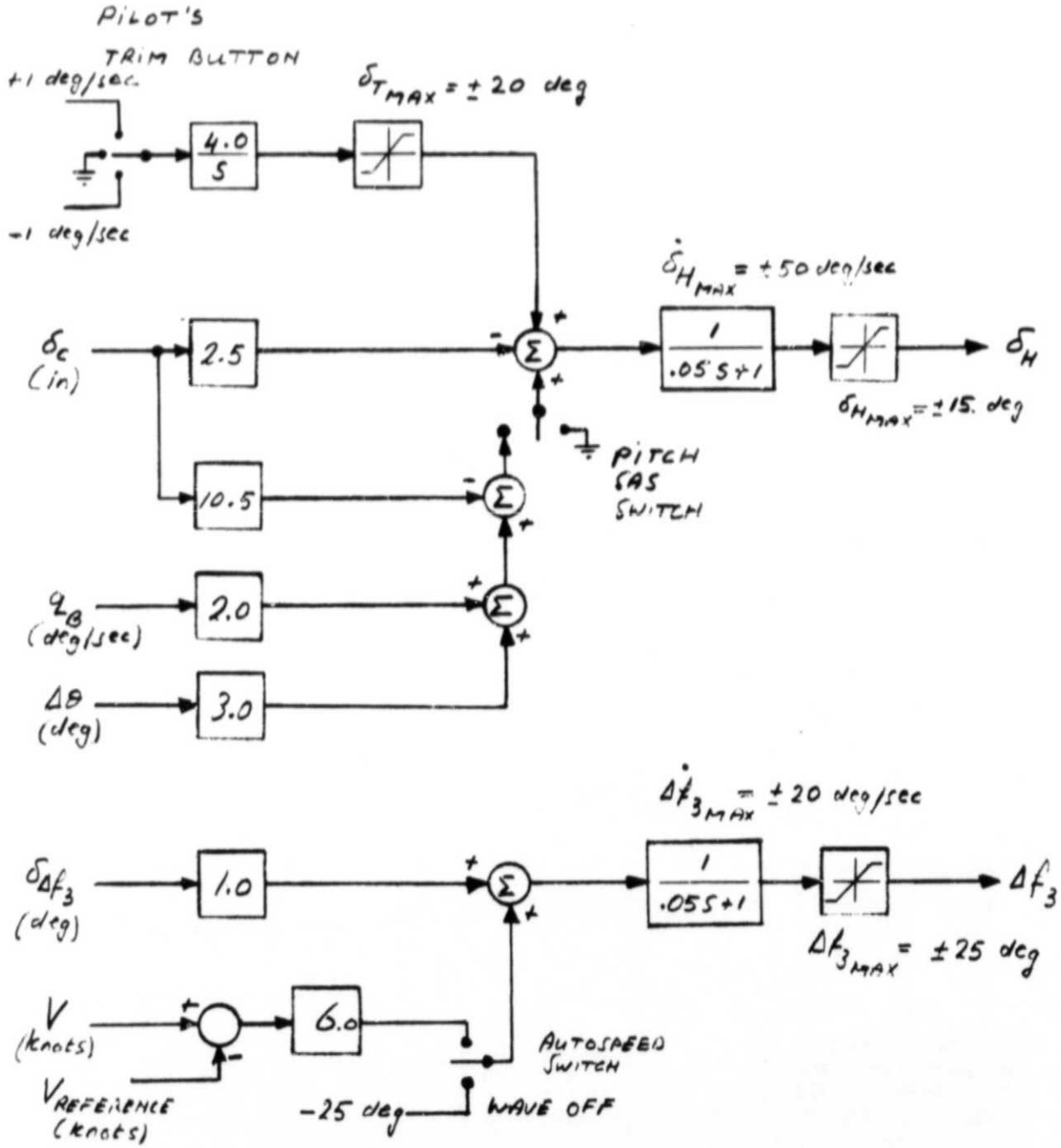

Figure 9. Longitudinal Stability and Command Augmentation System

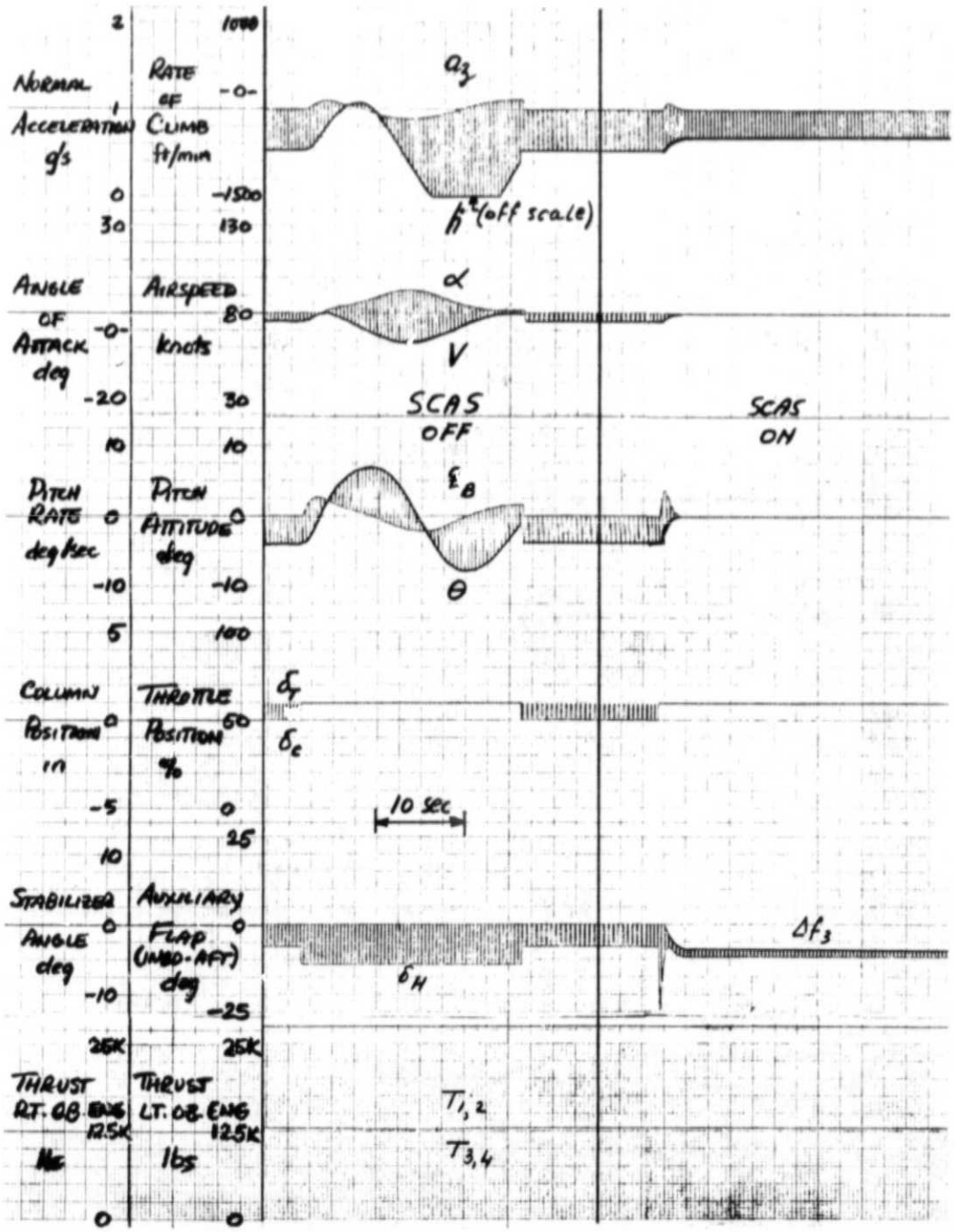

Figure 10. Longitudinal Response to a Step Column Input - SCAS Off and On

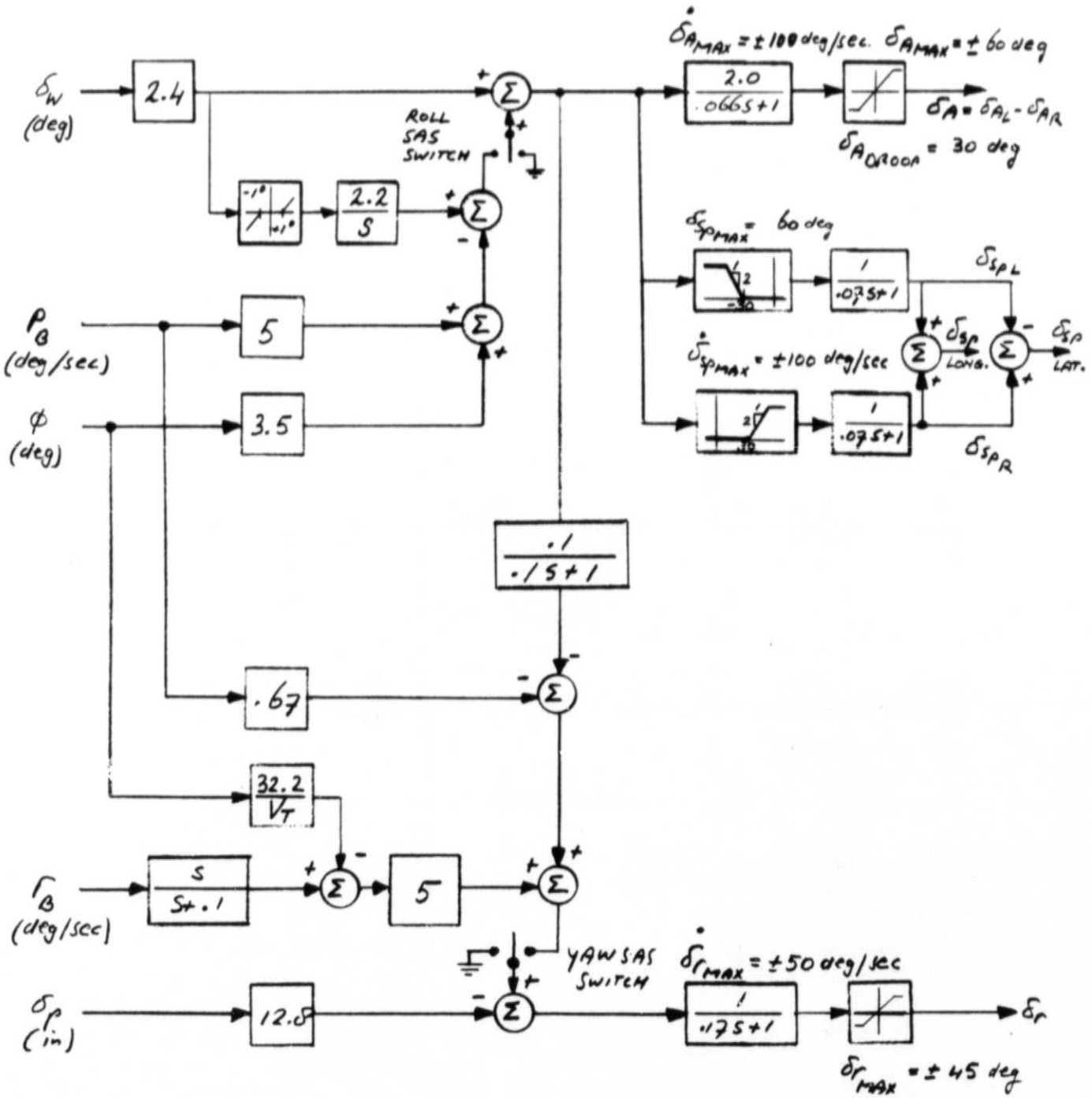

Figure 11. Lateral-Directional Stability and Command Augmentation System

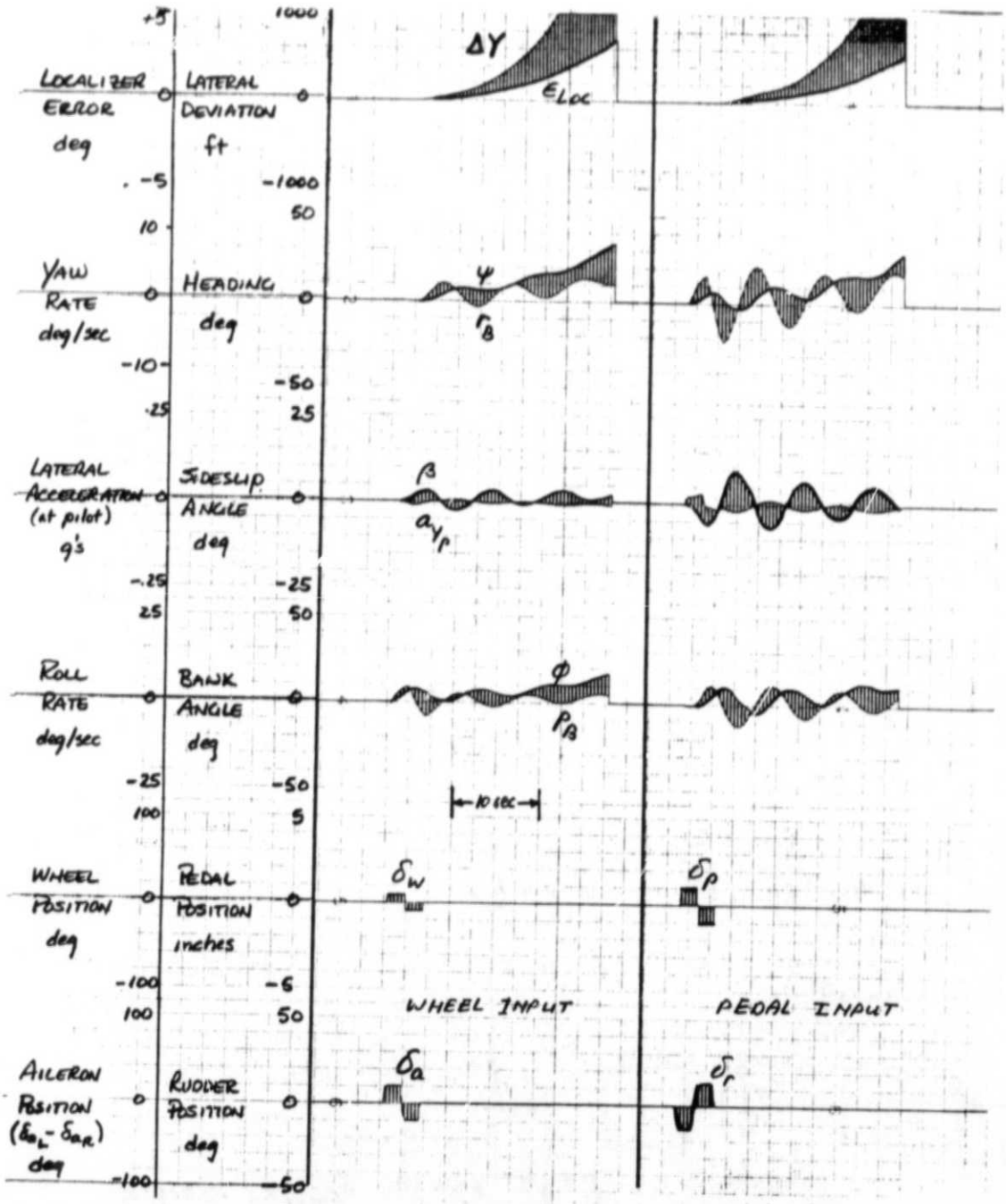

Figure 12. Lateral-Directional Response to Wheel and Pedal Doublet Inputs - SCAS Off

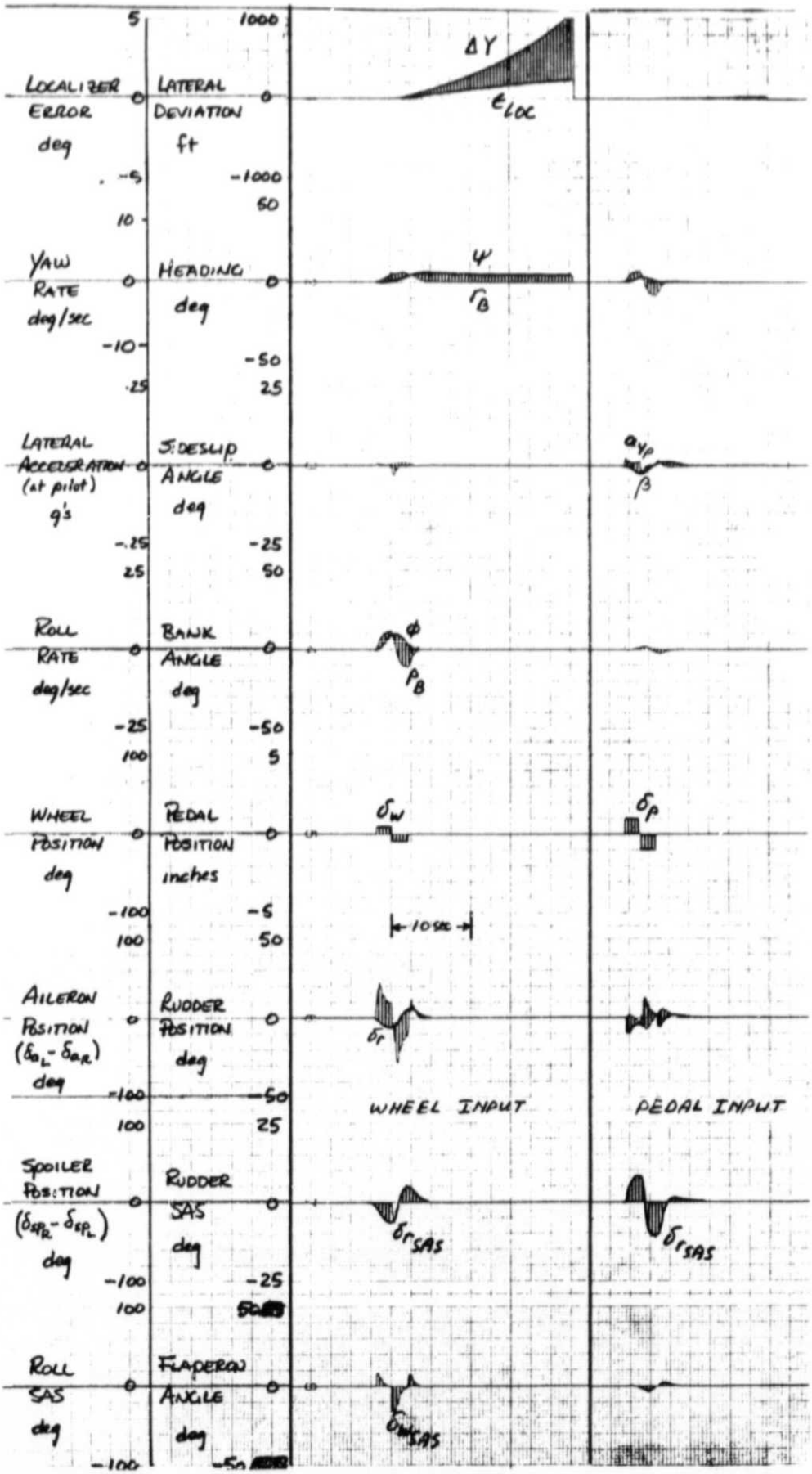

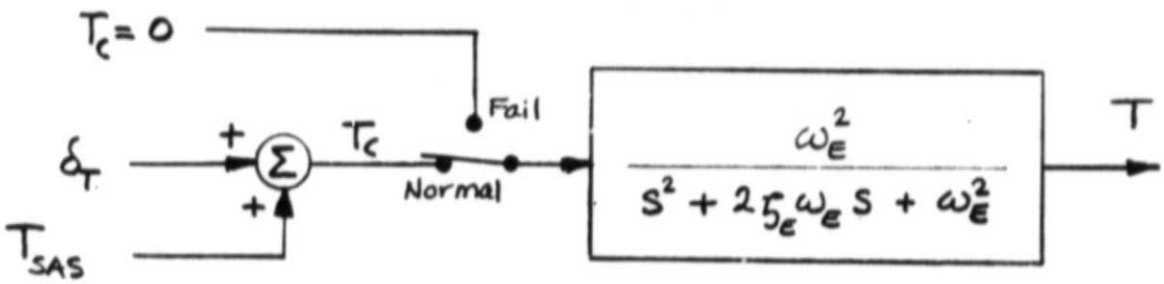

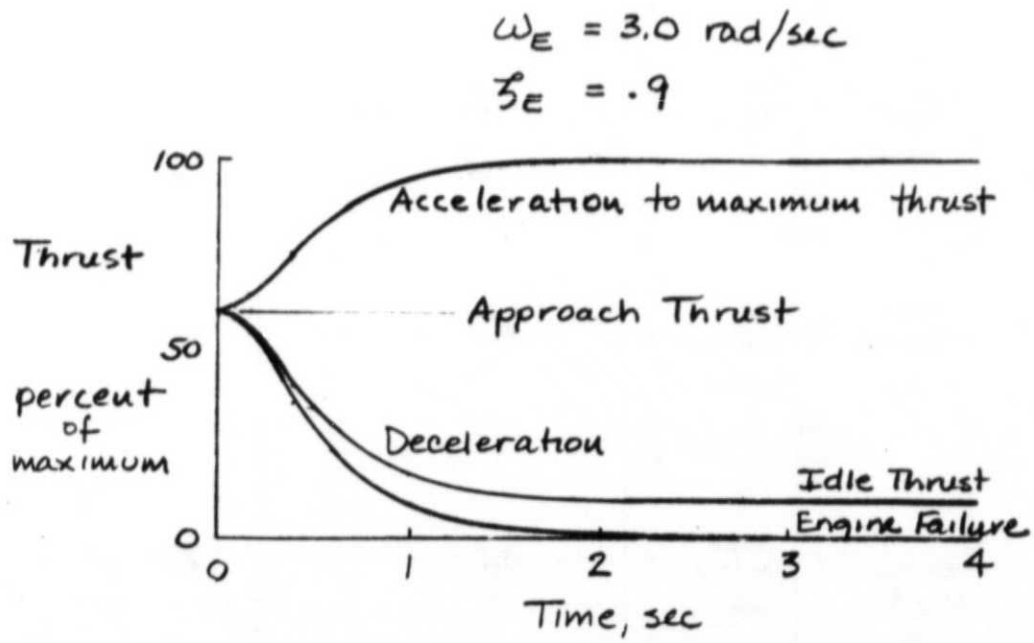

Figure 14. Engine Model and Thrust Transient Response Characteristics

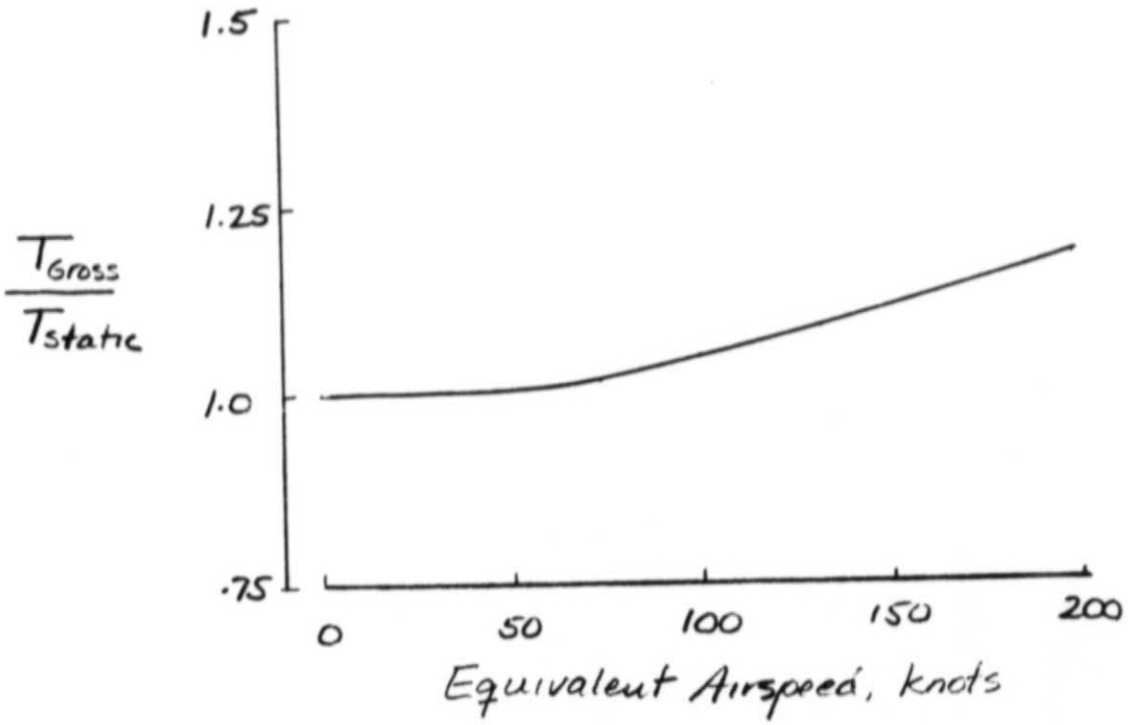

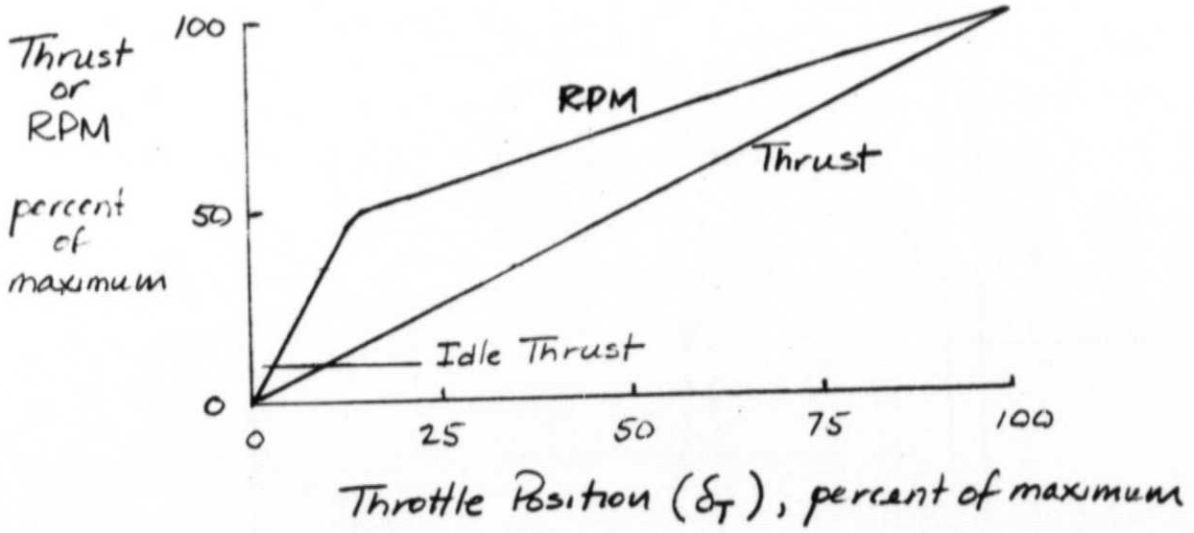

Figure 15. Engine Thrust and RPM Relationships

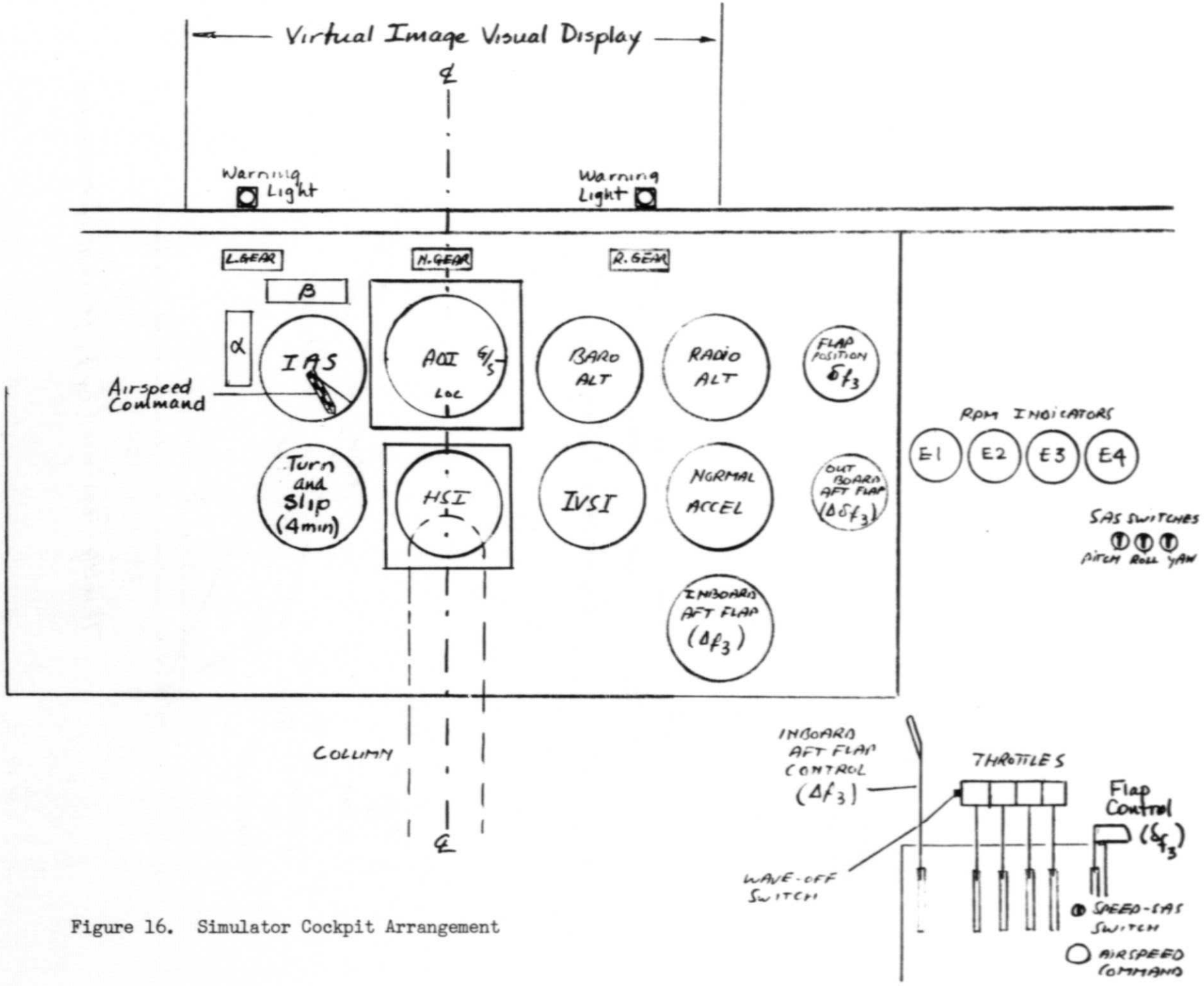

Figure 16. Simulator Cockpit Arrangement

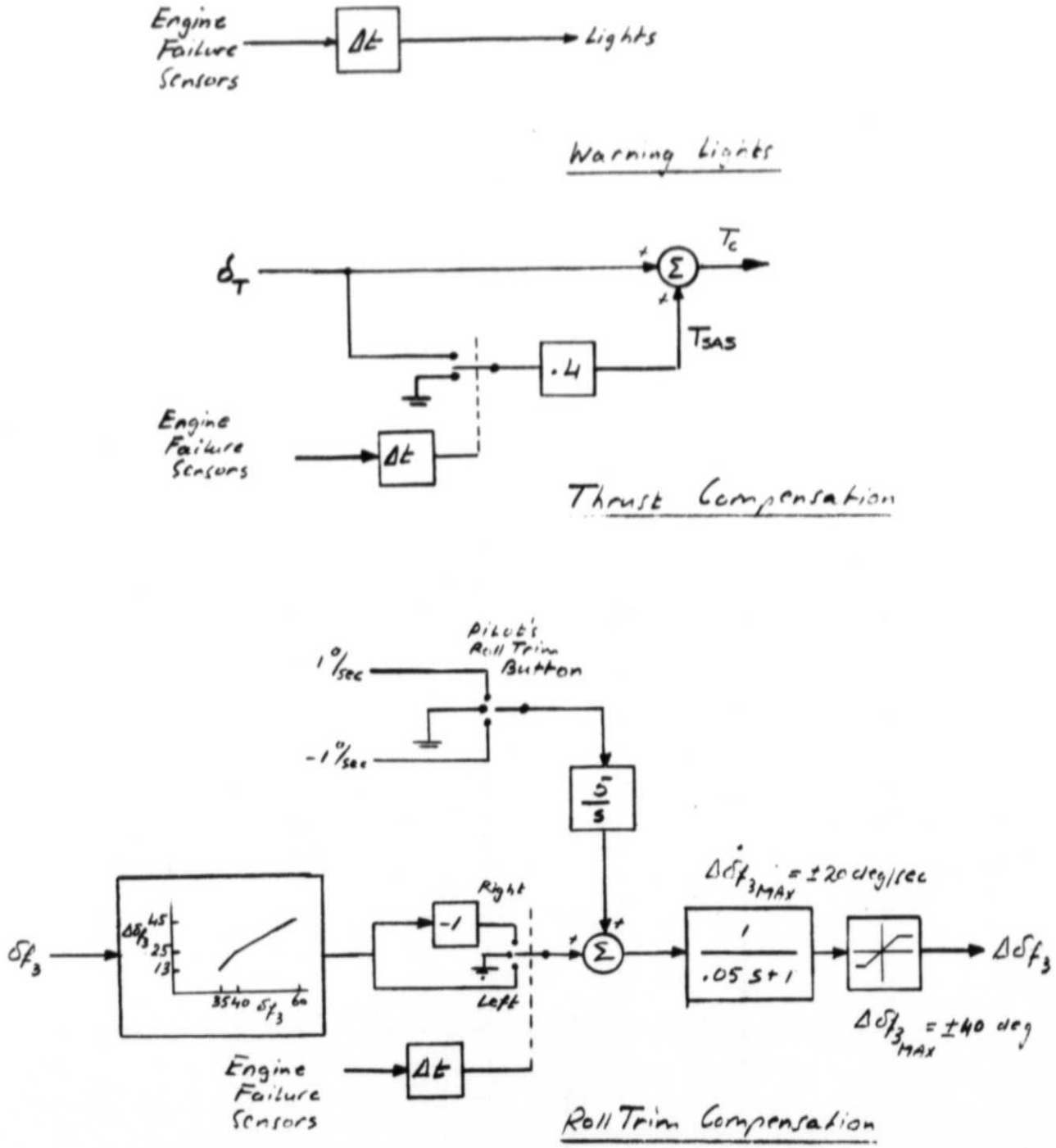

Figure 17. Failure Warning Light and Programmed Thrust and Roll Trim Compensation Systems

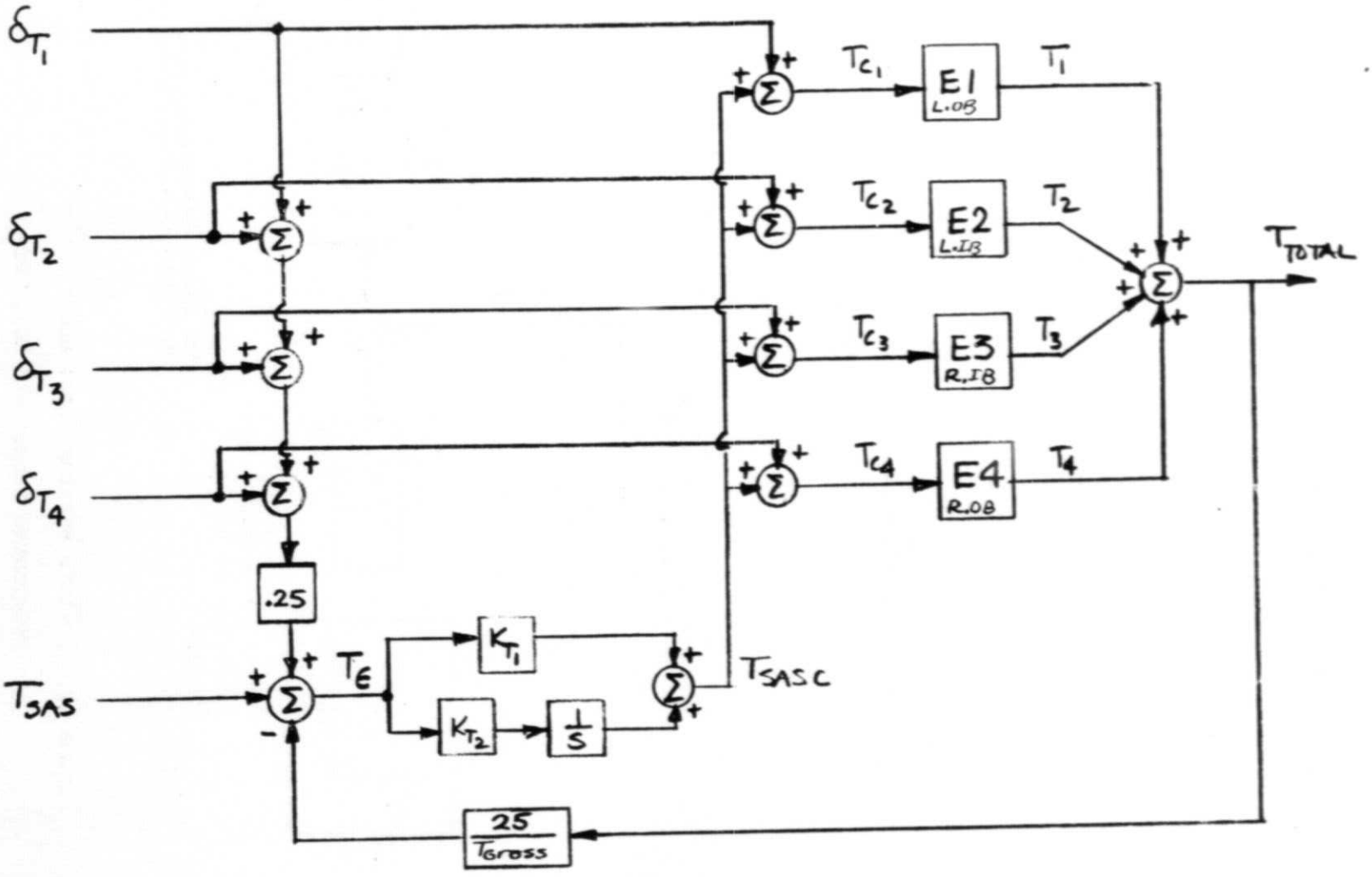

Figure 18. Thrust Command Control System

$$\frac{T}{T_\epsilon} = K_{T_2}\left(\frac{T_E s + 1}{s}\right)\left(\frac{\omega_E^2}{s^2 + 2\zeta_E\omega_E s + \omega_E^2}\right)$$

$T_E = \frac{K_{T_1}}{K_{T_2}} = .36$

$\omega_E = 3.0$ rad/sec

$\zeta_E = .9$

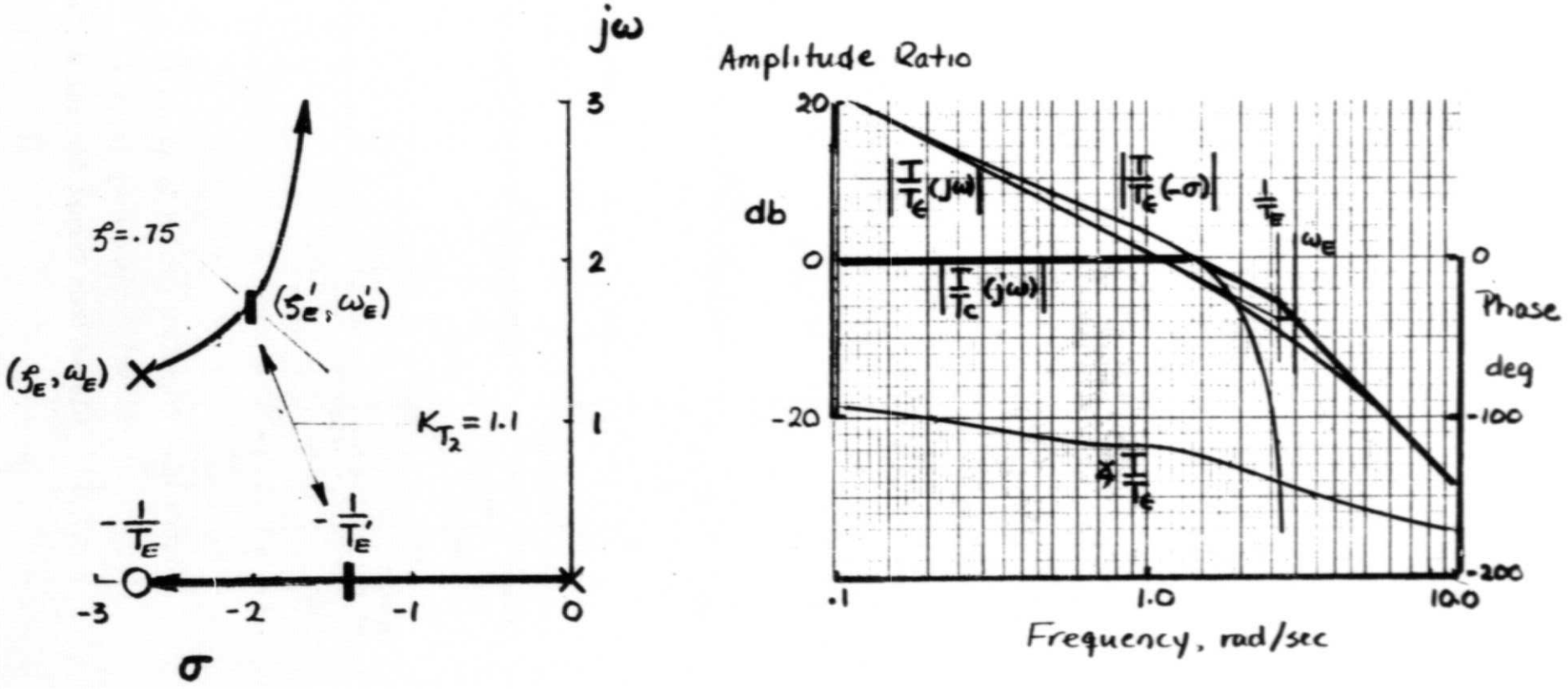

Figure 19. Root Locus and Bode Plots of Closed-Loop Thrust Control

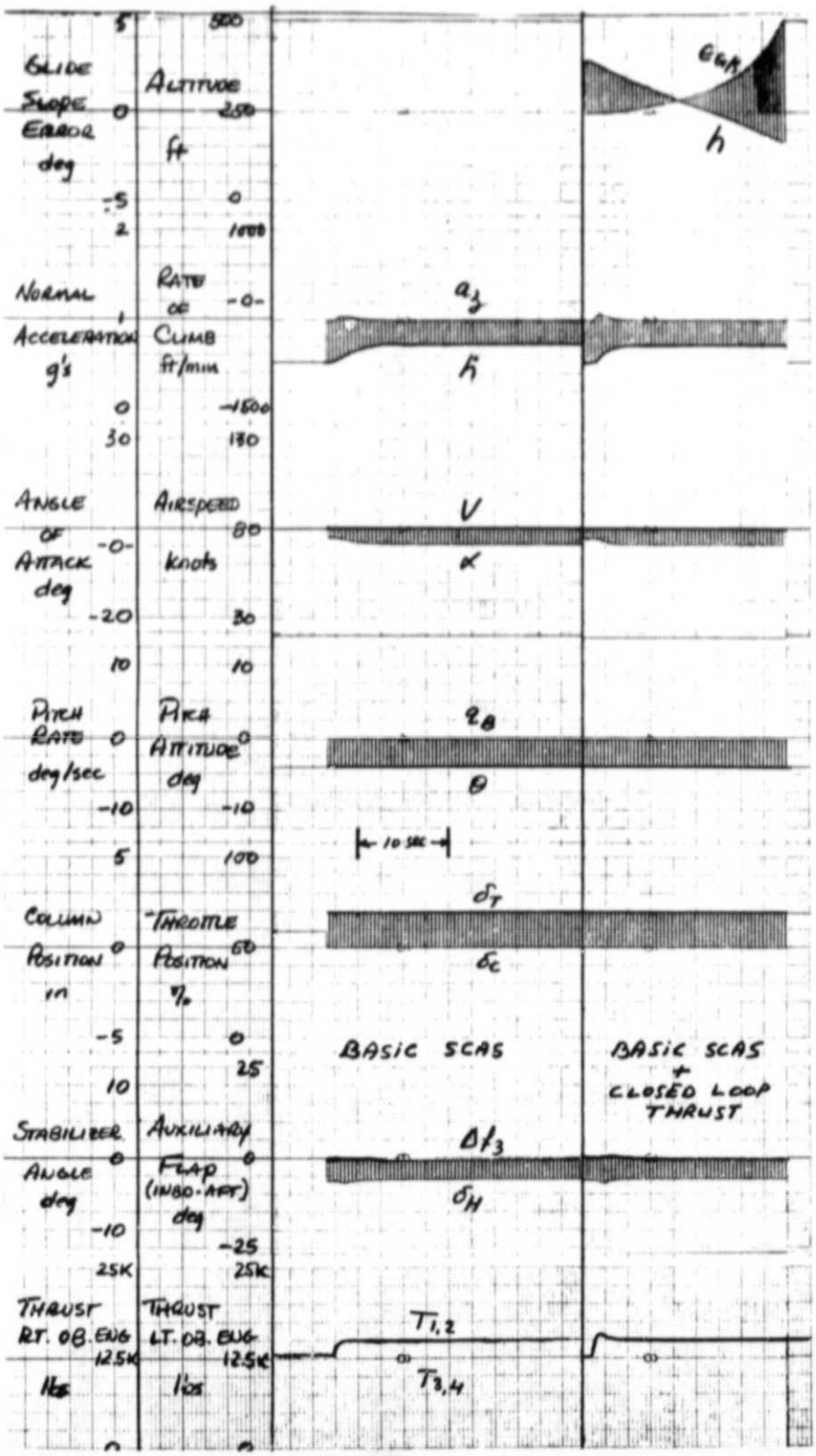

Figure 20. Transient Thrust Response to a Thrust Command Step Input - Closed Loop Thrust Control Off and On

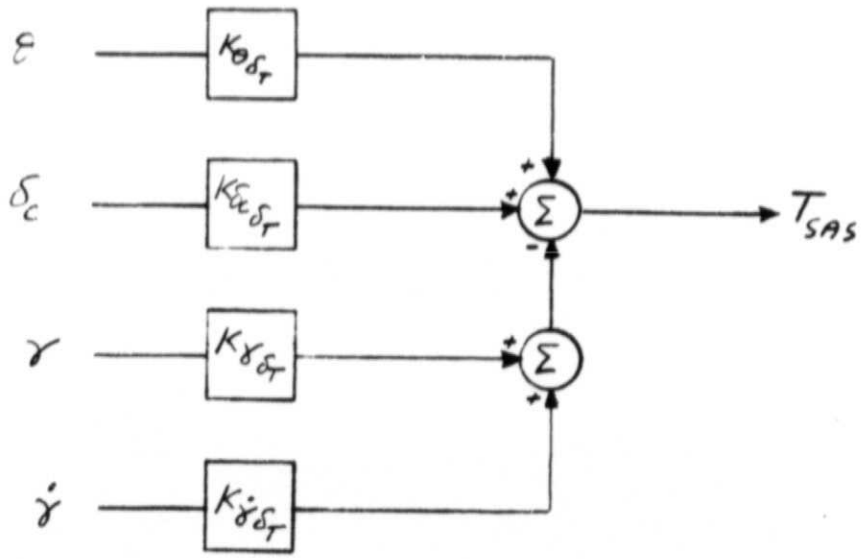

Figure 21. Flight-Path Stabilization System

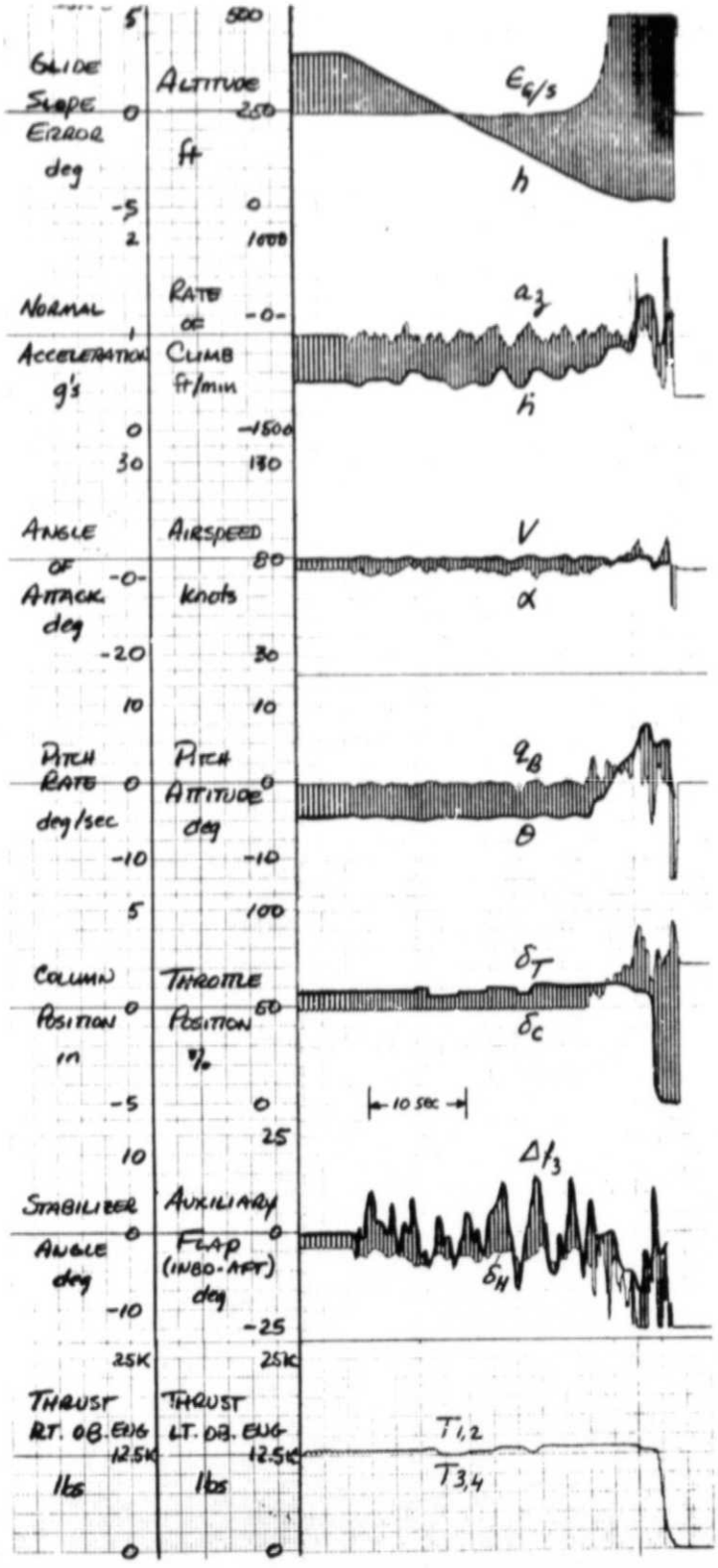

Figure 22. Time History of a Landing Flare Performed with Aircraft Rotation - All Engines Operating

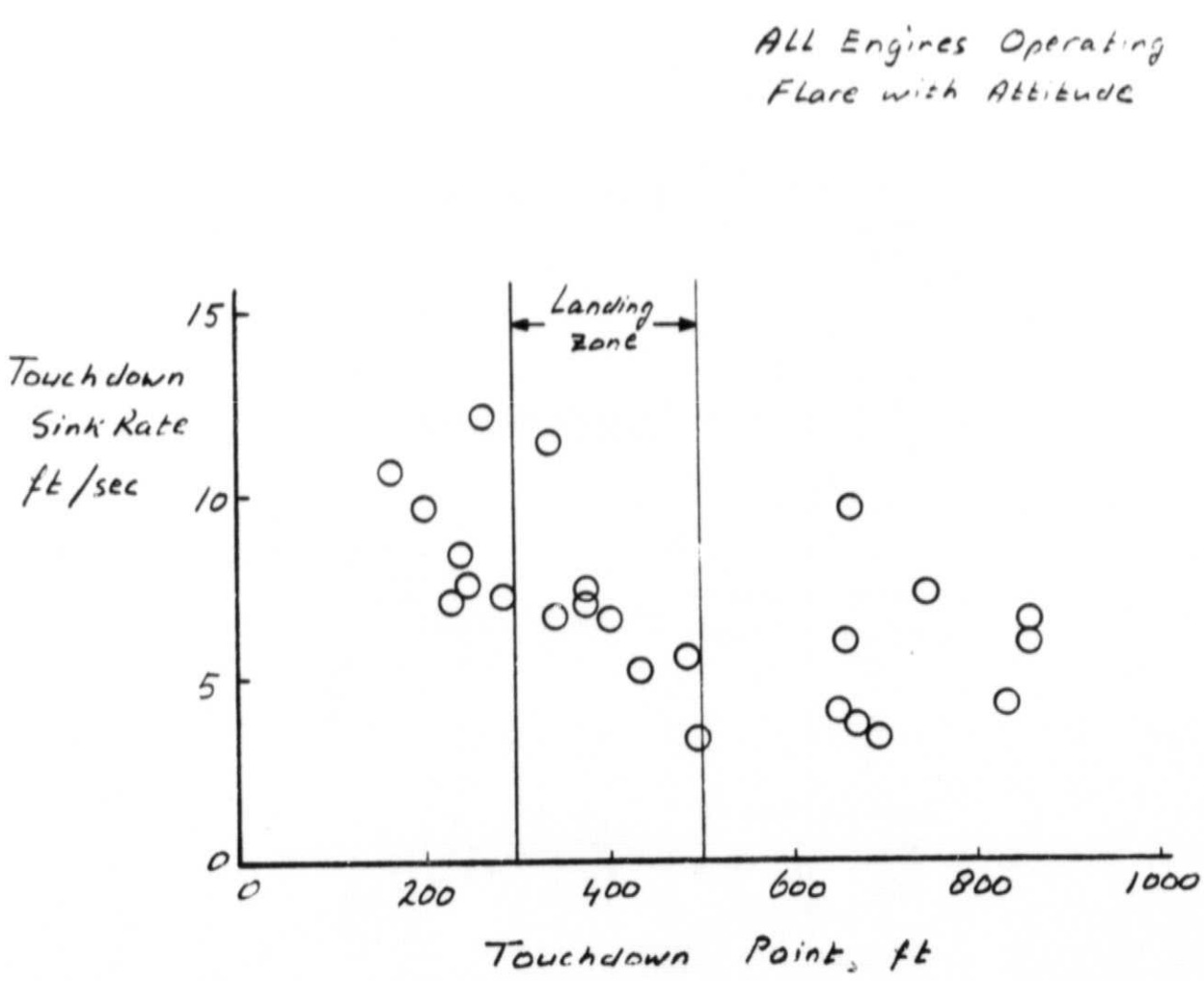

Figure 23. Landing Precision for Four Engine Operation

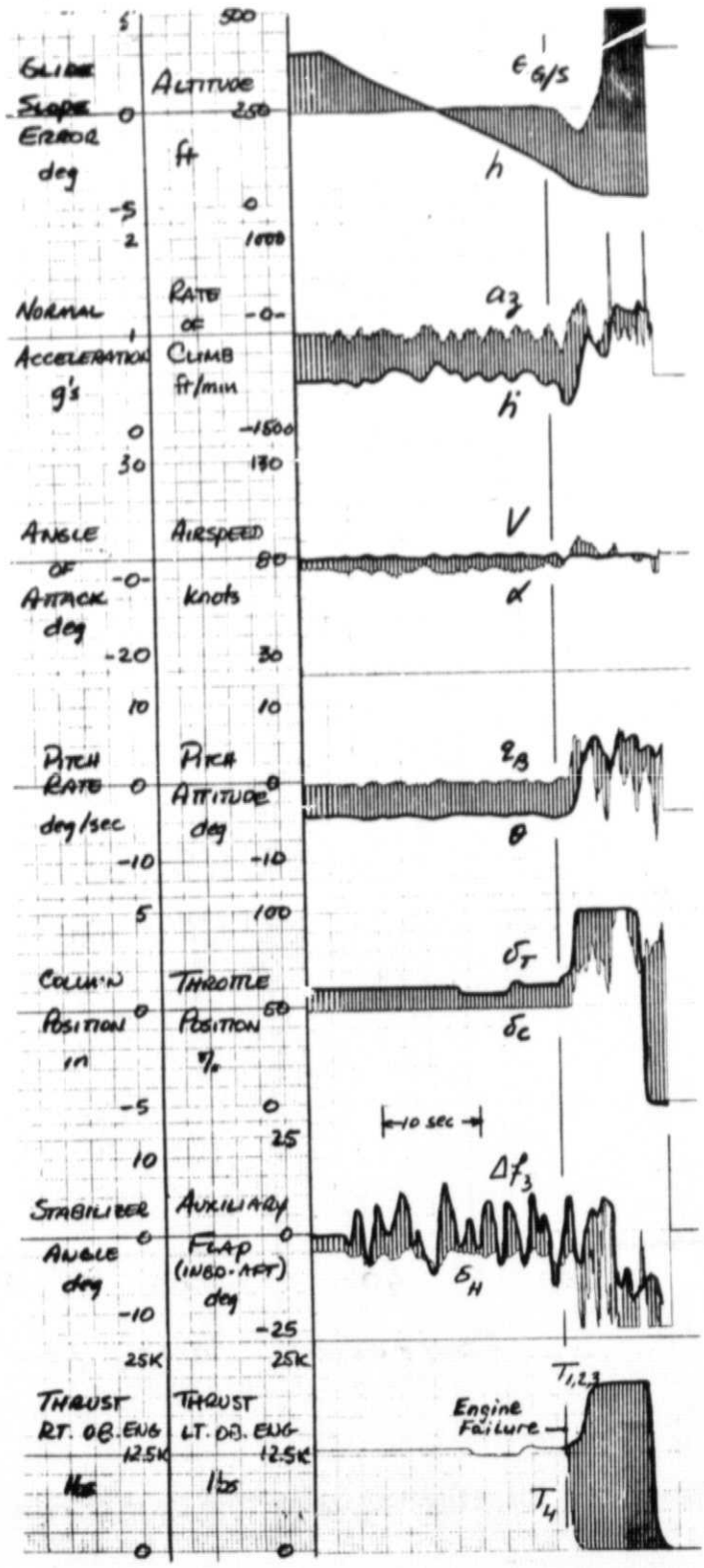

Figure 24. Time History of an Engine-Out Landing - No Compensation - Engine Failed at 86 Feet

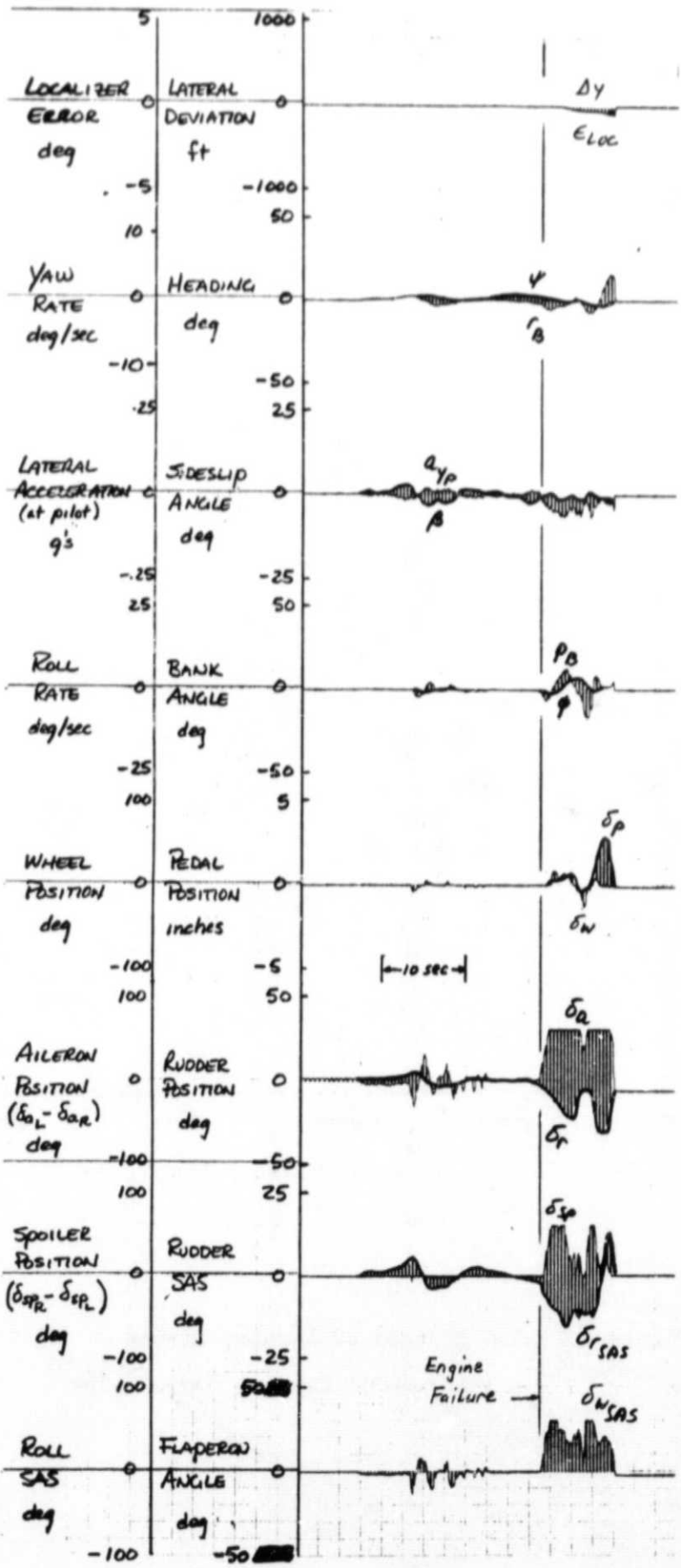

Figure 24 (concluded)

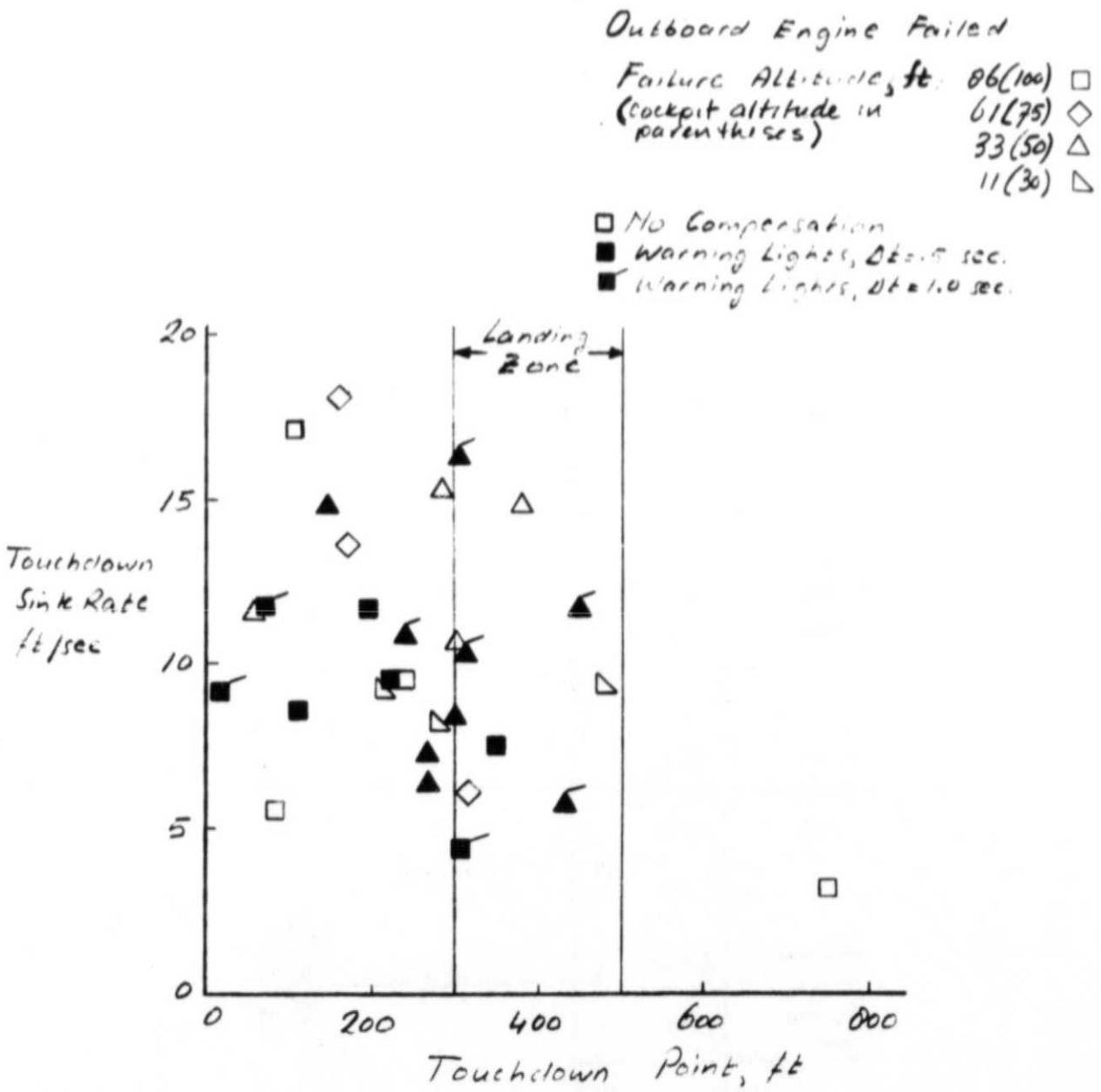

Figure 25. The Effects of Warning Lights on Engine-Out Landing Performance

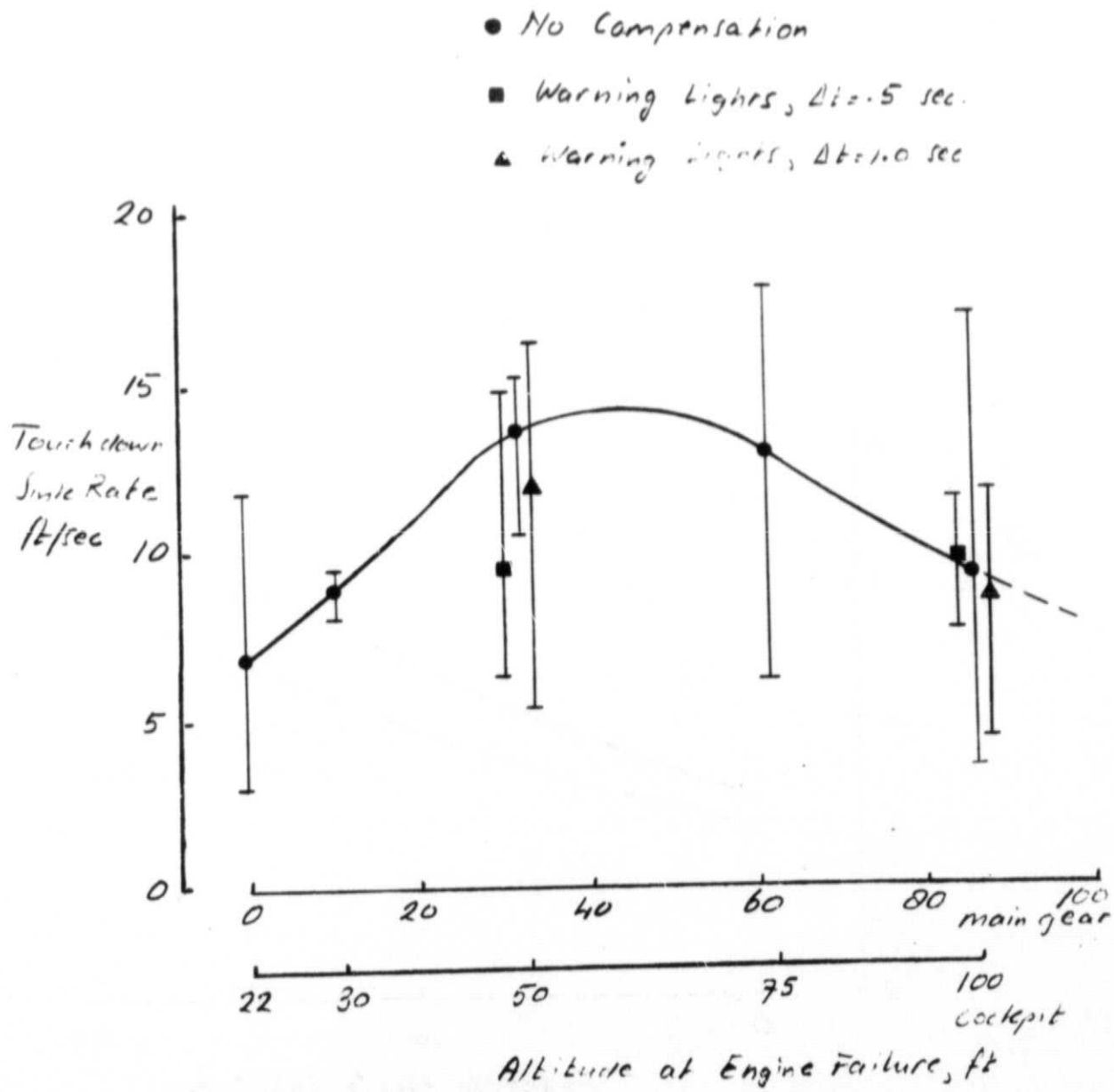

Figure 25 (concluded)

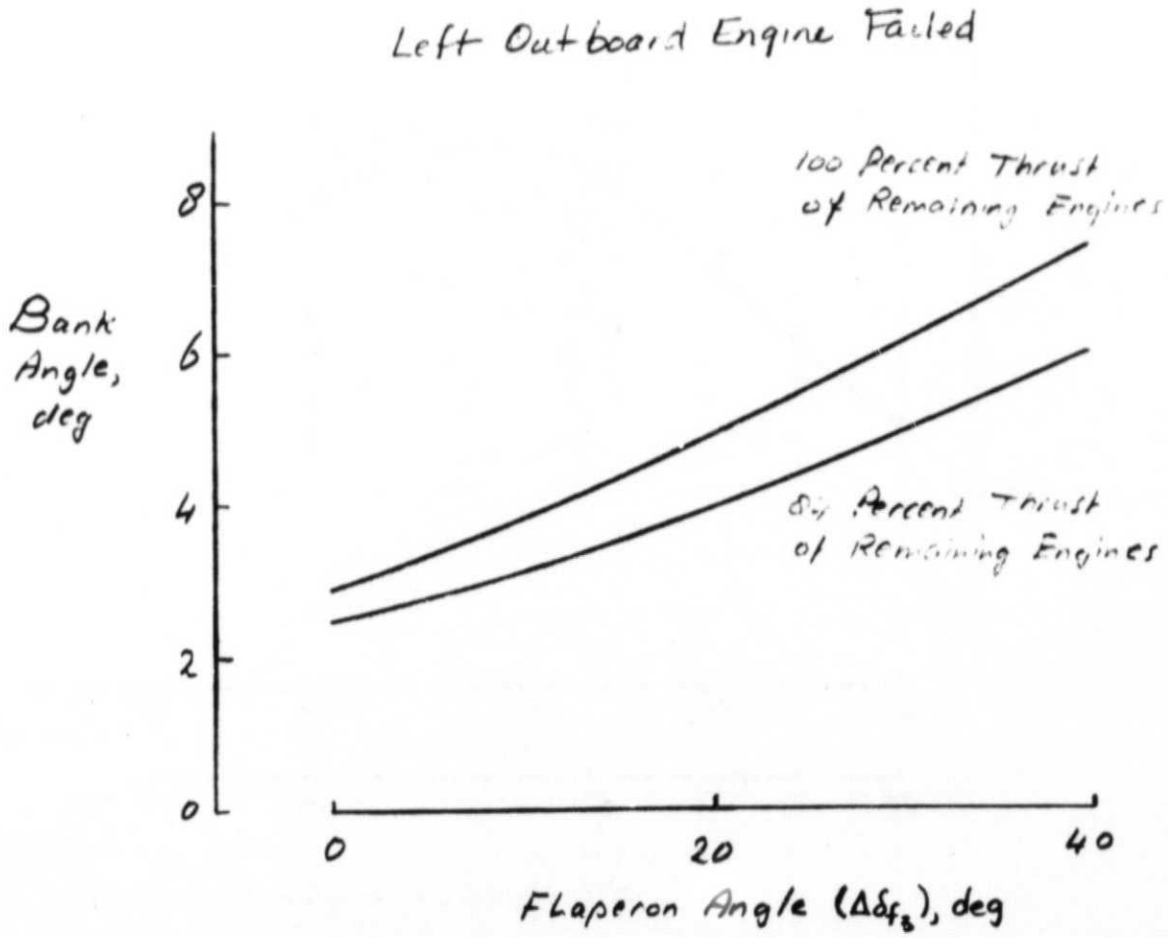

Figure 26. Steady State Bank Angle Required to Maintain Ground Track as a Function of Flaperon Angle Applied for Engine-Out Roll Trim

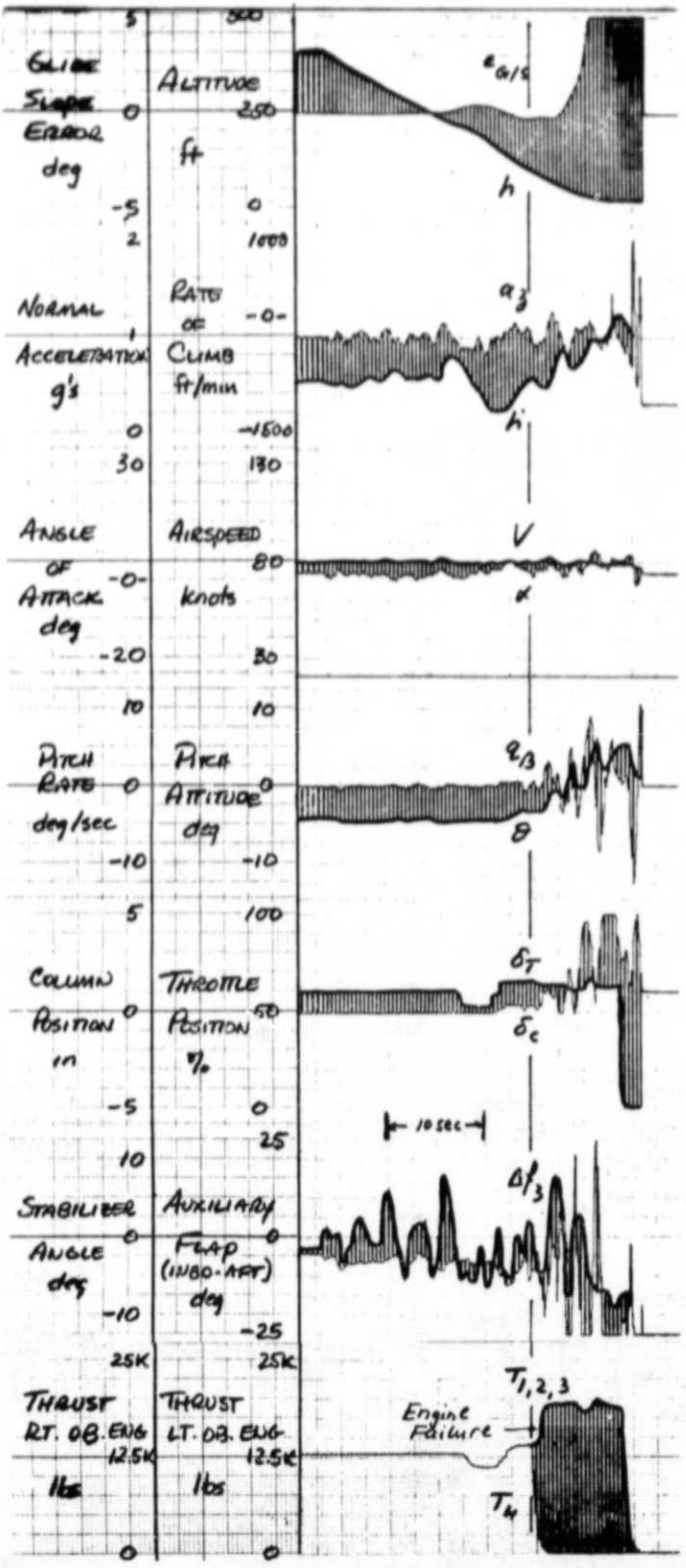

Figure 27. Time History of an Engine-Out Landing
- Programmed thrust and Roll Trim Compensation
($\Delta t = .5$ sec) - Engine Failed at 86 Feet

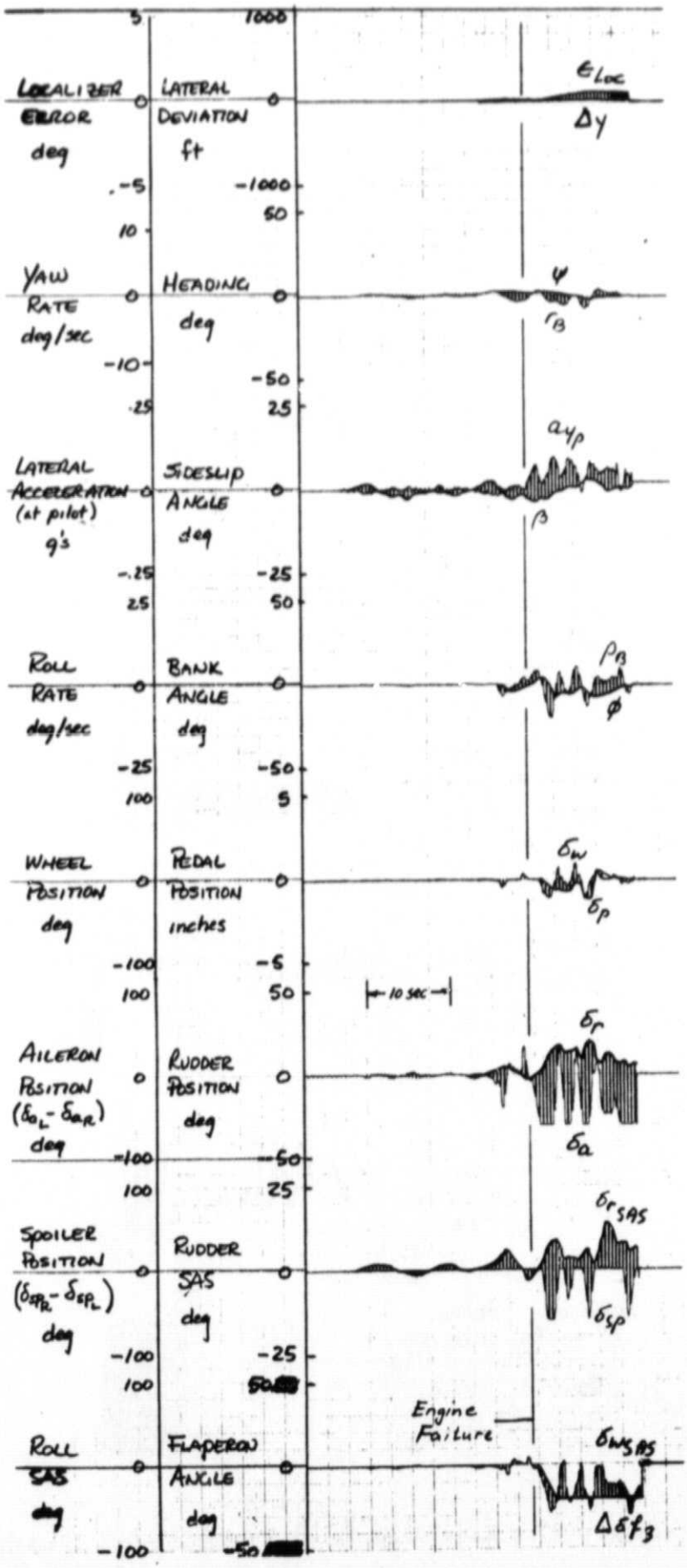

Figure 27 (concluded)

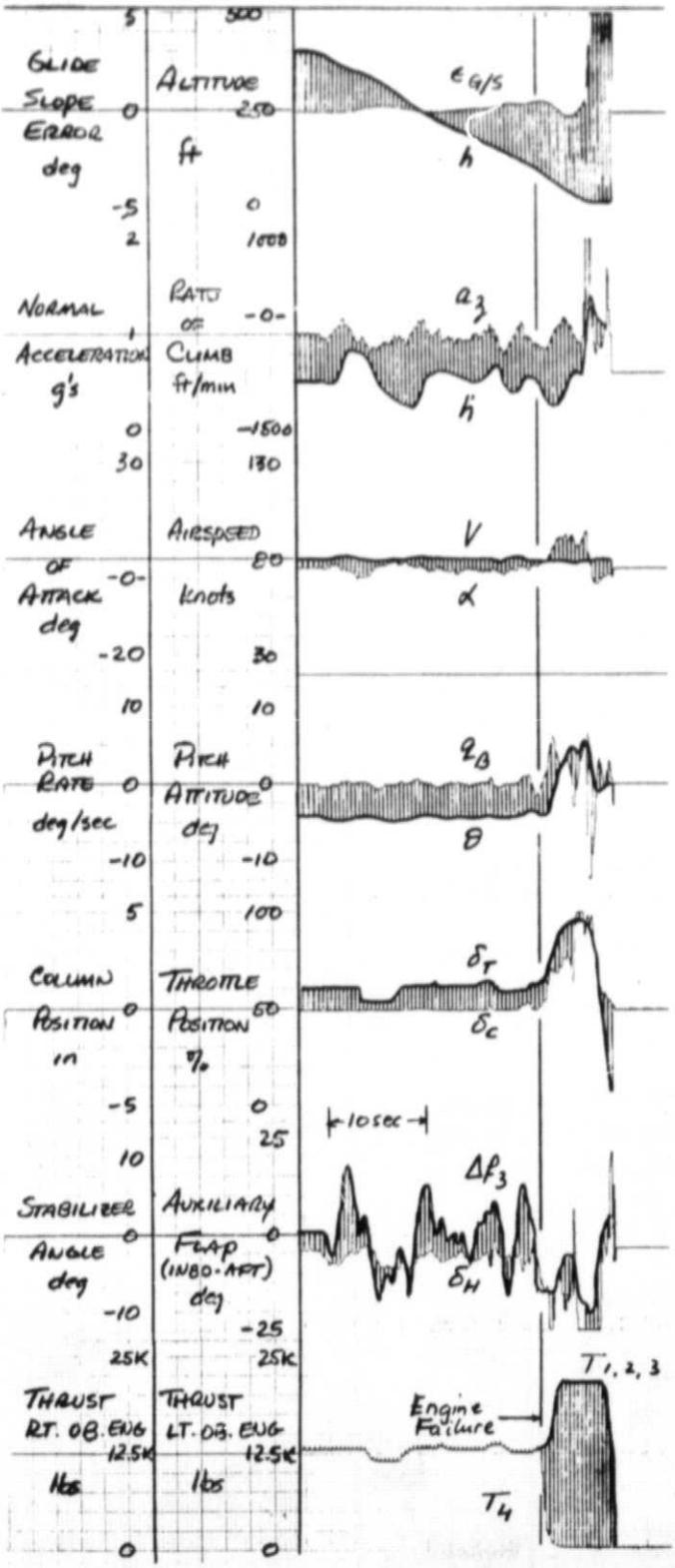

Figure 28. Time History of an Engine-Out Landing - Programmed Thrust and Roll Trim Compensation ($\Delta t = 1.0$ sec.) - Engine Failed at 86 Feet

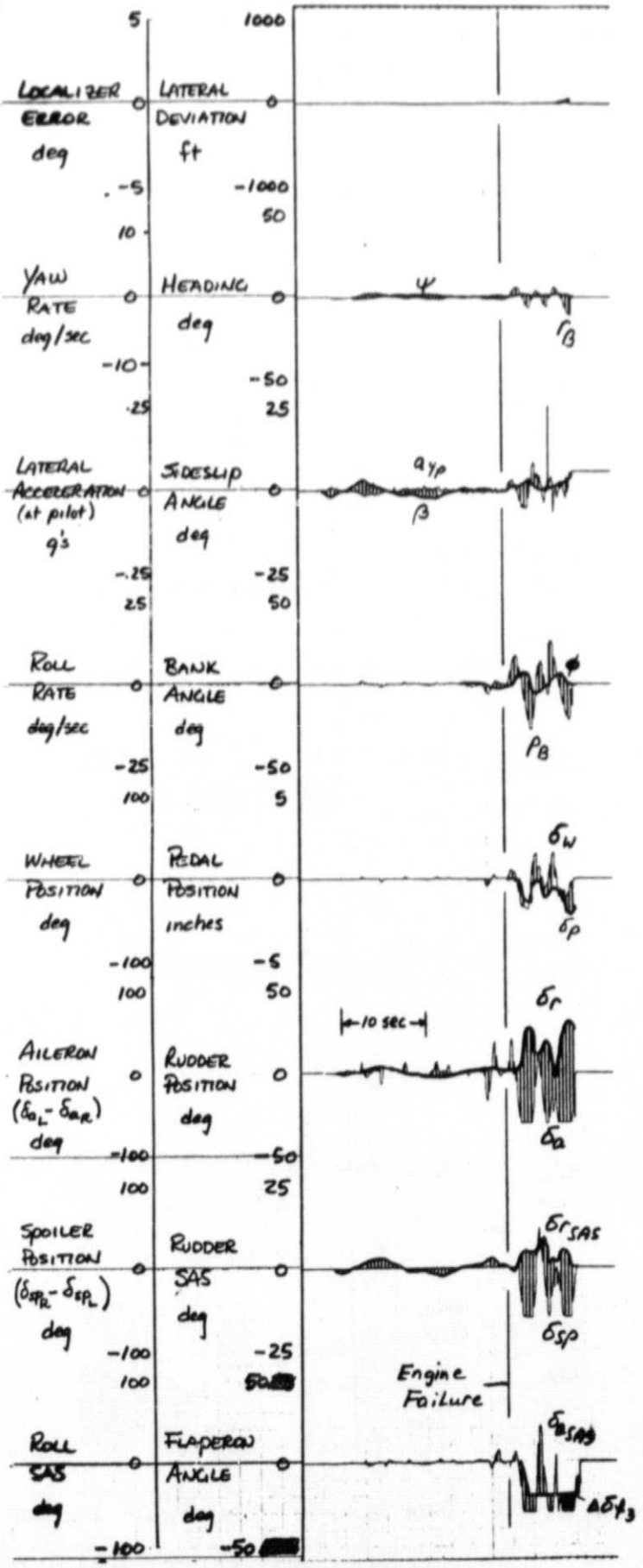

Figure 28 (concluded)

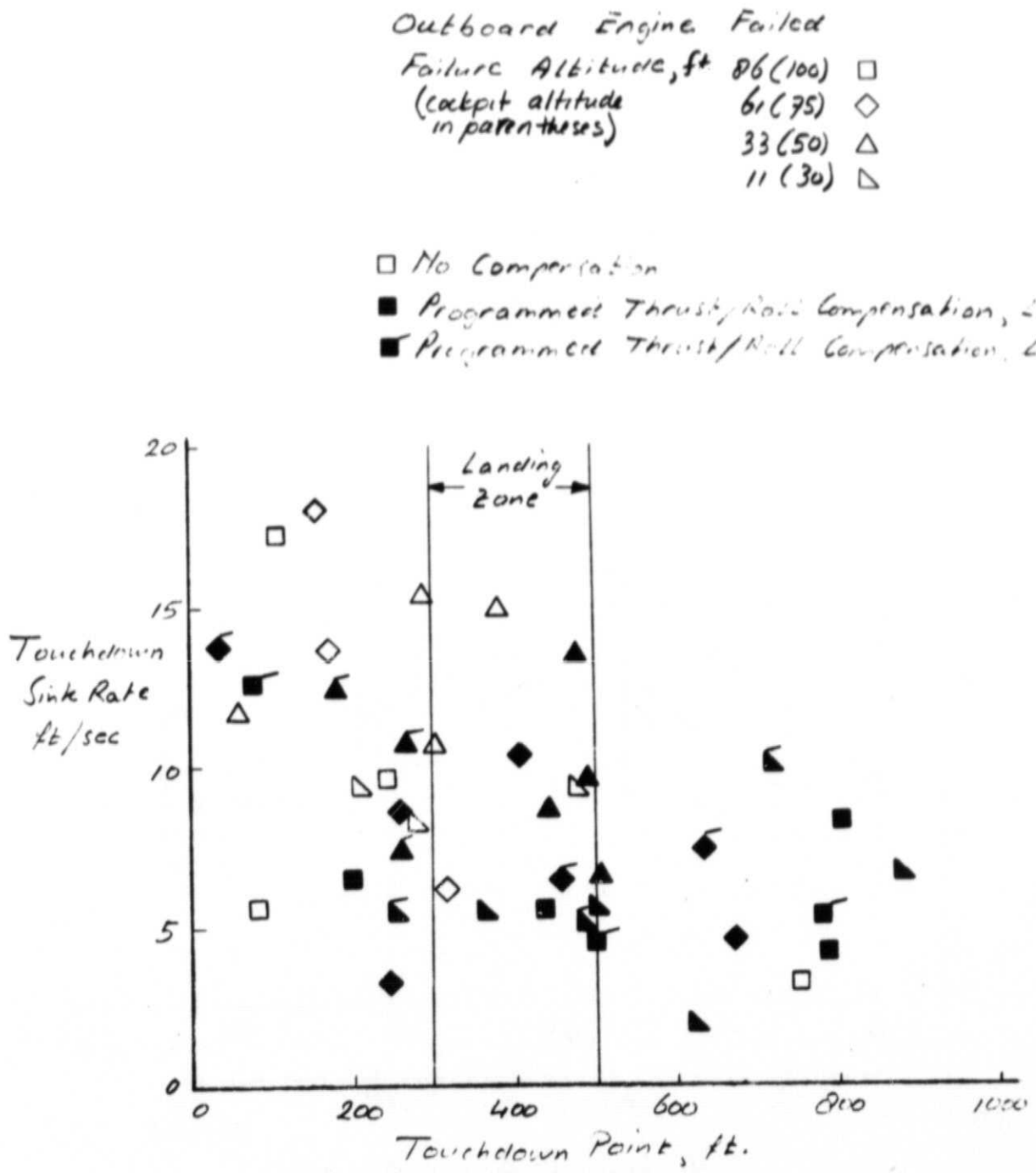

Figure 29. The Effect of Programmed Thrust and Roll Trim Compensation on Engine-Out Landing Performance

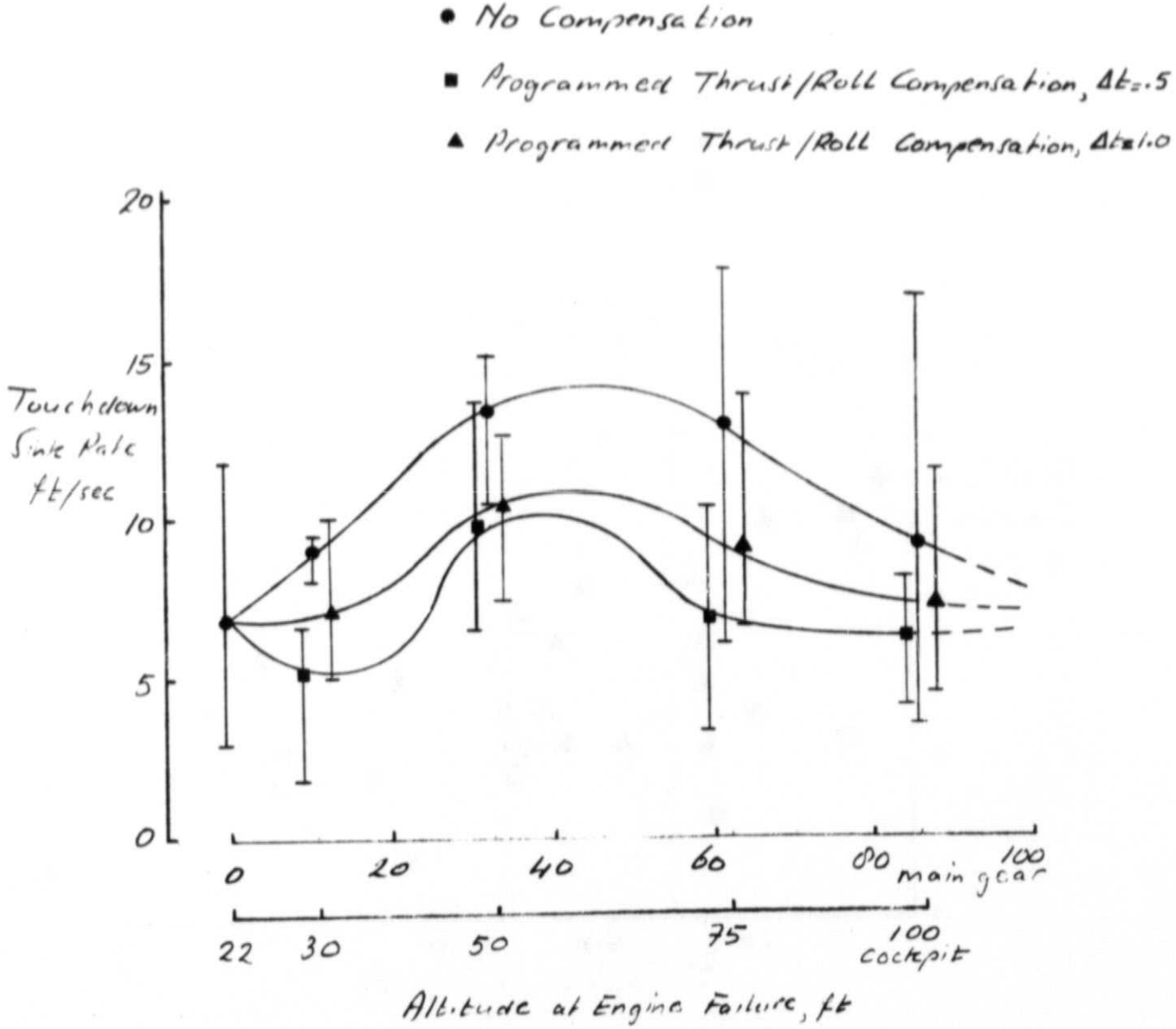

Figure 29 (concluded)

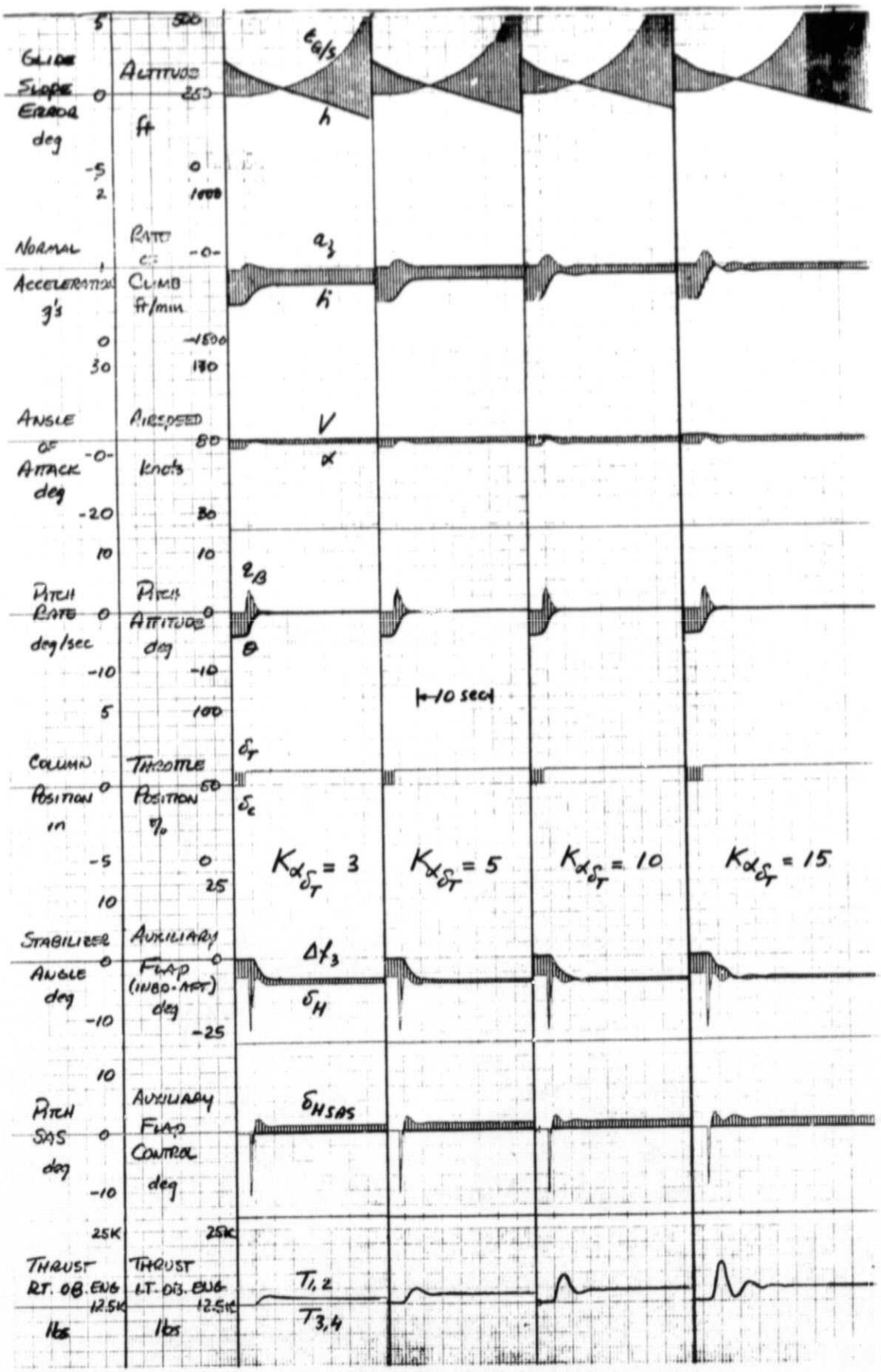

Figure 30. Longitudinal Response to a Step Column Input for Several Flight-Path Stabilization Feedback Gains

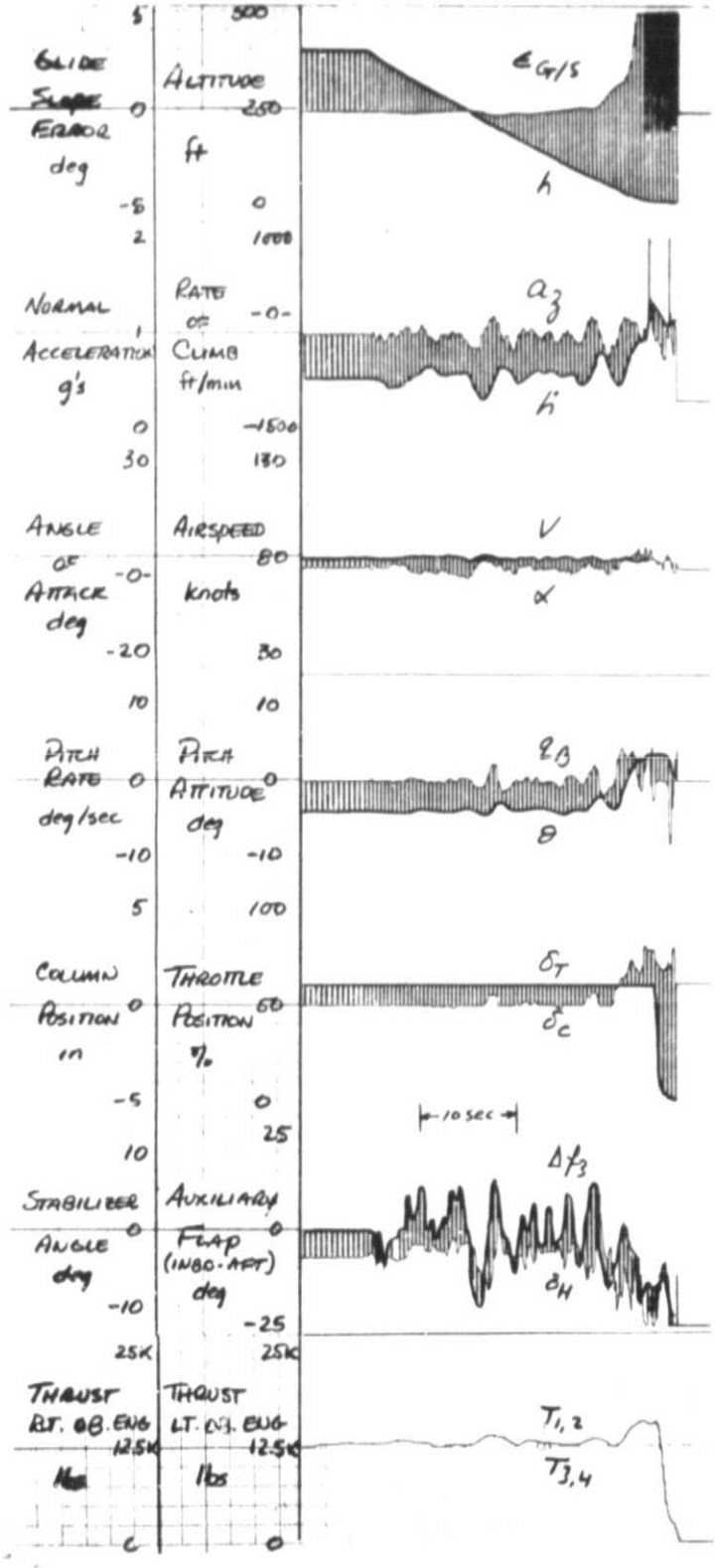

Figure 31. Time History of a Landing with Flight Path Statilization $K_{\alpha\delta_T} = 3$ percent per degree -All Engines Operating

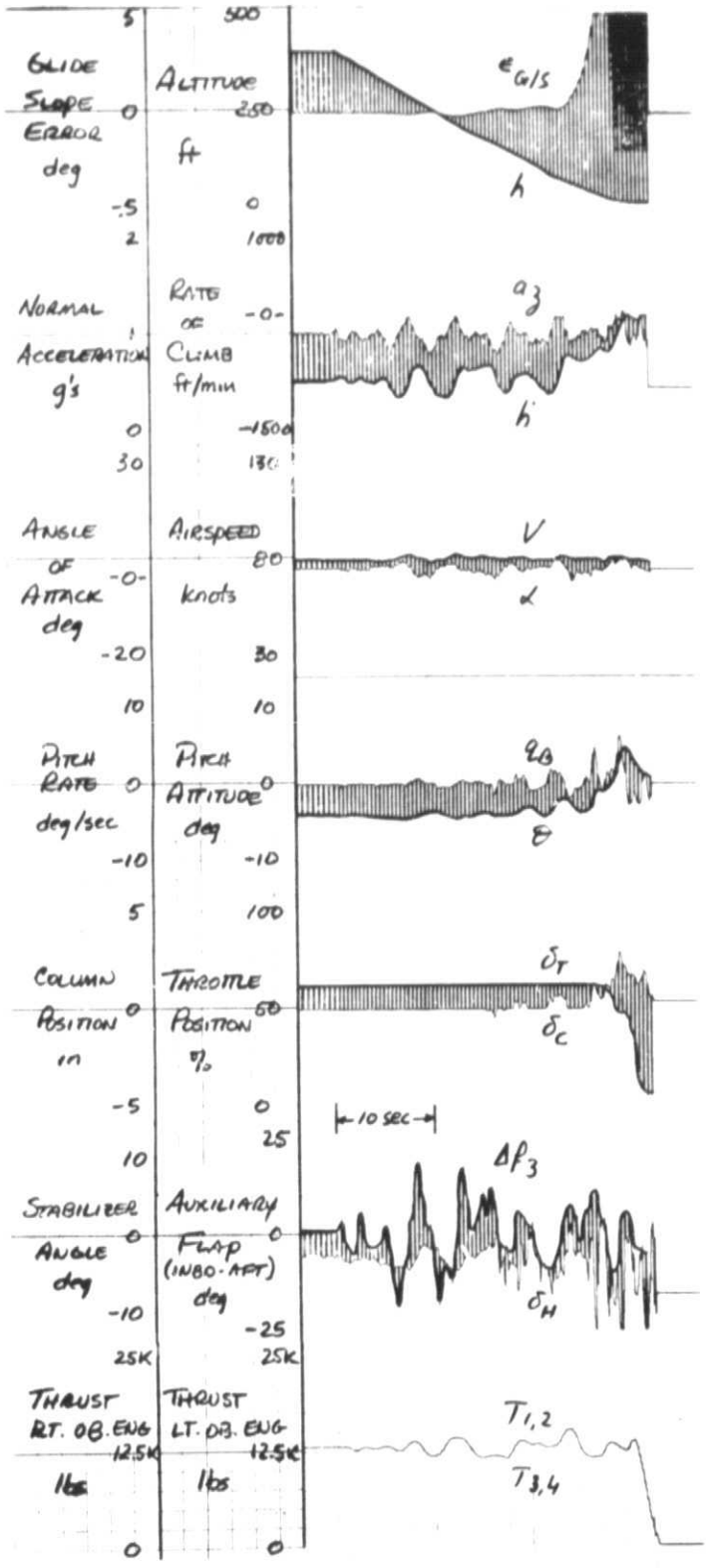

Figure 32. Time History of a Landing with Flight Path Stabilization $K_{\alpha_{\delta_T}} = 5$ percent per degree - All Engines Operating

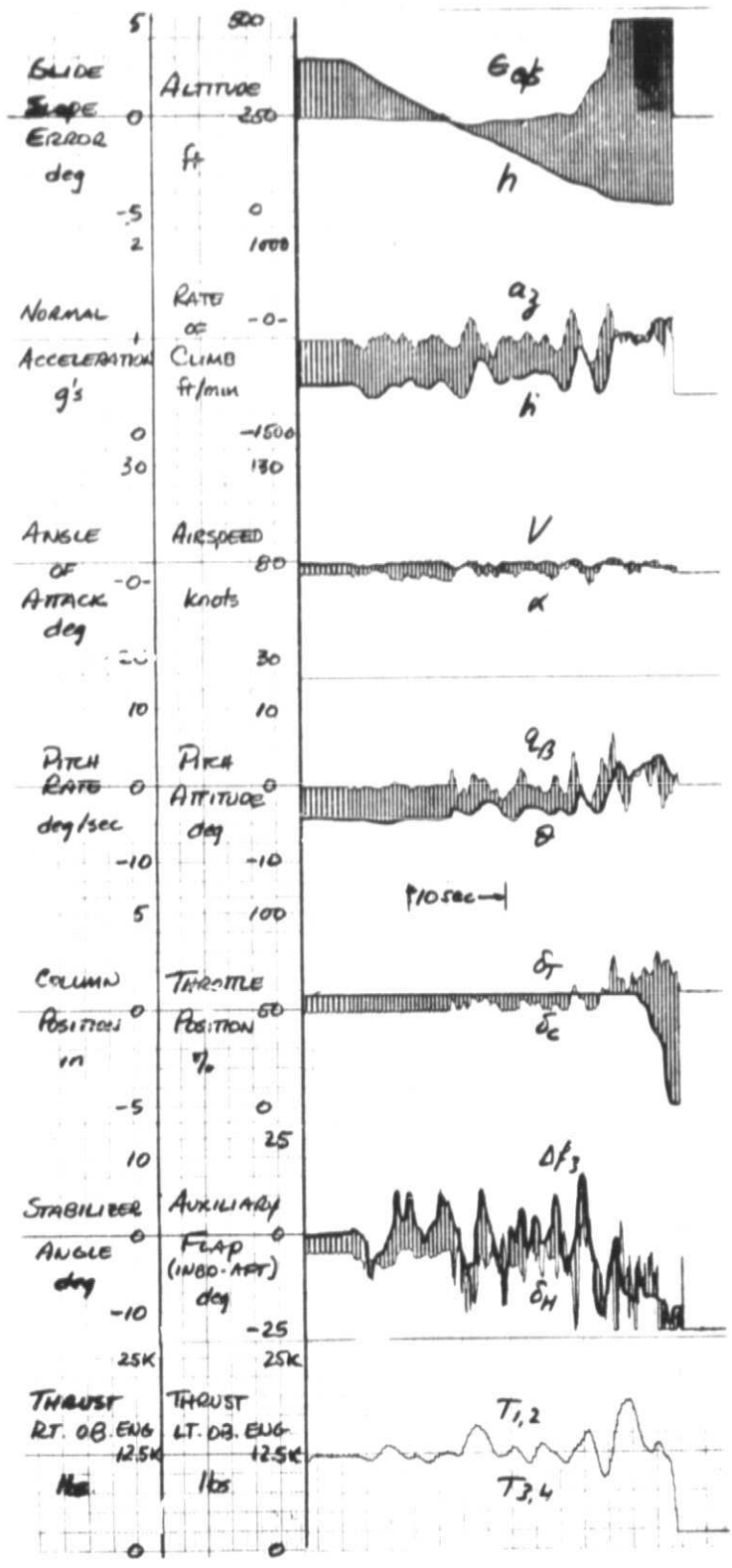

Figure 33. Time History of a Landing with Flight Path Stabilization, $K_{\alpha_{\delta_T}} = 10$ percent per degree - All Engines Operating

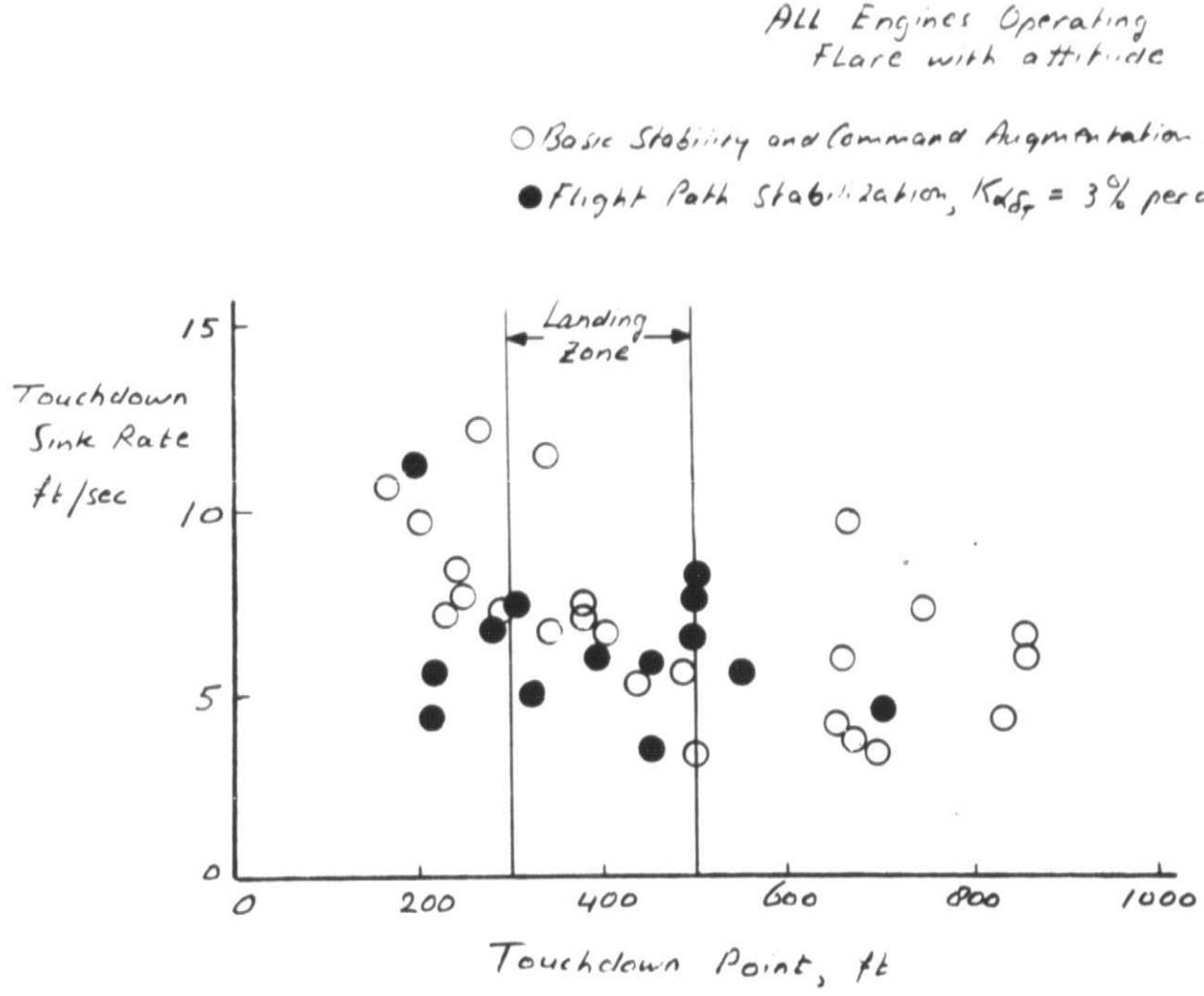

Figure 34. Comparison of Landing Precision of Basic Aircraft with and without Flight-Path Stabilization - All Engines Operating

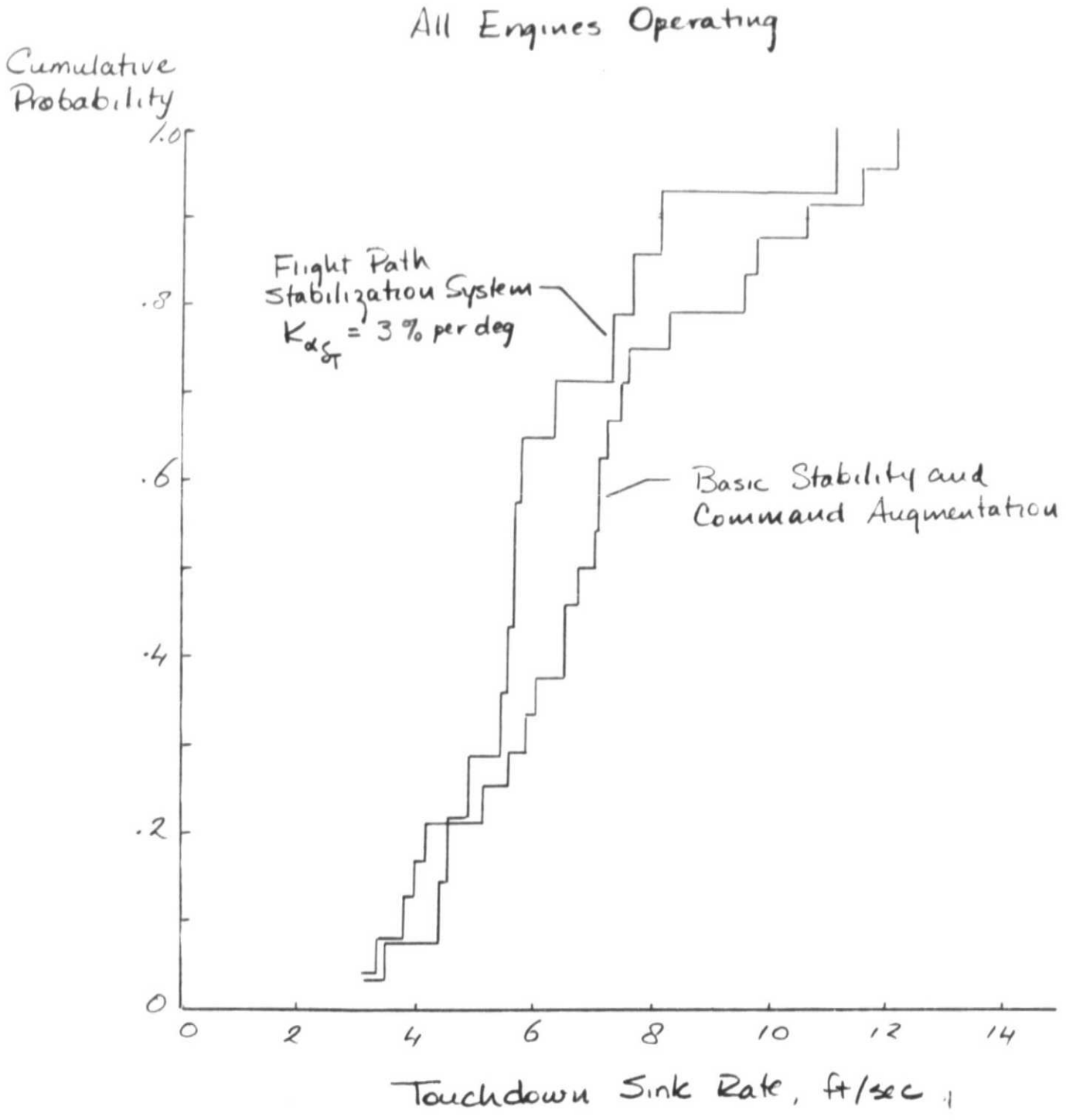

Figure 35. Comparison of Touchdown Sink Rate Probability for Aircraft With and Without Flight-Path Stabilization

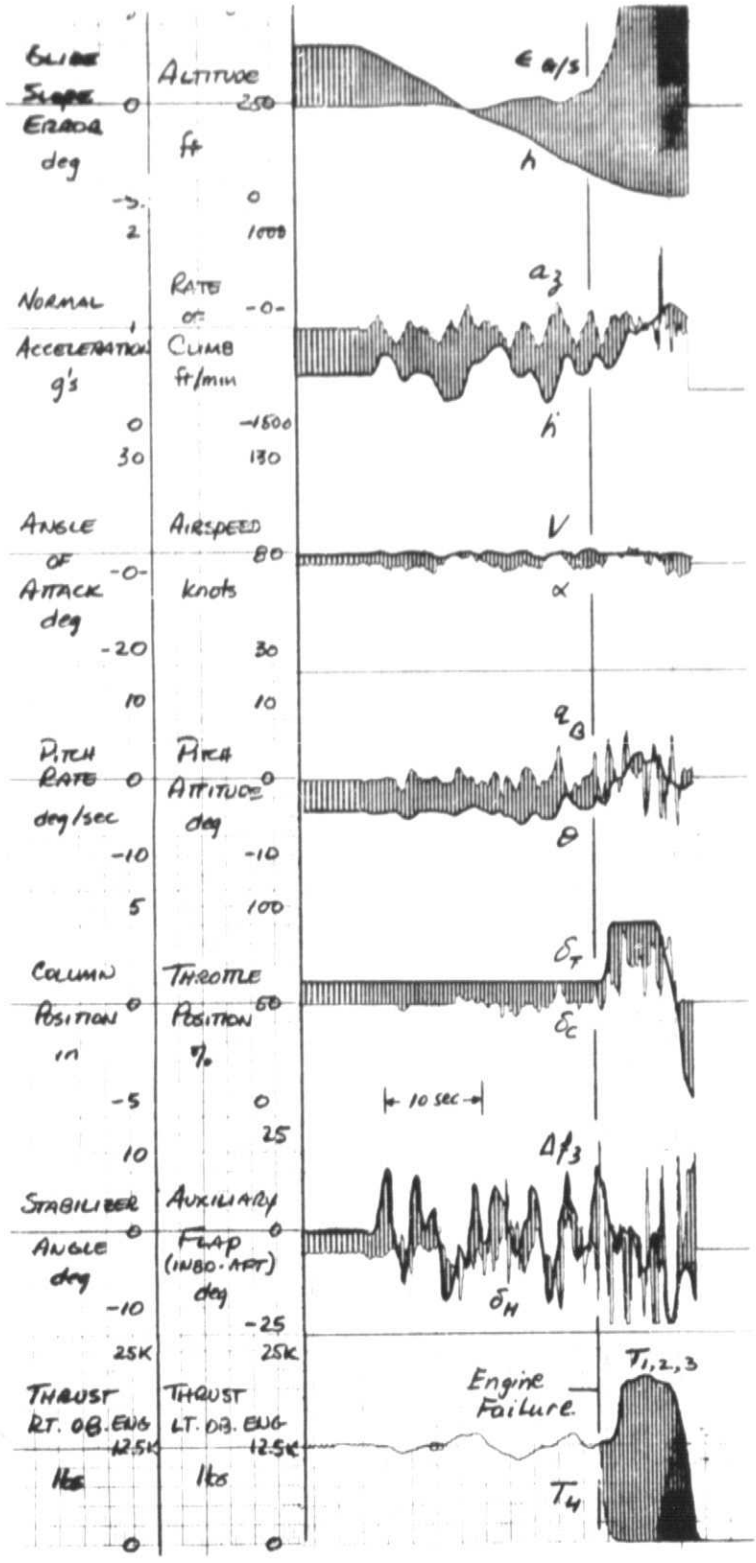

Figure 36. Time History of an Engine-Out Landing

- Flight Path Stabilization, $K_{\alpha_{\delta_T}} = 3$ percent per degree
- Engine Failed at 61 Feet

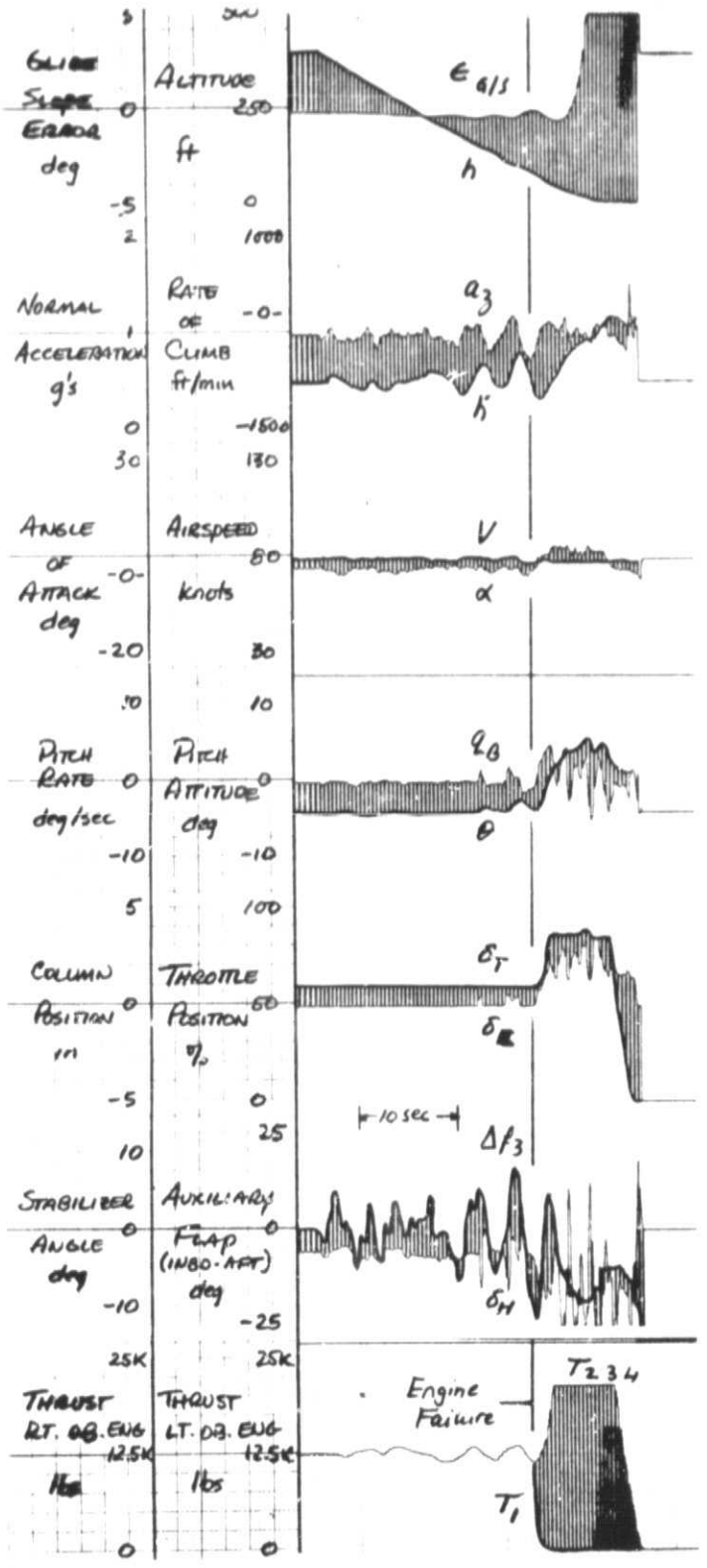

Figure 37. Time History of an Engine-Out Landing

- Flight Path Stabilization, $K_{\alpha_{\delta_T}} = 5$ percent per degree
- Engine Failed at 86 Feet

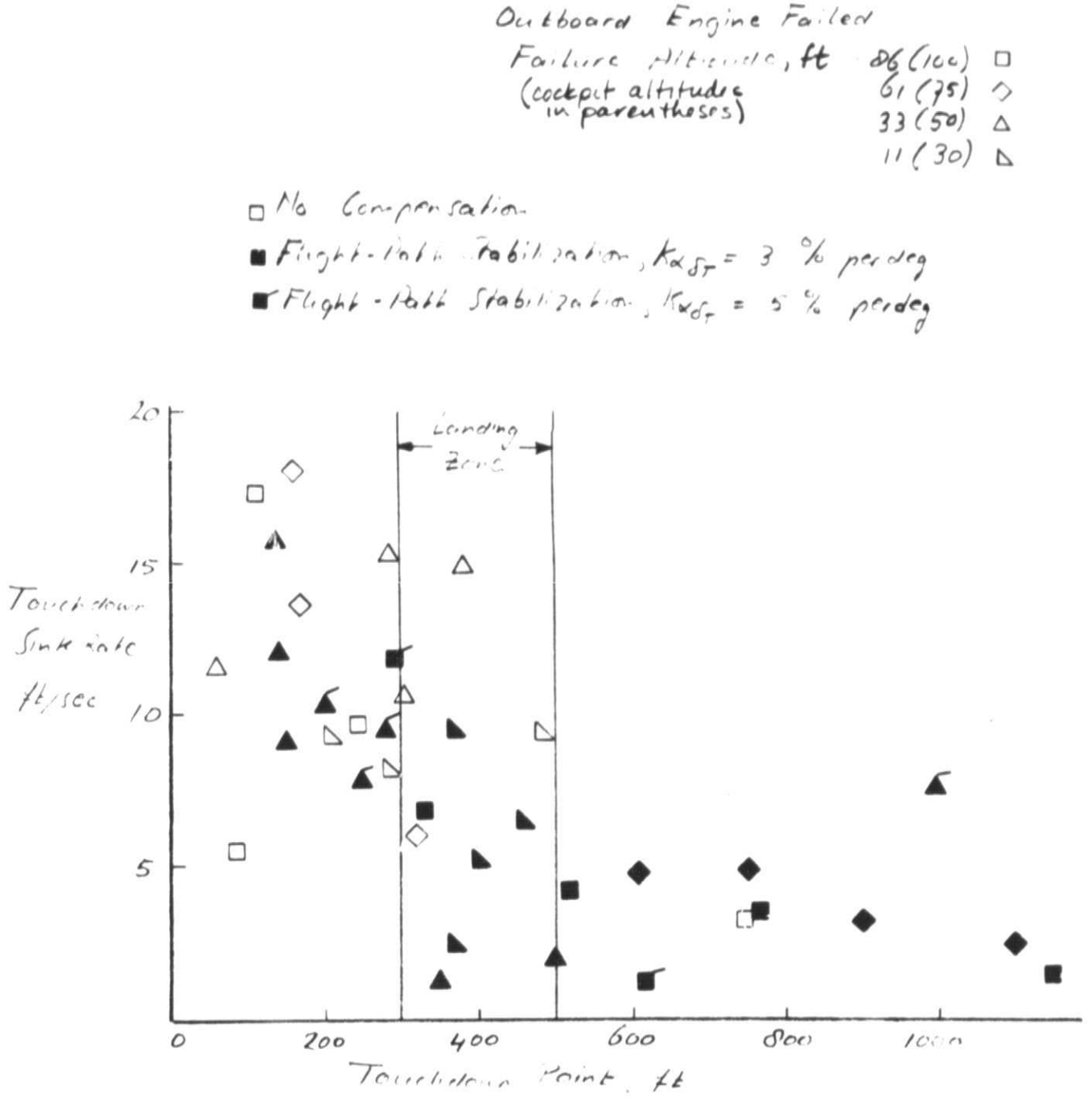

Figure 38. The Effect of Flight-Path Stabilization on Engine-Out Landing Performance

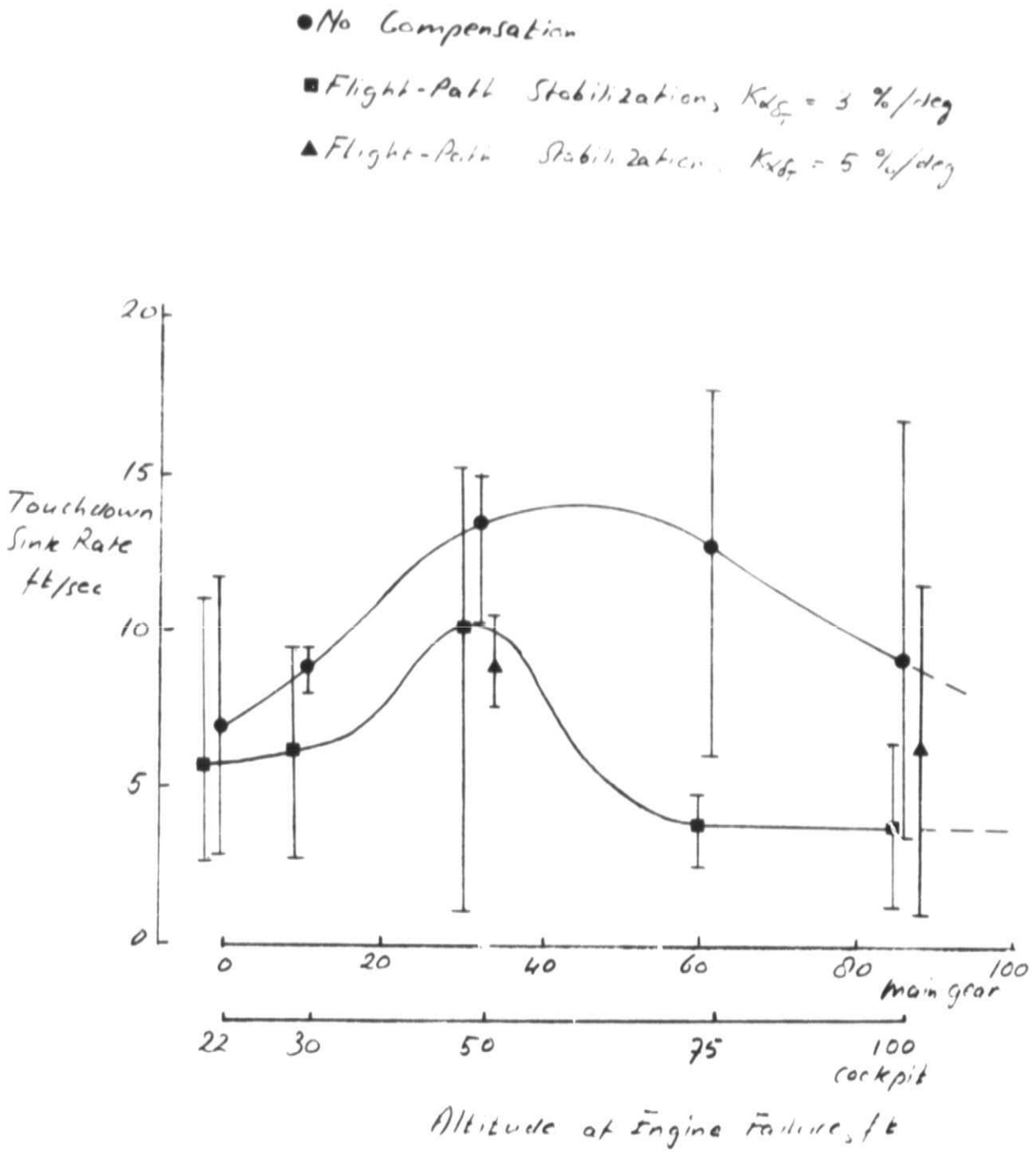

Figure 38 (concluded)

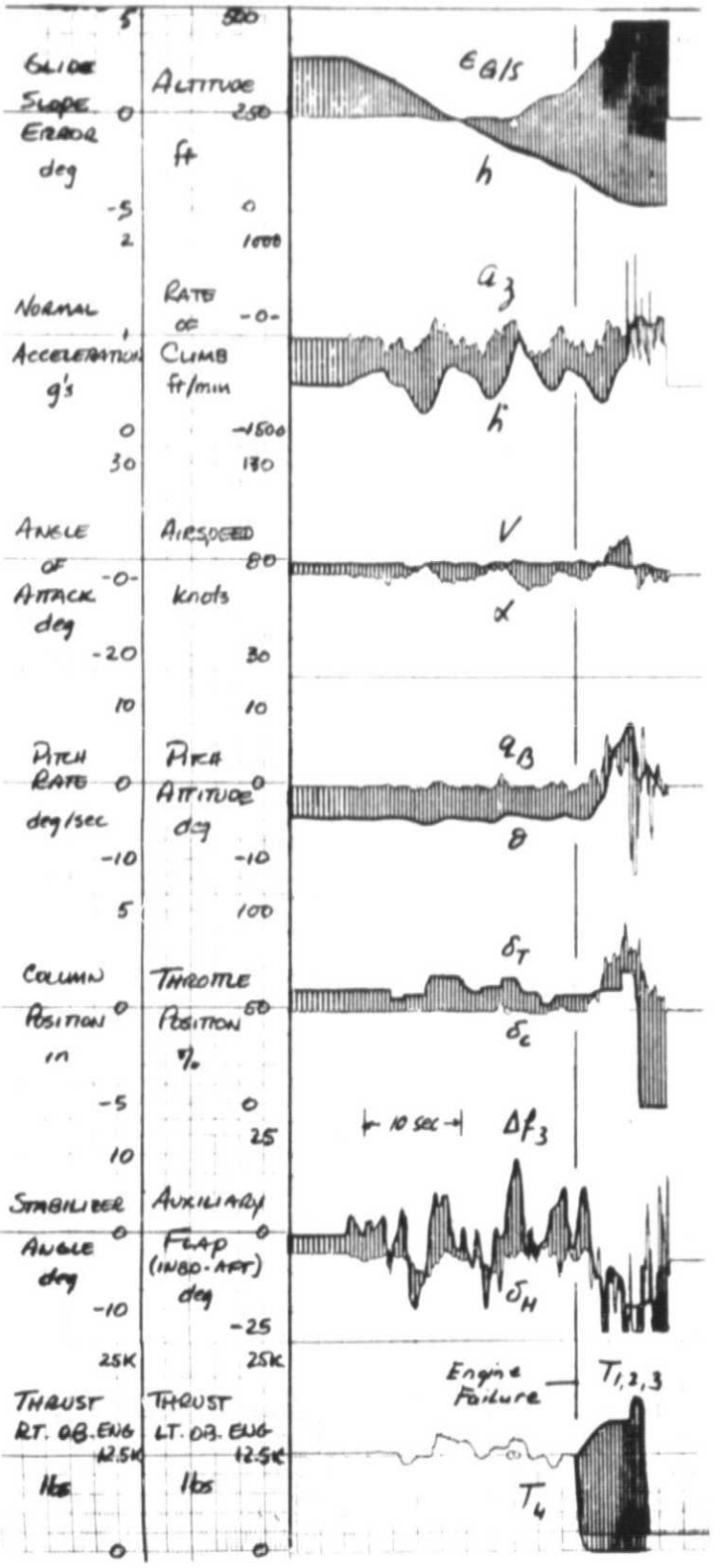

Figure 39. Time History of an Engine-Out Landing
- Closed Loop Thrust Control
- Engine Failed at 86 Feet

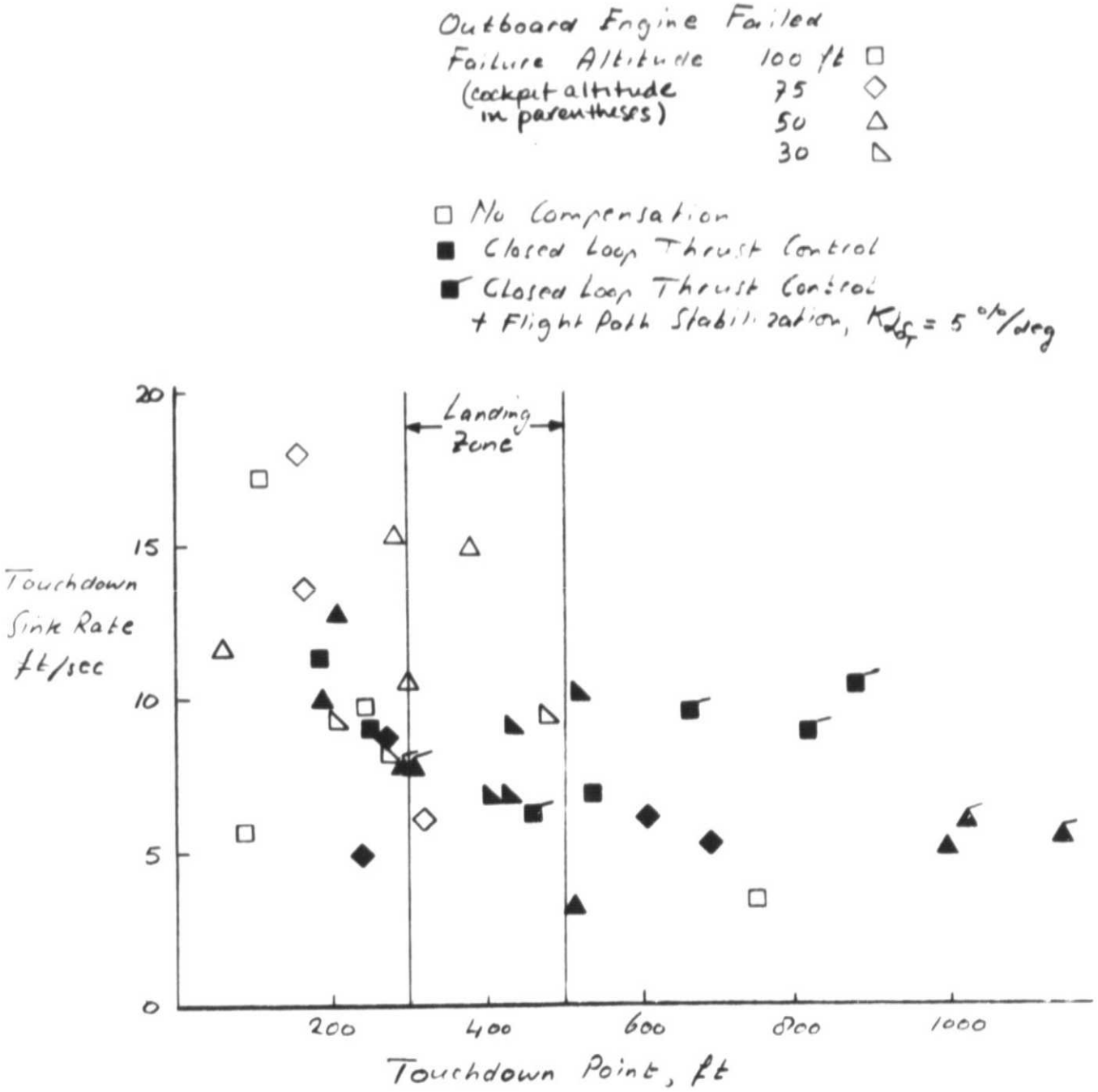

Figure 40. The Effect of Closed-Loop Thrust Control and Combined Closed-Loop Thrust Control/Flight Path Stabilization on Engine-Out Landing Performance

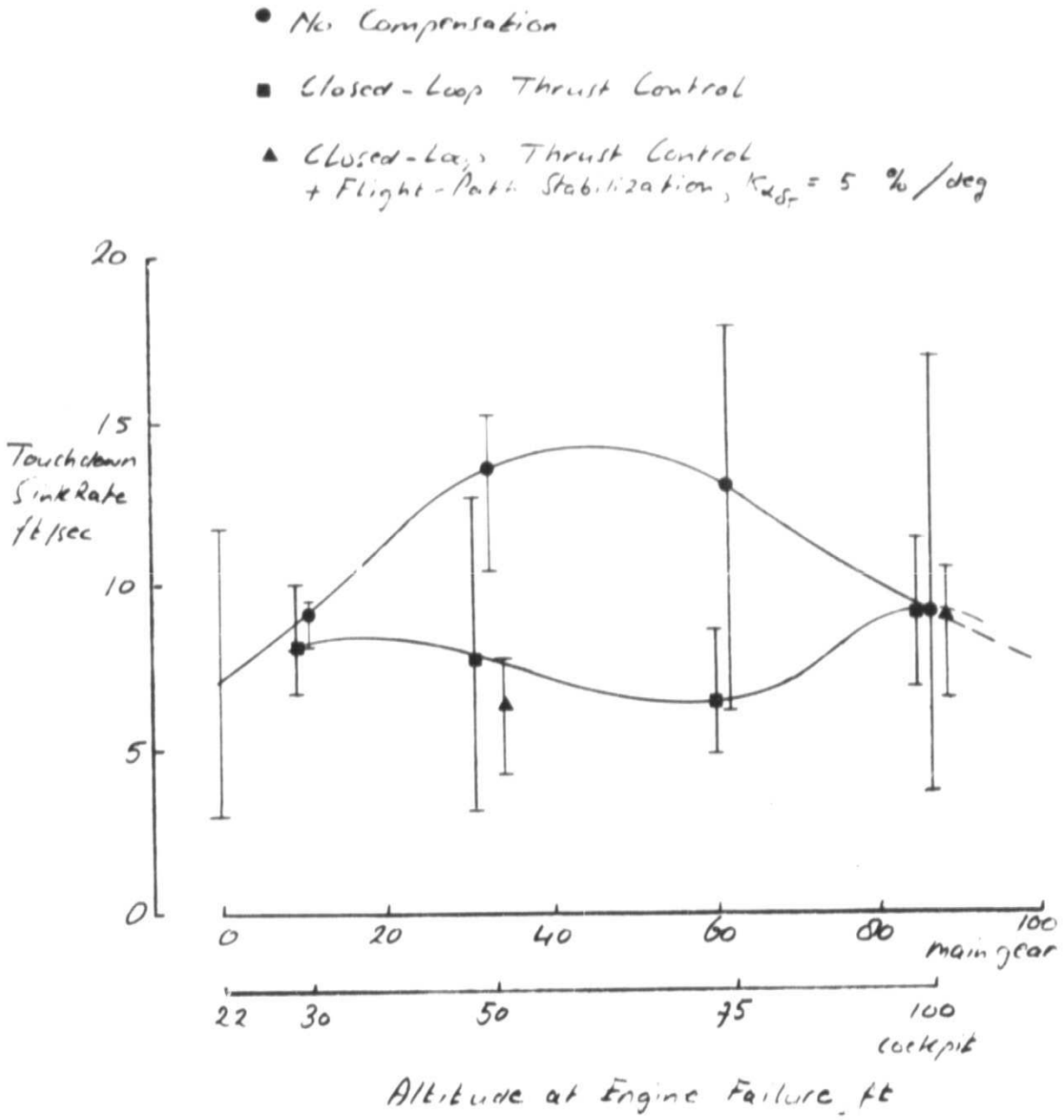

Figure 40 (concluded)

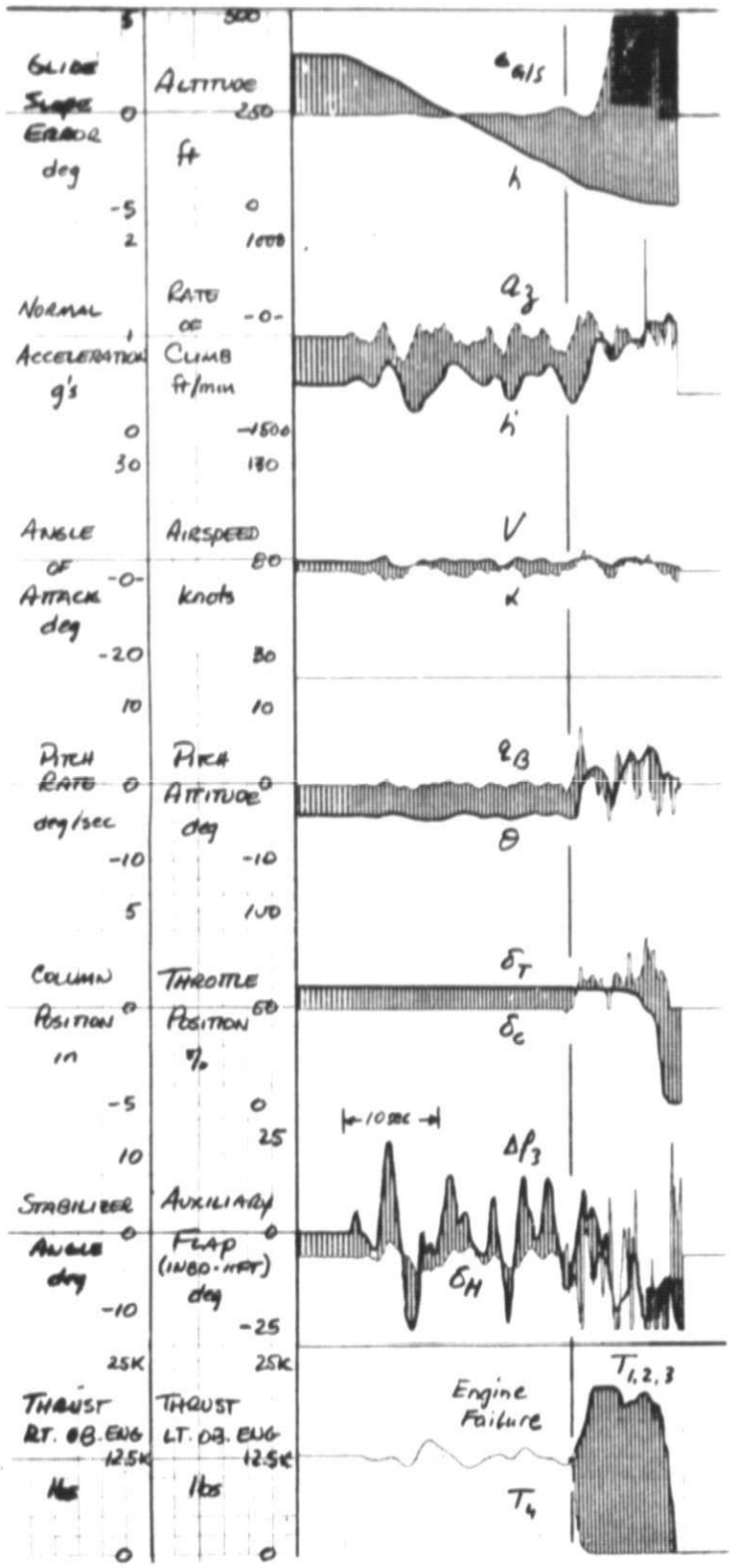

Figure 41. Time History of an Engine-Out Landing
- Closed-Loop Thrust Compensation and Flight Path Stabilization, $K_{\alpha_{\delta_T}} = 5$ percent per degree
- Engine Failed at 86 Feet

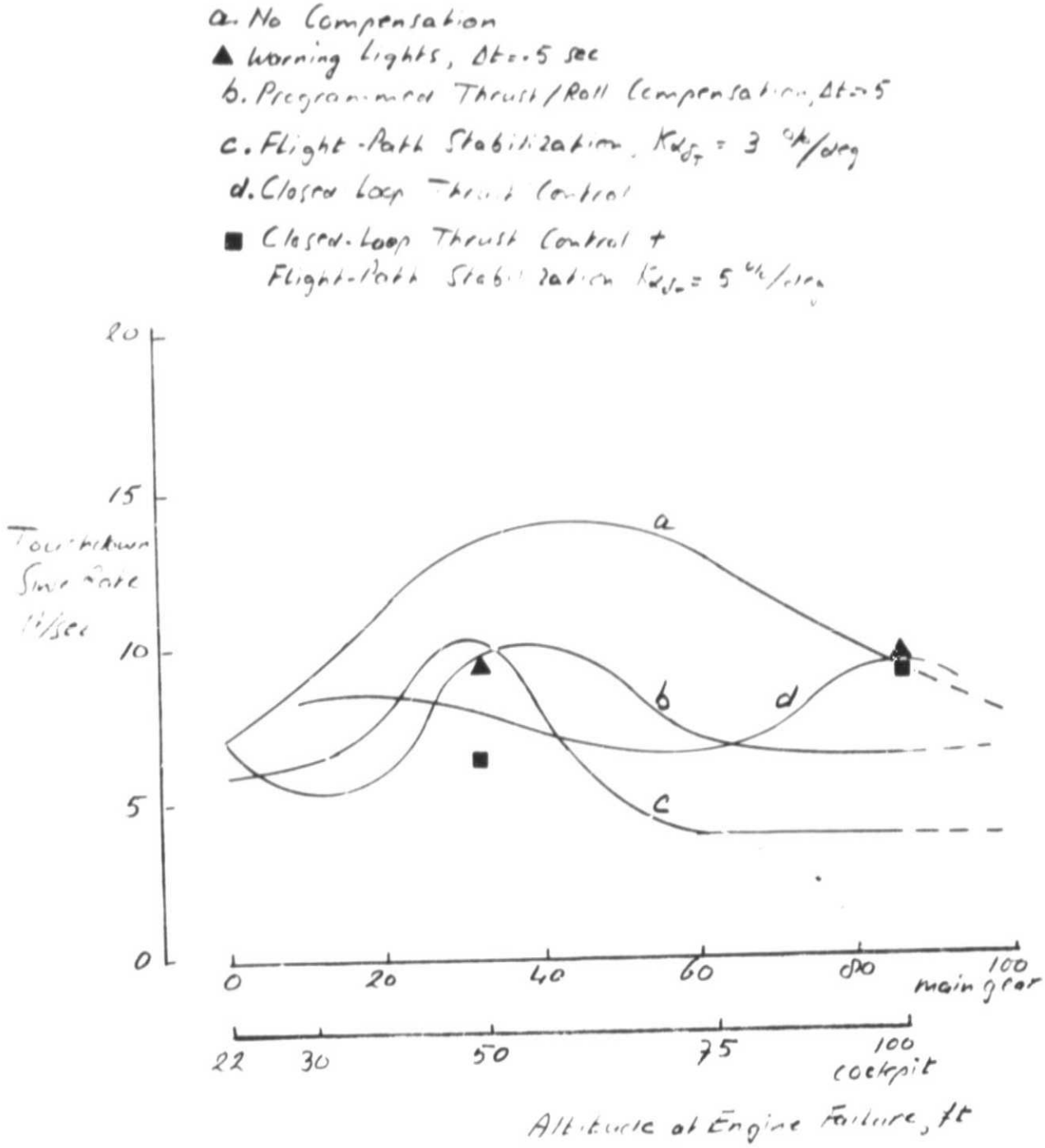

Figure 42. Comparison of Trends of Engine-Out Touchdown Sink Rate with Altitude of Engine Failure for the Engine Failure Compensation Concepts Investigated